1988

Compaction-induced inclination shallowing in natural and synthetic sediments /

Gay A. Deamer
Lehigh University

COMPACTION-INDUCED INCLINATION SHALLOWING IN NATURAL AND SYNTHETIC SEDIMENTS

by

Gay A. Deamer

A Thesis

Presented to the Graduate Committee

of Lehigh University

in Candidacy for the Degree of

Master of Science

in

Geological Science

Lehigh University

1988

This thesis is accepted and approved in partial fulfillment of the requirements for the degree of Master of Science.

May 16, 1988
(date)

Professor in Charge

Chairman of Department

Acknowledgements

I am extremely grateful to my world-famous and amazingly understanding thesis advisor, Ken Kodama, for his help and ideas throughout this project. He is a great scientist and really fine person. I would also like to thank the other members of my committee, Sibel Pamucku, of the Civil Engineering Department, and Bobb Carson, but especially Sibel, for being very patient with my many ignorent questions. Carl Moses also provided several extremely helpful suggestions for my work. George Yasko spent many, many hours designing and building improvements to the consolidometer, and his help has been inestimable. John Stamatakos deserves thanks for things like helping me with my experiments, answering stupid paleomag questions I didn't want to ask Ken, and writing my computer programs, but these things are trivial compared to his most significant contribution: cribbage playing. Thanks, John. I thank the head of the department, Laurie Cambiotti, for the millions of things she does for all of us who tend to take her for granted, and finally I'd like to thank the other students, graduate and undergraduate, who have made my time at Lehigh so much fun.

Table of Contents

List of Tables

List of Figures

Compaction-Induced Inclination Shallowing in Synthetic and Natural Sediments

ABSTRACT

A model proposing a mechanism for inclination shallowing of compacting sediments (Anson and Kodama, 1987) in which magnetite particles are electrostatically attracted to negatively charged clay particles was tested. Equidimensional and acicular magnetite (0.5 microns in size) were mixed with kaolinite, chlorite, montmorillonite or illite in either saline or distilled water to produce clay slurries which were given PDRM's by stirring them in fields with inclinations of 30^{o}, 45^{o}, 60^{o}, and 75^{o} and compacted to maximum pressures ranging from 0.14 to 0.19 MPa. Although no evidence for electrostatic attraction between magnetite and clay particles was found, there is evidence that clay and magnetite somehow interact.

The shallowing rate for most samples is rapid at low pressures, and decreases abruptly at higher pressures. This change in shallowing rate occurs at the same pressure as an abrupt change in compaction rate with pressure. This behavior closely resembles the behavior of compacted slurries studied by McConnachie (1974). He found that the orientation of clay particles during compaction was initially rapid, but then the clays stopped orienting at the same pressure at which he observed a change in the compaction rate. It is inferred that since clay orientation and inclination shallowing exhibit very similar behavior with increasing pressure, the magnetite particles are attached to clay platelets.

The change in intensity of magnetization according to field inclination angle during compaction suggests that magnetite particles are not perfectly aligned before compaction, but are dispersed about the mean direction. Compaction causes a decrease in magnetic intensity accompanying shallowing, suggesting that compaction increases the dispersion, similar to the effect found by Cogne (1987) in strained synthetic materials.

INTRODUCTION

Sedimentary rocks used in paleomagnetic studies introduce uncertainties which are not present in igneous rocks. Inaccuracies introduced by depositional and post-depositional processes can have a deleterious effect on tectonic interpretations and geomagnetic field studies which are based on the remanent magnetization of sedimentary rocks. In order to use the magnetic signal determined from sedimentary rocks, it is necessary to understand how these processes have affected the alignment of magnetic particles within the field.

Studies attempting to define these processes have been limited in several ways: 1)laboratory experiments designed to imitate natural depositional processes invariably do not, so that comparisons to real deposits are questionable (King, 1955, Irving, 1957, Irving and Major, 1964, Otofuji and Sasajima, 1981); 2) until recently, it was virtually impossible to collect in-situ deep sea sediments for study without severely disrupting them, thus destroying delicate depositional fabrics (Mayer, 1982); 3) the preparation of sediments for microscopic study generally results in some distortion of the sediment, making even qualitative observations difficult (Tovey and Wong, 1973). As a result, much of the quantitative information defining the relationship between the magnetic field and the resultant magnetization of deposited sediments has been questioned (Verosub, 1977).

Background

Early studies of depositional remanent magnetization (DRM) suggest that whether or not magnetic particles initially record the earth's magnetic field accurately (i.e., King, 1955), subsequent disturbances of the sediment can cause realignment of the magnetite signal (Irving, 1957), imparting an accurate post-depositional remanent magnetization (PDRM) to the sediment. Whether this more accurate signal is retained by the sediment while it undergoes further compaction is less certain.

Studies of deep-sea sediments cast doubt on the existence of compaction-induced inclination error. The classic study by Opdyke and Henry (1969) of 52 deep sea cores showed no inclination error exhibited by ocean sediments. Hammond, et. al. (1979) and Prince, et. al. (1980) also found no evidence of inclination error in the cores they examined.

However, one reason it has been difficult to demonstrate the existence of compaction error is because until recently, deep sea sediments have been sampled using piston cores, which sample only up to twenty meters of sediments. The development of the hydraulic piston corer in conjunction with the deep-sea drilling program has allowed the removal of relatively undisturbed marine sediments from depths of more than 200 meters (Mayer, 1982). Several recent studies of these deeper cores have revealed the possibility of compaction-induced error in deep sea sediments. Tauxe, et.al. (1984) found evidence for shallowing in sediments below 100 meters in DSDP Leg 73 sediments. Arason and Levi (1986) report finding a systematic

shallowing of inclinations in the top 120 meters of sediments at site 578 of DSDP Leg 86. Celaya and Clement (1988) found evidence of inclination shallowing in some of the sediments they studied, but only below a depth of 250 meters.

It is difficult to try to investigate the mechanism by which compaction error occurs (or even if it occurs) before having a clear idea of how sediments originally acquire a PDRM. The mechanism by which sediments may acquire post-depositional remanent magnetization is still uncertain. Several laboratory studies have suggested that the ability of magnetic particles to realign themselves after deposition is related to the water content of the sediment (Irving and Major, 1964; Hamano, 1980; Lovlie, 1974; Khramov, 1968). These studies imply that while the sediment maintains a high porosity near the sediment-water interface, small magnetite grains are free to rotate into alignment with the earth's field. Therefore, when the water content drops below a certain amount, the grains will become "locked in", unable to respond to any further changes in the field. Payne and Verosub (1982) demonstrated this idea using various sediment types and water contents to show that below a particular critical water content, the magnetic signal of the sediments could not be changed. Other experiments designed to determine lock-in depths and critical water content include work by Hamano (1980), who found a correlation between void ratio and lock-in depth which suggested that the magnetic signal is acquired at very low depths (1-2 meters below the sediment/water interface). Lovlie (1974) redeposited deep sea sediments to determine that when the sediments

reached a particular degree of compaction, they remained permanently aligned with the field.

Despite the many studies investigating the lock-in of PDRM, there are few which go farther to determine what may happen deeper in the sediment column as the sediment compacts. Blow and Hamilton (1978) used redeposited deep sea silty clay to try to determine the effect of compaction on the remanence of sediments. They found that as the sediment compacted, inclination shallowing occurred, which they termed compactive DRM. One of the problems with their study was that they allowed their sediment to compact by evaporation, and this process may have contributed as much to the shallowing effect as compaction. Noel (1980) suggests that the rotation of remanence of a sediment may occur during drying, probably due to surface tension effects in the pore spaces.

Other laboratory experiments designed to study compaction error in sediments have had limited success, usually because it is difficult to simulate the natural conditions which affect both the acquisition of PDRM and cause compaction error in the laboratory. Hall (1983) consolidated pure clay and natural sediments to pressures of 5.62 MPa, and found a 5-10^{o} decrease in the inclination angle during compaction. However, he applied an ARM to the sample for its signal, and this may not be a good model for the acquisition of PDRM.

More recently, Anson and Kodama (1987) performed a series of experiments to demonstrate the effect of compaction on clay slurries. Their model suggests that an electrostatic attraction exists between negatively charged clay particles and magnetic particles. The

assumption is that in a slurry consisting of a clay (kaolinite), magnetite, and water, the magnetite will have a positive surface charge, causing an attraction between the clay and magnetite grains, which then attach themselves to the surface of clay grains. The long axis (easy axis of magnetization) of the magnetic particles will rotate parallel to the clay particle surface. Subsequent compaction of the slurry causes a reorientation of the clay particles perpendicular to the direction of compaction. As the clay platelets rotate during compaction, the magnetic grains rotate with them, causing the bulk magnetization to be rotated toward the horizontal (inclination shallowing).

Anson and Kodama (1987) found that the amount of inclination shallowing depended on the inclination of the field in which compaction took place, with maximum shallowing occurring at 45-50^{o} and minimums at 90^{o} and 0^{o}, following a mathematical function expressed as:

$$\tan (I_r) = (1 - adV) \tan (I_o)$$

where I_r is the remanent inclination after compaction, dV is the amount of compaction, and I_o is the initial inclination of the sample. The coefficient "a" was suggested to be a factor relating the ratio of edge to face areas in the clay particles, and arises from the assumption that clay edges are also negatively charged, so that any magnetite particles which became attached to the clay edge rather than the face would tend to offset shallowing during compaction.

Anson and Kodama also found that the inclination angles of a statistically significant number of samples in their study became shallower during AF demagnetization. Anson and Kodama suggested that magnetite grains having a lower coercivity (larger grain size) did not rotate or shallow as much as the smaller magnetic grains. According to their model, the smaller magnetic grains attached to the clay flakes are shallowed more by compaction than the larger grains which are free to reorient parallel to the ambient field. The results of their af demagnetization of the samples were the primary piece of evidence suggesting attachment of the magnetite grains to the clay fabric.

The present study was designed to test Anson and Kodama's model. The work investigates the effect of various clay minerals, magnetic grain shape, and pH on laboratory-induced compaction error in sediments. Different behavior of the clay under various conditions will help to determine the validity of their model in which electrostatic attraction between negatively charged surfaces of clay particles and positively charged magnetic grains caused compaction shallowing. The experimental work also attempts to define the extent of compaction error occurring in clay-rich sediments, and to determine whether the use of pure clay analogs for simulating the effect in natural sediments is valid. The first phase of the study includes compaction of acicular and equidimensional magnetite in various types of pure clays (kaolinite, illite, chlorite, montmorillonite). The use of different clay types was expected to affect the results in at least two ways: 1) Since different clays

have different surface charge densities, it was hoped that there would be a corresponding difference in the attractive force between the clay and magnetite which would be reflected in the amount of compaction error; 2) The different clays may also experience different degrees of orientation during compaction (Quigley and Thompson, 1966; von Englehardt and Gaida, 1963; Meade, 1965). If Anson and Kodama's model is correct, it was assumed that the effect of compaction would produce increased shallowing in clays which orient themselves more readily.

Additional experiments involve the use of different pH values in the clay slurries, since ph should have an effect on the amount of attraction between the clay and magnetite. Parks (1964) determined that the zero point of charge (ZPC) on the surface of magnetite occurs at a pH of 6.5 +/- 0.3. This means that a magnetite particle present in a slurry having a pH of less than about 6.2 should have a positive surface charge, and in a slurry having a pH above 6.8 should be negatively charged, and if the slurry has a pH of about 6.5, the particle should have no surface charge. By altering the pH of the slurries used for compaction, it should be possible to see a change in the amount of attraction between particle types. In the case where the magnetite particles are negatively charged, the model would predict a net repulsion, which would presumably be reflected in a difference in the amount of inclination shallowing.

Anson and Kodama's model also predicts a different amount of shallowing depending on the shape of the magnetic grains present in the sediment. It suggests that acicular shaped magnetite grains will

produce more shallowing than equi-dimensional ones, so a series of experiments is also performed using different shapes of magnetite to determine whether there is a relationship between grain shape and amount of shallowing.

Finally, a series of compaction experiments are conducted on both a natural sediment, and a "reconstructed" analog of the natural sediment using the pure clay material to reconstruct the clay portion of the natural sediment. The use of natural and reconstructed sediments is intended to demonstrate that if inclination shallowing behavior in the natural sediments is similar to that of the pure clays and the reconstructed analog, it is reasonable to use non-natural sediments in future compaction experiments, recognizing that it is easier to characterize the synthetic analogs.

PROCEDURE

Summary of compaction experiments

Compaction experiments were performed on four types of pure clays (kaolinite, chlorite, illite, and montmorillonite) mixed with acicular-shaped magnetite using two fluid types (distilled, deionized water and saline water), at field inclination angles of 30^{o}, 45^{o}, 60^{o}, and 75^{o}. Identical clay/fluid combinations containing equidimensional magnetite were compacted in a single field inclination angle of 50^{o}. Two natural sediments collected off the coast of Oregon, and a "reconstructed sediment", all containing natural magnetite were compacted at the four different field inclination angles. Finally, three of the pure clays mixed with water, and one with NaOH and water, were compacted using a combination of natural and equidimensional magnetite in a 60^{o} field.

Material

Four types of clay were obtained from Ward's Inc.: illite-bearing shale from Fithian, Illinois; kaolinite from Twigg's County, Georgia; chlorite from Calaveras County, California; and sodium montmorillonite from Clay Spur, Wyoming. The clays were broken up in a Spex ball mill, and then further ground in a Fisher automatic mortar grinder. The grain size of each clay type was determined using an Elzone Rapid Particle analyzer. The mean grain size for each clay type is as follows: kaolinite, 1.2 microns; illite, 2.0 microns; montmorillonite, 1.0 microns; chlorite, 44 microns. The specific gravity of each clay type was determined according to ASTM Specification D-854. The values determined for specific gravity are

as follows: illite, 2.75 gm/cm^3; kaolinite, 2.64 gm/cm^3, montmorillonite, 2.94 gm/cm^3, chlorite, 2.71 gm/cm^3.

Synthetic magnetite was obtained from Pfizer Minerals and Pigments Company. Acicular magnetite (type MO-4232) has an average length of 0.45 microns and a length to width ratio of 6:1 (Hall, 1982). The equidimensional magnetite (type MO-7029) has an average diameter of 0.5 microns.

Two marine sediments collected from off the Oregon coast were used for a series of compaction experiments. The sediment containing a higher proportion of clay was separated by settling into sand, silt and clay fractions. By weight, the sediment was determined to be 8.5% sand, 49.0% silt and 42.5% clay. The clay fraction was analyzed using a Phillips X-ray diffractometer, and consisted of 64% chlorite, 22% illite, and 14% montmorillonite. No attempt was made to analyze the sand and silt fractions mineralogically; they were assumed to consist primarily of quartz. An analog of the marine sediment was constructed using the pure clays from Ward's, plus the sand and silt fractions from the marine sediment removed during settling. The sand, silt, and clay fractions were added in the same proportions as were present in the natural sediment, and the clay fraction was added in proportion to the amounts indicated by the X-ray analysis (Table 1). Chlorite comprised 64% of the clay fraction of the natural sediment, but the chlorite added to the reconstructed sediment had a mean grain size larger than clay size. No attempt was made to correct this discrepancy when reconstructing the sediment. The magnetic fraction for the reconstructed sediment was obtained from

TABLE 1

Grain Type and X-Ray Results for Natural Sediment

Grain type	% present
clay	42.4
silt	49.1
sand	8.5

X-ray results on clay fraction

Clay type	% present
chlorite	64
illite	22
montmorillonite	14

magnetic separation of the natural sediment, although no attempt was made to first determine the weight fraction of magnetic component. The magnetite was added to make up approximately 0.1 weight percent (dry) of the sediment.

The grain size of the magnetic component of both the natural sediment and the reconstructed sediment was estimated by determining the ARM versus susceptibility ratio (Banerjee, et. al, 1981). The ARM was induced in an alternating field of 100 mT, and a steady field of 0.06 mT. The susceptibility was measured using a Sapphire Instruments SI-2 magnetic susceptibility and anisotropy instrument.

An examination of the magnetic separates was made using a scanning electron microscope. At least several magnetite grains were observed which were approximately 20 microns in size, but it was not possible to determine whether these larger grains comprised a significant proportion of the total magnetite population.

Sample Preparation

Slurries were prepared using oven-dried clay, magnetite, and either distilled, deionized water or "instant ocean", a solution which chemically approximates the composition of ocean water. Usually, enough slurry for several samples was prepared at one time. Magnetite was weighed and added to whichever fluid was being used, and sonicated for several minutes to evenly distribute the magnetite and break up clumps. The dry clay was then added, and the mixture was transferred to plastic bottles and shaken until the slurry was homogeneous. The approximate water content of the clay slurries was as follows: kaolinite, 170% (distilled water) and 150% (instant

ocean); illite, 75% (distilled water and instant ocean); chlorite, 70% (distilled water and instant ocean); montmorillonite, 1300% (distilled water) and 190% (instant ocean). The magnetite comprised approximately 0.1% by dry weight of the slurry.

The slurry was compacted in an acrylic cylinder (1.37 cm. OD, 1.63 cm. ID, 4.4 cm. long). The cylinder has a removable acrylic bottom plate, so that the sample can be easily extruded after compaction (see Figure 1 of Anson and Kodama, 1987). A porous stone covered with a piece of filter paper was set over the bottom plate, and the slurry was poured into the cylinder. The slurry was stirred inside a set of 1 meter Helmholtz coils (Parry, 1967) capable of maintaining a controlled magnetic field of 0.05 mT over a 5 cm^3 region, within which the sample would be subsequently compacted. Stirring (with a wooden toothpick) was designed to impart a post-depositional remanent magnetization (Tucker, 1980) which would be parallel to the field inside the Helmholtz coils. The magnetization was measured on a 2-axis CTF superconducting rock magnetometer after stirring. The sample was measured at four 90^o intervals to obtain a complete 3-axis measurement and an estimate of magnetization homogeneity. This allowed measurements to be made while the slurry was still liquid, since the sample was not inverted. The magnetization was measured 2-3 times. If, after stirring, the signal did not approximate the field in the Helmholtz coils, the sample was restirred inside the coils and remeasured until the field was approximated. Another porous stone and piece of filter paper was placed on top of the slurry, and sample's magnetization was measured

once more before compaction began. The porous stone had a weak magnetization (approximately 10^{-6} mA/M), which was not strong enough to affect the slurries' signal. Placing the porous stone in the sample holder, however, did tend to change the signal. Almost invariably, when the sample was remeasured, the signal steepened by up to two degrees. An acrylic piston transferred the load to the slurry. The piston had holes drilled through its length which allowed water to drain out during compaction.

Sample preparation for the natural sediment samples consisted of adding enough instant ocean solution to make a slurry from the sediment. The water contents for these two slurries were approximately 250% for clay-rich sediment, and 105% for the siltier sediment. Once the slurry was mixed, these sediments were treated in the same manner as the pure clay slurries.

The reconstructed sediment consisted of three parts: sand and silt, clay, and magnetite. The sand and silt proportion used in the reconstructed sediment was simply separated from the natural sediment by settling. The clay fraction was made up from the pure clays from Ward's, in the proportions determined by the X-ray analysis of the clay portion of the natural sediment. The magnetic component also originated from the natural sediment, and was separated magnetically by allowing portions of the sediment to settle through a water column past a magnet. The components were mixed with instant ocean to form a slurry (water content = 85%), and from this point was handled like the other slurries.

In samples containing both natural and synthetic magnetite, each magnetite type was weighed separately and added in the same proportion (approximately 0.05 weight percent) to the fluid before sonicating.

The pH of a representative sample of each of the slurry types was measured using an Orion Research digital pH meter. The pH values for each slurry type are shown in Table 2. One slurry consisting of kaolinite, with a combination of half natural and half equidimensional magnetite, had its pH adjusted by the addition of a 10% solution of NaOH to distilled, deionized water prior to sonicating with the magnetite.

Sample Compaction

An individual sample was compacted by applying a continuous load to an acrylic ball resting on top of the plunger. The load was provided by slowly filling an acrylic water tank over the sample holder (Hamano, 1980; Anson and Kodama, 1987) as shown in figure 1. Pressure on the sample is then determined by the amount of water in the tank. The pressure was monitored by noting the height of the water in the acrylic tank. A pressure transducer mounted at the bottom of the tank to automatically record pressure was found to not have sufficient sensitivity to accurately monitor pressure. The amount of compaction was determined by the decrease in sample height. This could be directly measured using a vernier caliper, but the water tank also included a position sensitive detector connected to a computer which continuously monitored downward movement of the tank.

TABLE 2

pH values for slurries

Water slurries	pH
kaolinite	4.9-5.0
illite	6.1-6.6
chlorite	8.2-8.4
montmorillonite	8.9-9.2
kaolinite with NaOH	9.5
Instant ocean slurries	
kaolinite	3.8-4.0
illite	6.2-6.7
chlorite	7.2-7.5
montmorillonite	7.3-7.5
Marine sediment	7.3
Reconstructed sediment	7.2

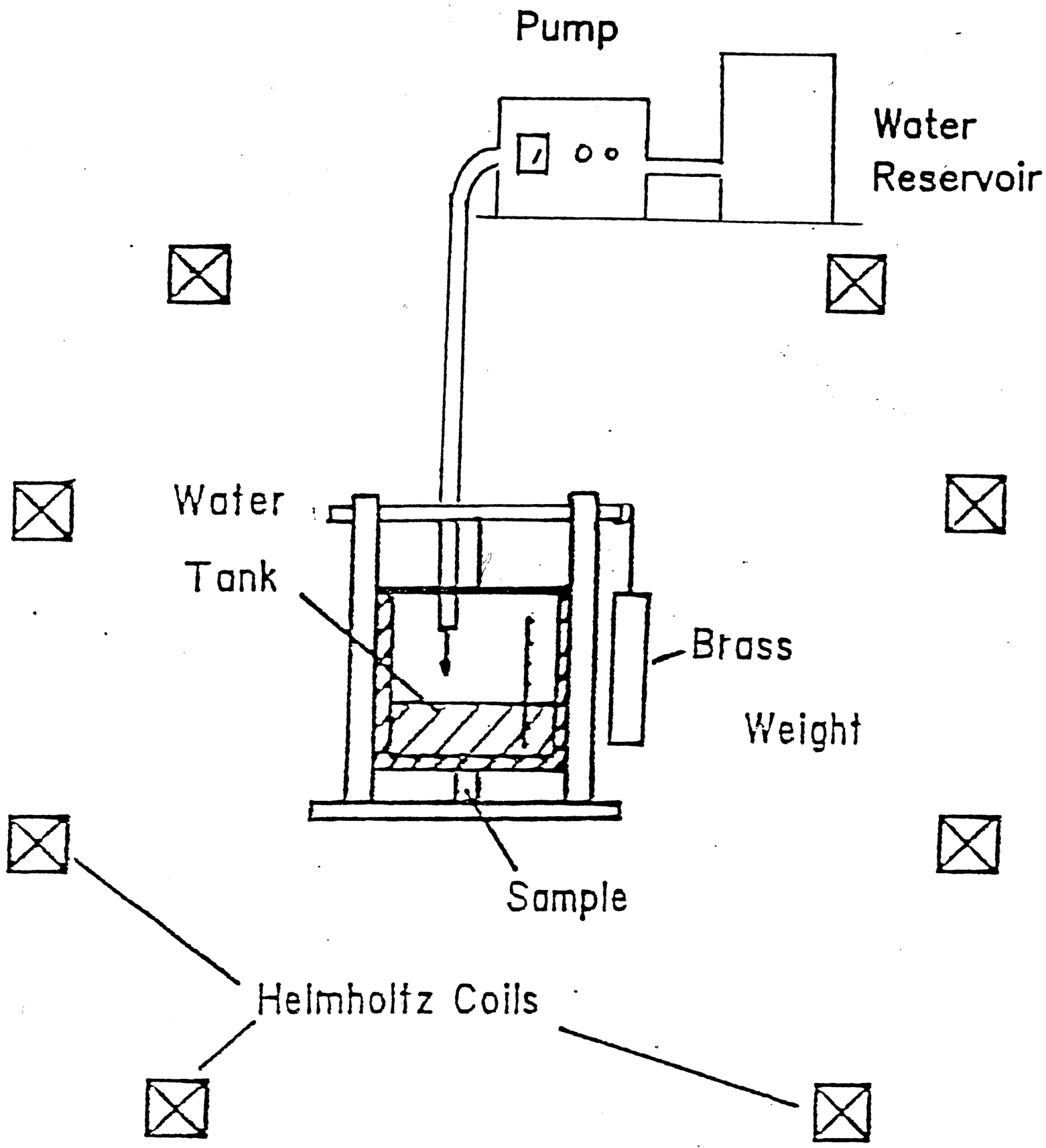

Figure 1: Schematic diagram of Helmholtz coils and water tank consolidometer (Hamano, 1980; Anson and Kodama, 1987). Water from a reservoir is pumped into the water tank whose weight is balanced by a brass weight. The increasing weight of the water tank applies a slowly increasing load on the sample. The consolidometer is surrounded by 2 sets of Helmholtz coils to control the magnetic field.

Samples were removed from the consolidometer approximately 10 times during the experiment to measure the magnetization at different compaction steps. Magnetization measurements took about one minute to complete, and at each compaction step, the sample was measured 2-3 times. After measurement, the sample was replaced in the consolidometer in the same orientation in the field. The water tank was lowered carefully back onto the plunger, so as not to compact the slurry too quickly. Occasionally, the height of the water tank was measured after replacement of the sample as well as before the sample was removed, in order to insure that any rebound experienced by removal of the load was eliminated after the load was reapplied. Most runs lasted between 5-10 hours with maximum pressures of 0.12-0.20 MPa exerted on the sample.

A series of loading rate experiments were performed on the pure clay slurries to determine whether the slurries were overpressured at a particular loading rate. This was determined by loading at the desired rate to the maximum desired pressure (0.15 MPa) and then allowing the sample to remain at that load overnight. If the sample height decreased between the time loading stopped and the time it was measured the next day, it was obvious that the sample was dissipating pore water pressures, therefore undergoing deformation during loading). All of the slurries except montmorillonite/water slurries were loaded at a rate of approximately 0.03 MPa/hour. Montmorillonite/water slurries were loaded at a rate of less than 0.02 MPa/hour, and dissipated excess pore water pressures more slowly than the other slurries.

Due to the presence of a very strong vertical field (75,000 nT) at the mouth of the cryogenic magnetometer, a set of Helmholtz coils were set up around the top of the magnetometer to offset this vertical field. One compaction run was completed with the vertical field cancelled. When the vertical field was cancelled, a horizontal field caused a progressive change in declination of the sample, and thereafter, no attempt was made to correct the vertical field.

Alternating Field Demagnetization

Following compaction, the sample was extruded from the acrylic sample holder in which it was compacted, and pushed carefully into a shorter acrylic holder. This was necessary because the compaction sample holder was too long to fit in the demagnetizer. Unfortunately, the extrusion process occasionally destroyed the sample to the point that it could not be demagnetized.

Those samples not destroyed were progressively demagnetized on a Schoenstedt GSD-5 tumbling AF demagnetizer to at least 80 mT, at which point less than 10% of the original intensity remained. Intensity, stereographic, and orthogonal projection (Zijderveld, 1967) plots were constructed from the AF demagnetization data. Characteristic directions were determined using principle component analysis (Kirschvink, 1980).

Fabric Experiments

An attempt was made to quantitatively measure the fabric of the compacted clay sample containing no magnetite by measuring its anisotropy of magnetic susceptibility on a Sapphire Instrument SI-2

magnetic susceptibility meter. The sample was too weakly magnetic, and extremely inconsistent values were obtained.

Volume change, water content, void ratios and porosity

Volume change (dV/V) in percent was monitored throughout each compaction experiment. Volume change is inversely proportional to water content and void ratio, and porosity.

The water content for representative samples of each slurry type were determined before and after a compaction experiment. This was done by weighing the oven-dried clay prior to mixing with water, and then weighing again after the water or saline solution was added to make the slurry of the proper consistency. Water content was calculated by dividing the weight of the water divided by the weight of the dry clay. Void ratio (volume of voids divided by volume of solid material) was obtained from water content by multiplying by the specific gravity of the solid material, and porosity was calculated by dividing the void ratio, e, by the quantity (1 + e).

Although the specific gravity was measured for each of the pure clay types, this was not done for the natural sediments. Instead, bulk grain density values listed by Hamilton (1979, Table A-1a) for clayey silt and silty clay were used as approximate values in these calculations.

RESULTS

The data collected for all of the compaction experiments are listed in Appendix 1. A summary of the results (change in inclination, volume and intensity) for each experiment is shown in Table 3. The results of AF demagnetization for all samples are given in Appendix 2.

I. Acicular magnetite/distilled water

Inclination shallowing occurred in all four clay types, although not to the same degree. Chlorite exhibited both the least amount of shallowing (1.2-4.7°) and the least volume change, and montmorillonite shallowed the most (8.1-11.5°) and experienced the largest volume loss. The rate of inclination angle decrease varied both with volume and pressure. Figures 2 and 3 show the inclination versus pressure plots for the four clays. It can be seen that kaolinite and illite have similar curves, with little change in inclination at the low and high pressure ends, and a rapid drop at an approximate pressure of 0.04-0.05 MPa. The curve for chlorite is nearly horizontal, and the curve for montmorillonite maintains a constant slope with increasing pressure.

AF demagnetization of these samples did not show any particular trend. For most samples, however, the direction of magnetization remained very stable through the demagnetization steps. That is, within approximately 2° of inclination, the signal usually maintained the same direction throughout demagnetization. If inclination did shallow or steepen, it did so only over the last several steps, almost always at a field strength greater than 70 mT. At this point,

Table 3

Summary of Results

Acicular Magnetite/Distilled Water

clay-field	I_o-I(°)	dV/V(%)	dJ(%)
Kaolinite			
75	6.5	59.0	44.2
60	5.4	48.8	18.3
45	9.8	56.1	41.5
30	9.1	48.3	28.1
Illite			
75	6.8	46.2	45.9
60	8.9	45.6	41.9
45	13.0	51.8	33.3
30	11.1	54.4	25.8
Chlorite			
75	3.3	24.0	4.8
60	1.2	34.7	17.9
45	4.7	38.5	3.5
30	3.5	24.2	0.2
Montmorillonite			
75	8.1	71.9	30.1
60	11.2	68.6	19.0
45	11.1	61.6	13.3
30	11.5	67.8	4.4

Acicular Magnetite/Instant Ocean

Kaolinite			
75	3.6	54.6	42.5
60	12.0	51.9	30.8
45	11.3	55.0	28.7
30	7.9	56.3	18.5
Illite			
75	6.3	46.7	35.8
60	6.1	39.7	37.6
45	8.5	39.3	28.1
30	7.8	37.5	23.2

Chlorite			
75	1.9	32.8	5.5
60	3.3	36.6	10.9
45	4.3	32.7	6.7
30	3.0	34.5	5.3
Montmorillonite			
75	9.8	50.3	48.5
60	14.1	56.1	42.1
45	14.4	59.5	37.6
30	10.8	55.7	26.9

Equidimensional Magnetite/Distilled Water (field = 50°)

Kaolinite	3.6	53.5	40.0
Illite	6.5	40.5	57.9
Chlorite	8.4	29.6	13.5
Montmorillonite	9.1	61.4	35.2

Equidimensional Magnetite/Instant Ocean (field = 50°)

Kaolinite	15.9	53.7	23.0
Illite	7.2	44.6	47.3
Chlorite	6.0	38.5	12.2
Montmorillonite	9.4	52.2	59.2
Natural Sediment (muddy)/Saline			
75	5.1	55.4	41.0
60	12.4	54.4	36.4
45	9.4	57.6	33.3
30	10.4	56.1	27.6
Natural Sediment (silty)/Saline			
75	3.3	38.7	39.7
60	5.0	40.0	40.7
45	9.5	45.9	39.4
30	5.5	42.5	31.1
Reconstituted Natural Sediment/Instant Ocean			
75	5.1	43.9	39.7
60	5.3	44.8	34.0
45	5.1	33.2	30.9
30	6.0	37.9	28.7

Natural + Equidimensional Magnetite/Distilled Water (field = 60°)

Kaolinite	7.5	58.8	24.0
Kaolinite + NaOH	4.2	47.3	30.0
Illite	6.0	39.6	23.0
Montmorillonite	6.8	67.3	15.5

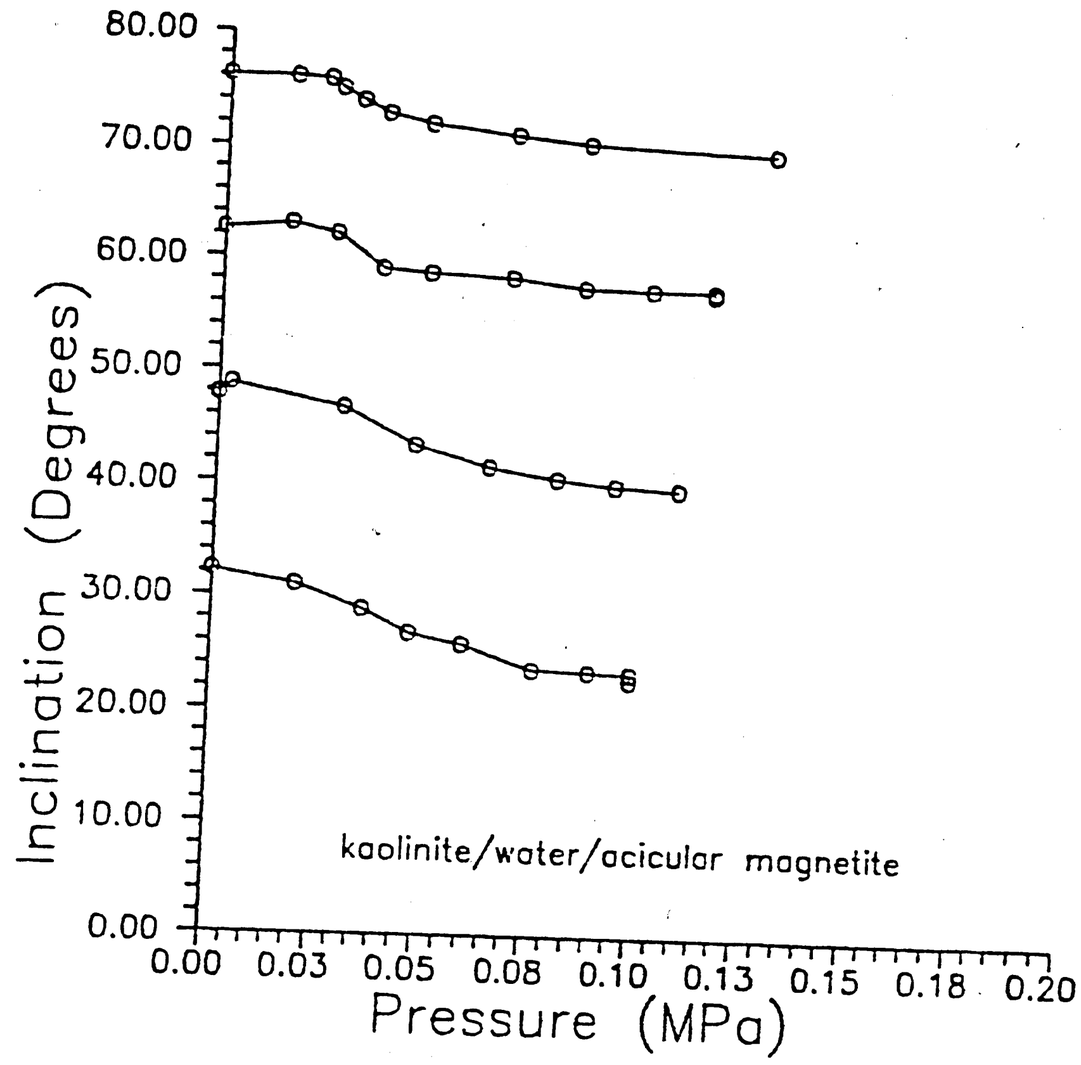

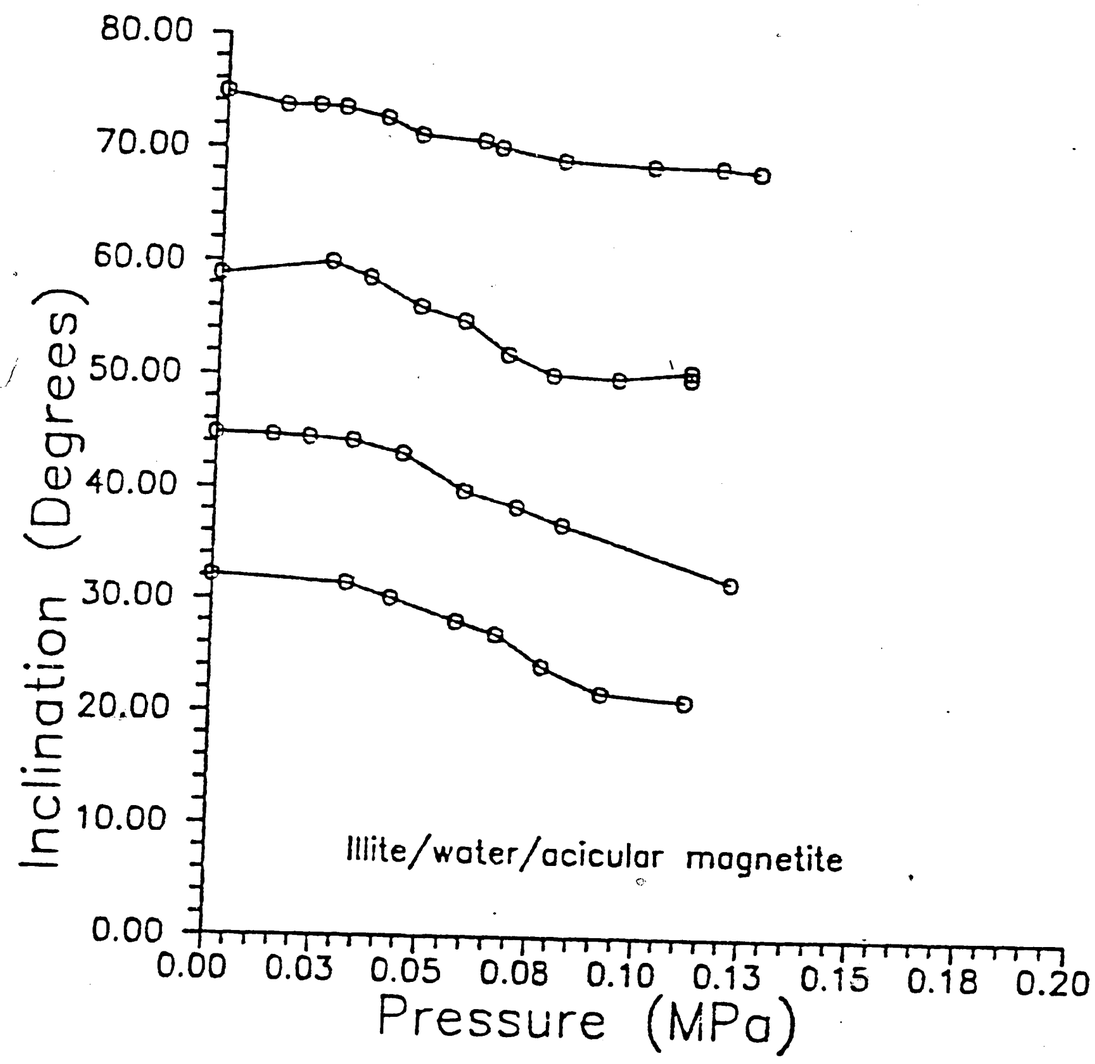

Figure 2. Plot of inclination versus pressure for kaolinite and illite clays in distilled water using acicular magnetite. The curves generally exhibit a nearly horizontal or slightly steepening inclination at very low pressures, then a more rapid decrease at slightly higher pressures followed by a flattening of the curve at still higher pressures resulting in a modified double-inflection curve.

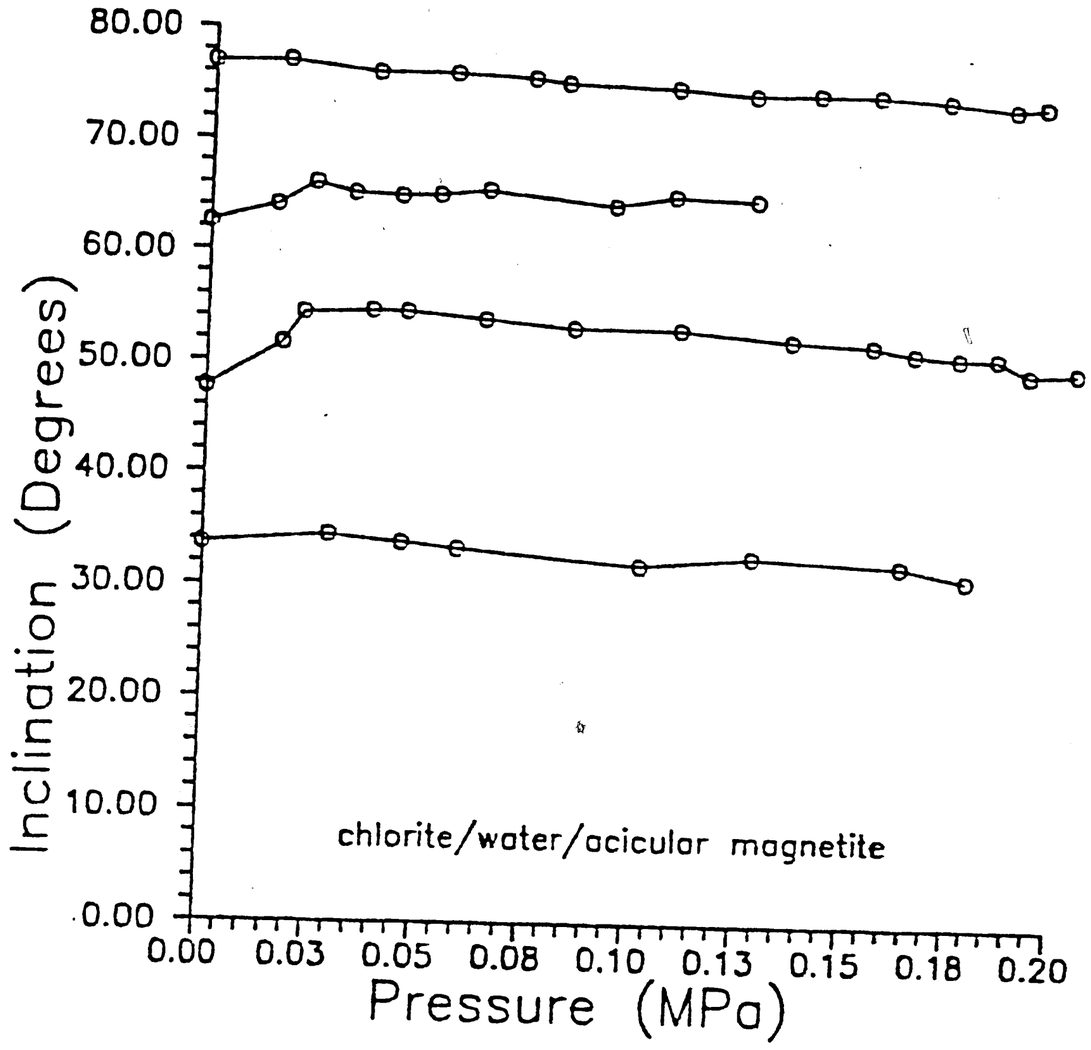

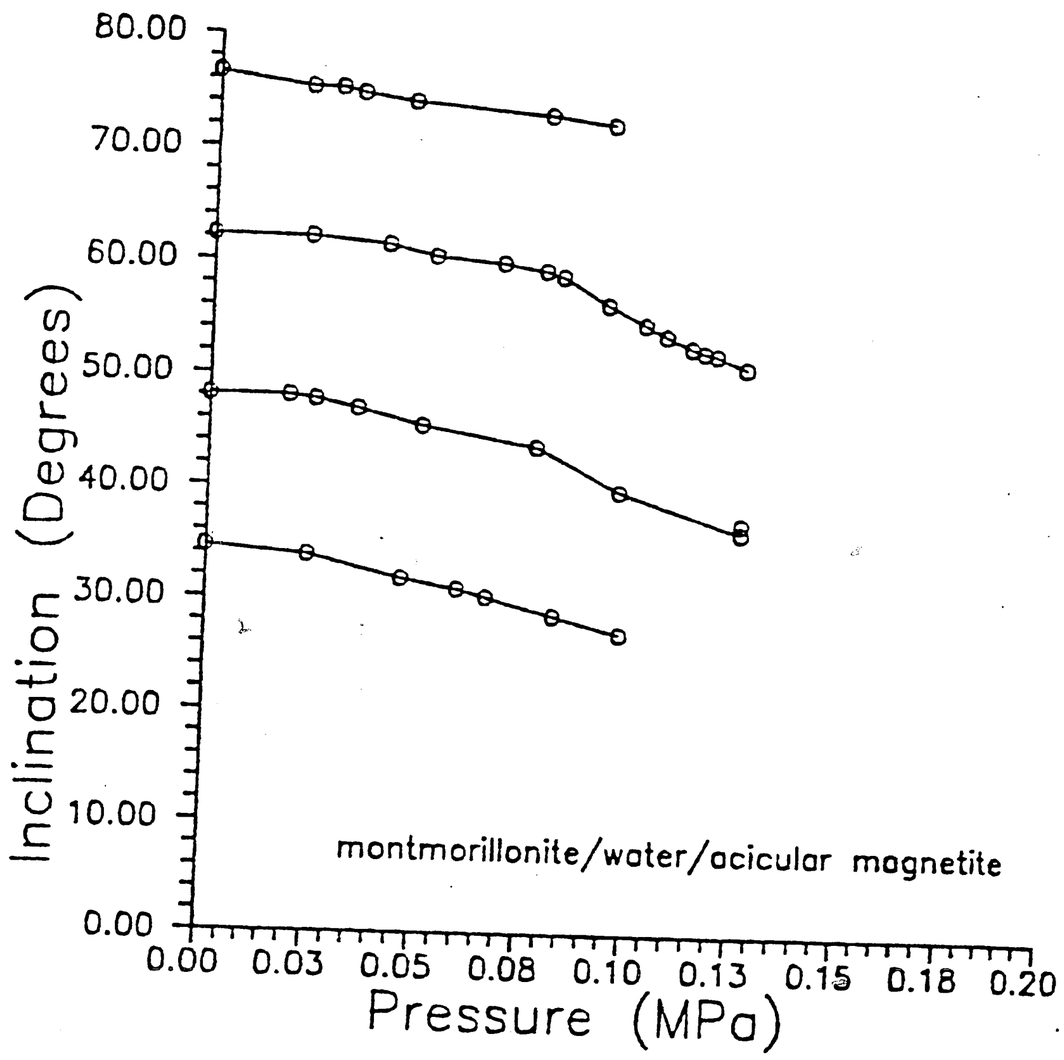

Figure 3. Plot of inclination versus pressure for chlorite and montmorillonite. Both curves are unlike the illite and kaolinite curves; montmorillonite changes slope only once, and chlorite is nearly flat.

the signal was already very weak, and making an interpretation as to whether shallowing or steepening had actually occurred was difficult. When viewed in orthogonal projection (Zijderveld, 1967), the trend can be very difficult to see. In other samples in which the signal did not remain stable, the inclination would tend to shallow and then steepen, or vice-versa, again making an interpretation of an overall steepening or shallowing difficult to determine.

In this group of samples, twelve were demagnetized. Of the twelve, the magnetization of four of the samples became slightly steeper, four became slightly shallower, three maintained the same direction, and one exhibited variable (shallower and steeper) behavior. The samples all had a fairly narrow coercivity range, with intensity beginning to fall off at about 40 mT (see figure 4). Chlorite was an exception; in these samples, the intensity began to fall off almost immediately (figure 5).

Representative orthogonal projection (Zijderveld, 1967) plots for these samples are shown in figure 6.

II. Acicular magnetite/saline water

The results for this set of experiments did not differ substantially from those in which distilled water was used as the fluid medium. Again, each clay exhibited inclination shallowing and volume decrease to different degrees. Chlorite exhibited the least shallowing (1.9-4.3^{o}) and the least volume decrease, and montmorillonite shallowed the most (9.8-14.4^{o}) and experienced the largest volume decrease. Figures 7-8 show the inclination versus pressure plots for these experiments. The curves for kaolinite,

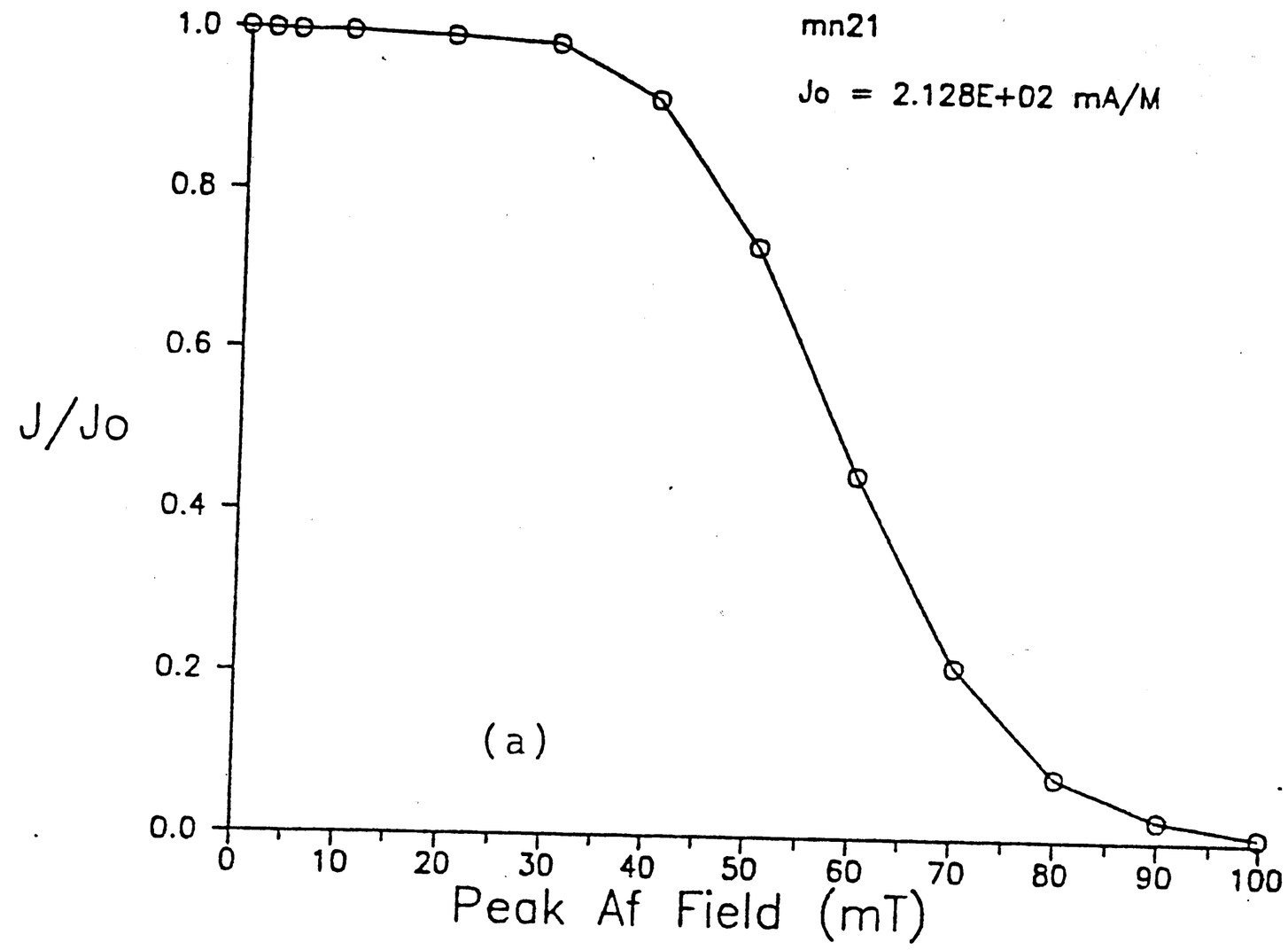

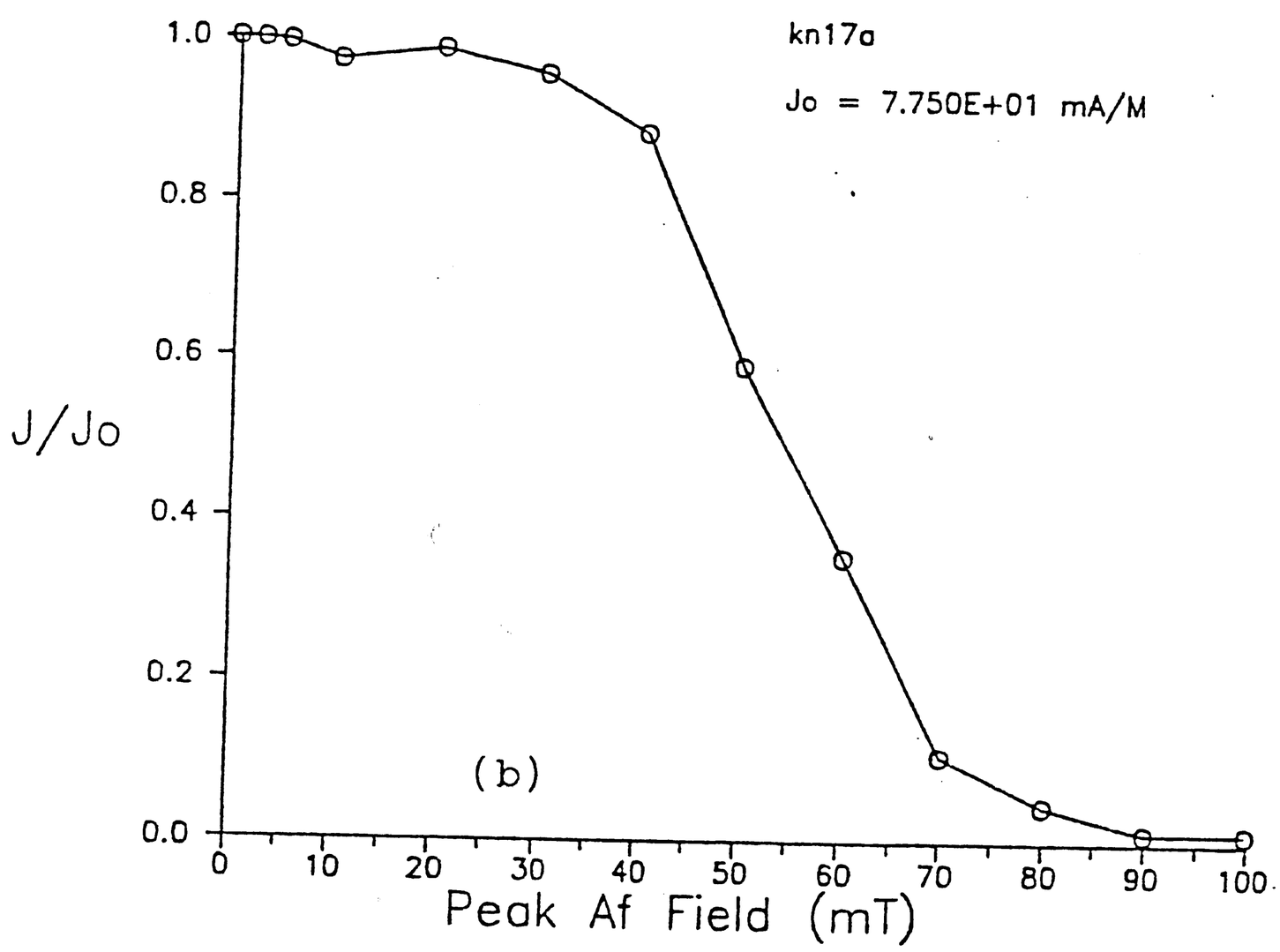

Figure 4: Plot of J/Jo versus peak af field for montmorillonite (a) and kaolinite (b) in distilled water using acicular magnetite.

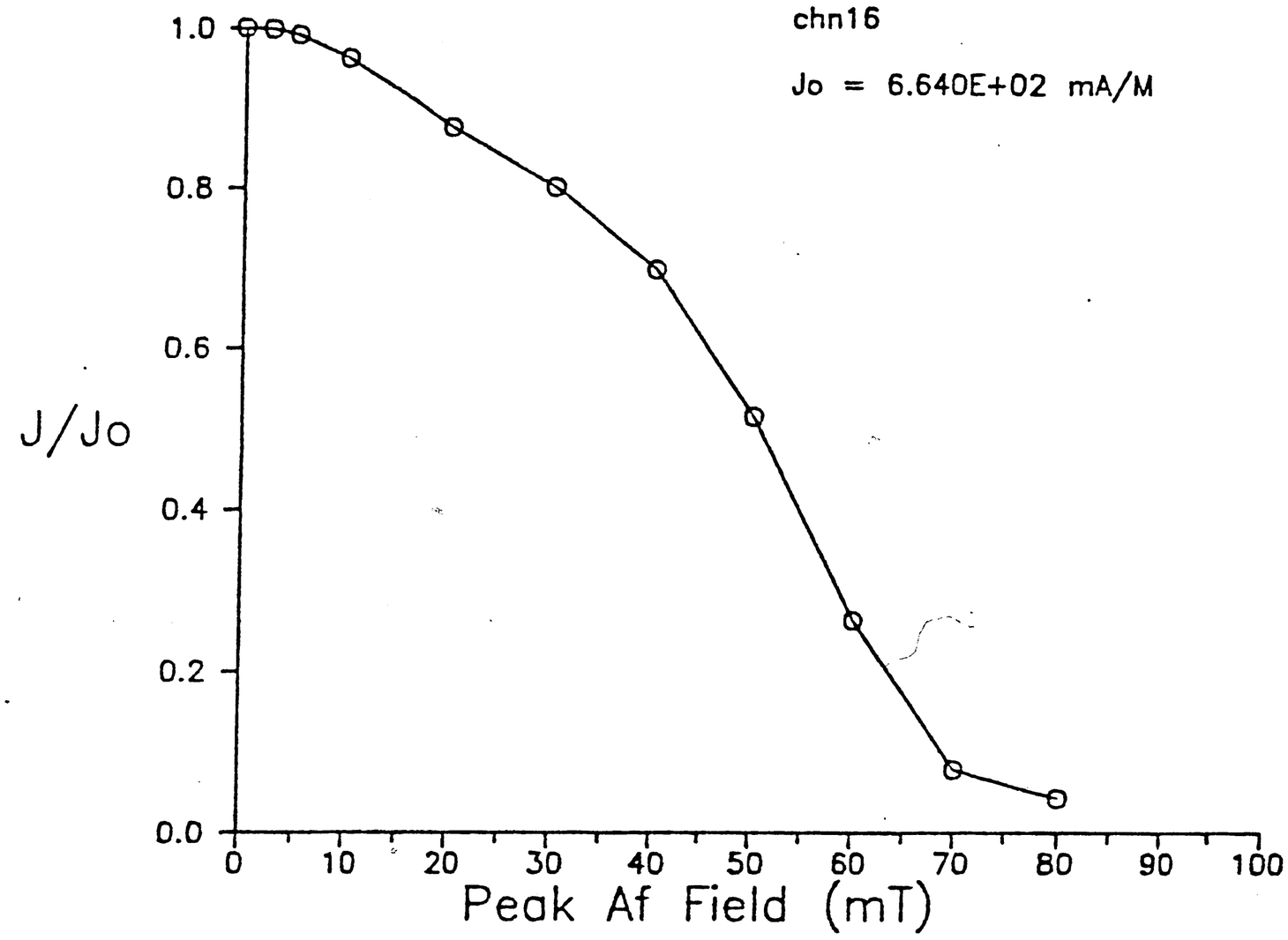

Figure 5: Plot of J/Jo versus peak af field for chlorite in distilled water using acicular magnetite.

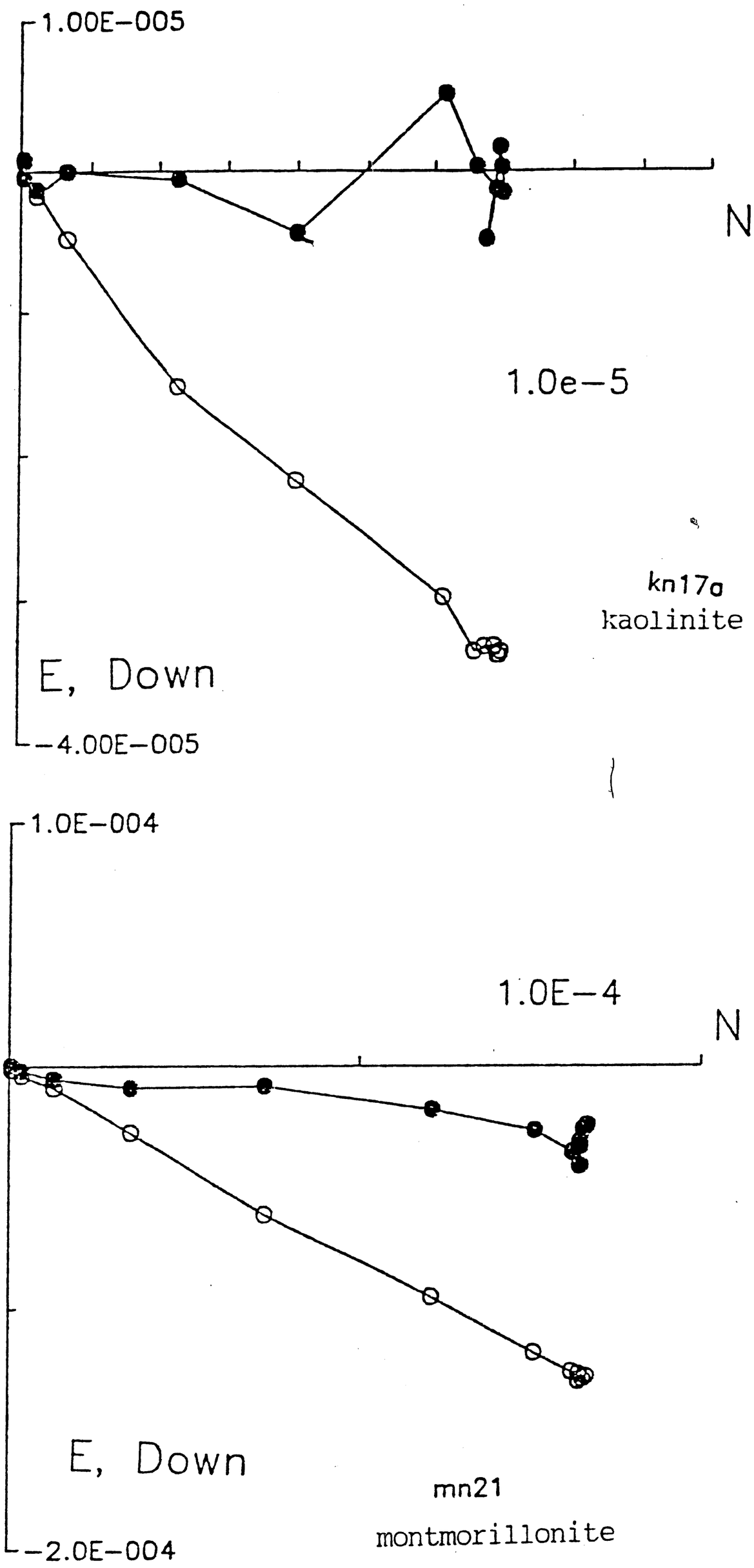

Figure 6. Representative Zijderveld plots for kaolinite and montmorillonite in distilled water. Montmorillonite shows slight shallowing during the last several steps of demagnetization, and kaolinite steepens slightly and then shallows in the final steps of demagnetization.

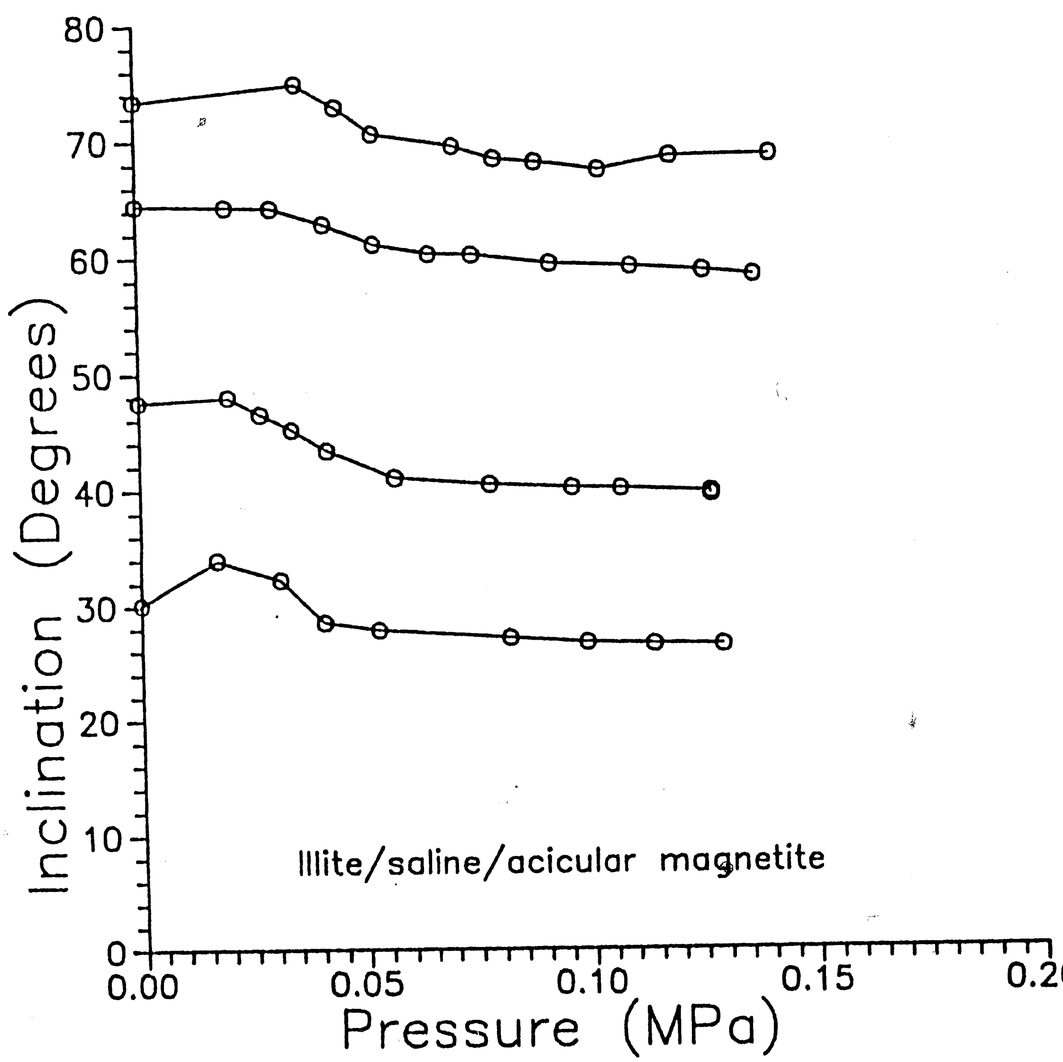

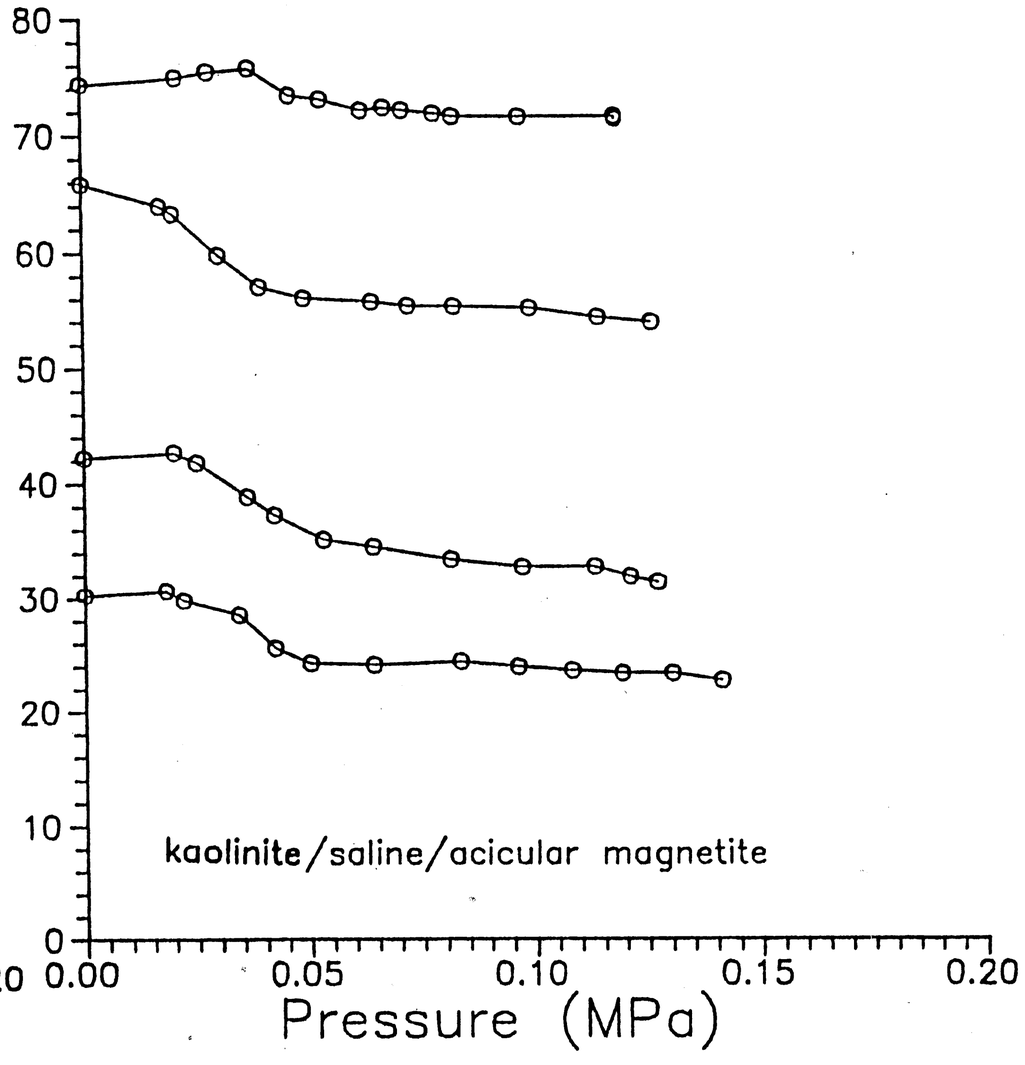

Figure 7. Plots of inclination versus pressure for illite and kaolinite in instant ocean, with acicular magnetite. These curves have a similar shape to the distilled water curves in figure 2.

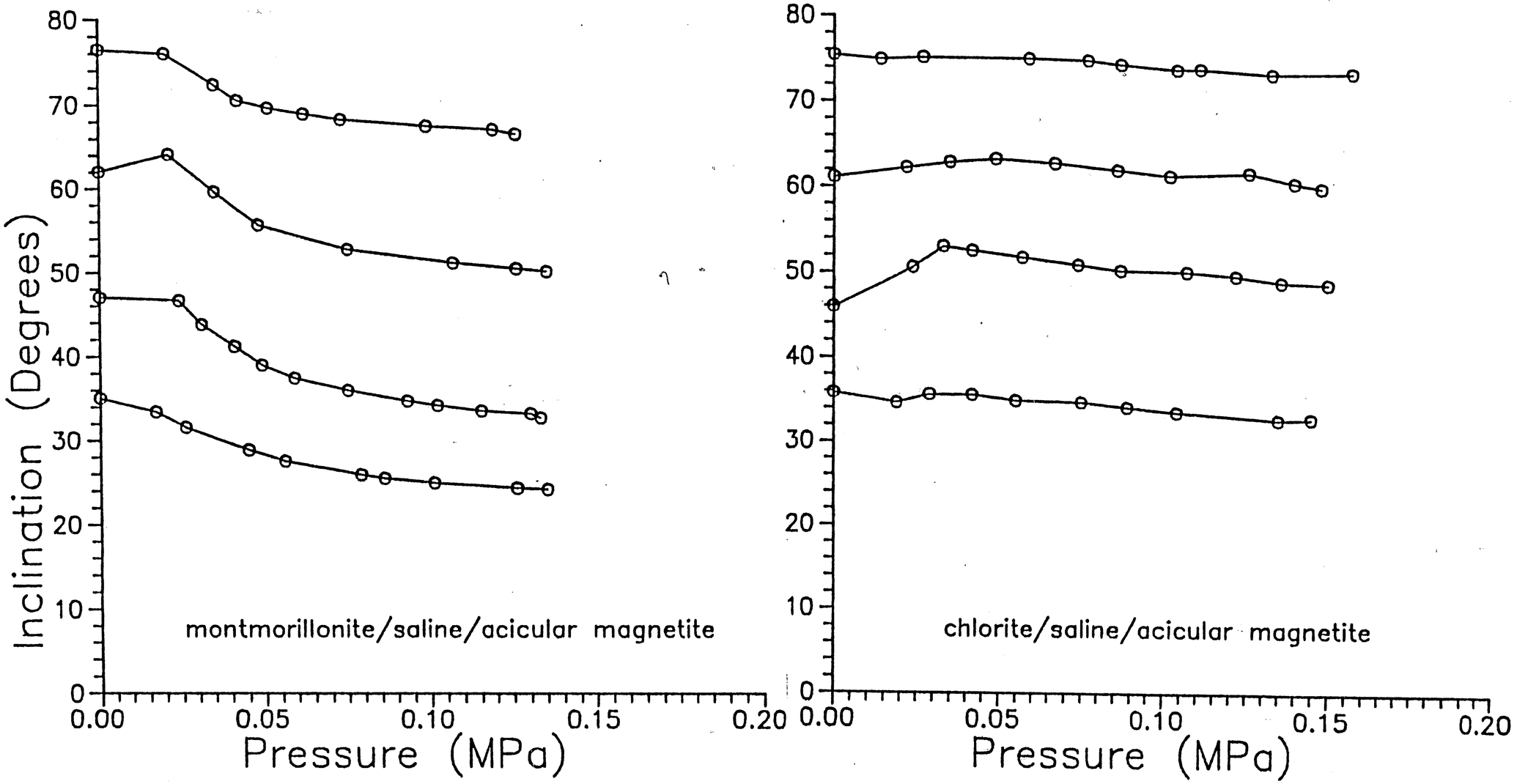

Figure 8. Plots of inclination versus pressure for montmorillonite and chlorite in instant ocean. The chlorite curve is very flat, but the montmorillonite curve resembles illite and kaolinite, acquiring the double-inflection.

illite and chlorite are similar in shape to the plots of the clays using distilled water (figures 2-3), but the montmorillonite curves do not have the same appearance as before. They have a shape more closely resembling the double-inflection curves of kaolinite and illite, with flatter sections at the high and low pressure ends, and a steeper drop at a pressure of about 0.05 MPa.

The Af demagnetization for these samples gave similar results to the distilled water samples. Most samples maintained a steady signal during demagnetization, and became shallower or steeper only during the last steps. In this set of experiments, only 10 samples were demagnetized; none of the chlorite samples were successfully demagnetized. When the chlorite samples were demagnetized, the resultant directions for subsequent steps fluctuated as much as 180°, with totally unrelated jumps. Of the samples which were demagnetized, four steepened slightly, two shallowed slightly, three maintained the same direction, and one exhibited both shallowing and steepening behavior. The samples all showed a narrow coercivity range, with intensity beginning to decrease at about 40 mT (figure 9). A representative orthogonal projection is shown in figure 10.

III. Equidimensional magnetite/distilled water

Overall, the behavior of slurries containing equidimensional magnetite does not differ substantially from those containing acicular magnetite. The illite slurry did not exhibit as large a volume decrease (40.5%) as the illite/acicular magnetite slurries (46.2-54.4%), and the inclination angle decrease is also slightly smaller (6.4° versus a range of 6.8-13.0° for the acicular magnetite

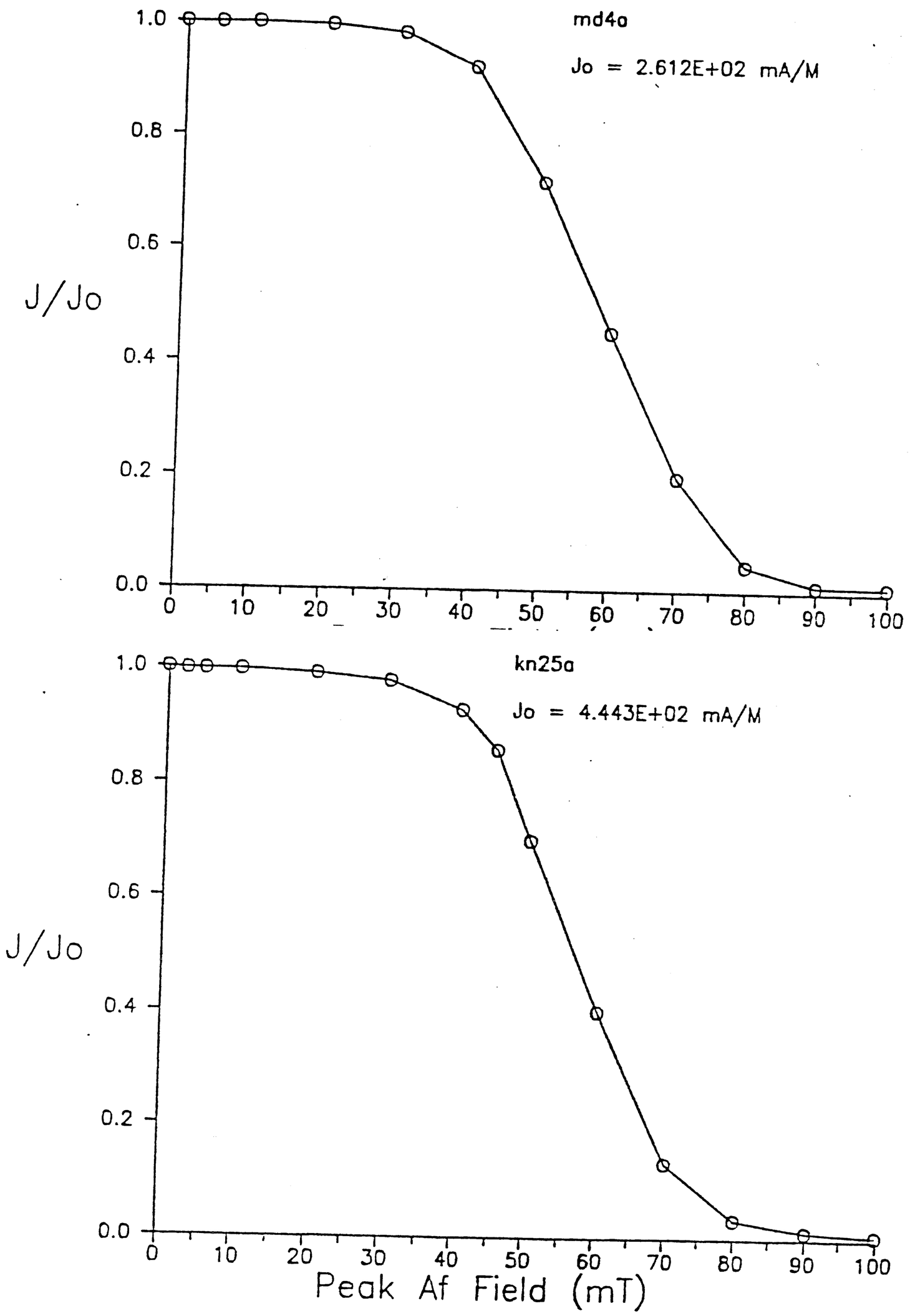

Figure 9. Representative J/Jo versus peak af field for kaolinite and montmorillonite in instant ocean with acicular magnetite.

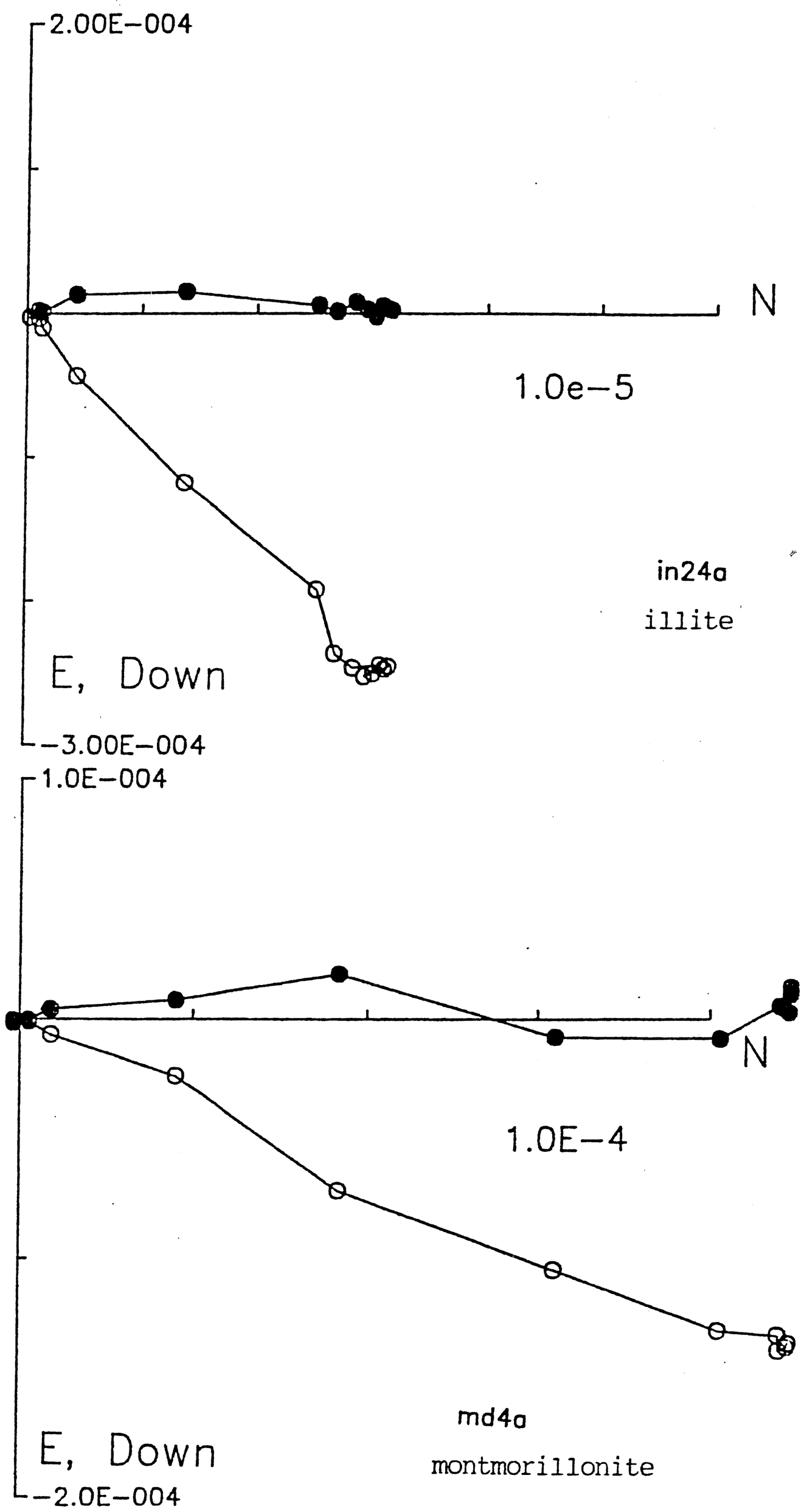

Figure 10. Representative Zijderveld plots for illite and montmorillonite in instant ocean. Both clays initially maintained the same direction during demagnetization, but illite steepened slightly in the final steps, and montmorillonite steepened, then shallowed in the final steps.

experiments), but this is not a substantial difference. The chlorite exhibited more shallowing (8.4°) than was typical for the acicular magnetite/water experiments (range = 1.2-4.7°). The plot of inclination versus pressure for these experiments is shown in figure 11a. These curves are similar in shape to the curves shown in figures 2-3 for acicular magnetite and water slurries. Kaolinite and illite exhibit curves containing a double inflection, and montmorillonite has a generally uniform downward slope. The chlorite curve slopes downward, reflecting a higher amount of shallowing in this compaction experiment, and exhibits behavior more like the illite and kaolinite, although the slope does not flatten out as much as for the other two clays.

The demagnetization results for equidimensional magnetite show a wider range of coercivity, with magnetic intensity beginning to decrease at about 20 mT (figure 12). Of the four samples in this set of experiments, only montmorillonite and illite were demagnetized; illite maintained the same direction during demagnetization, and montmorillonite became steeper.

IV. Equidimensional magnetite/saline water

Values for change in inclination shallowing and volume loss were similar to those obtained for the experiments using acicular magnetite and saline water. Kaolinite exhibited an unusually high (15.9°) amount of inclination shallowing, but several of the acicular magnetite/saline experiments for kaolinite also resulted in fairly high inclination shallowing (11.3-12.0°). The shapes of the inclination versus pressure curves for these experiments are similar

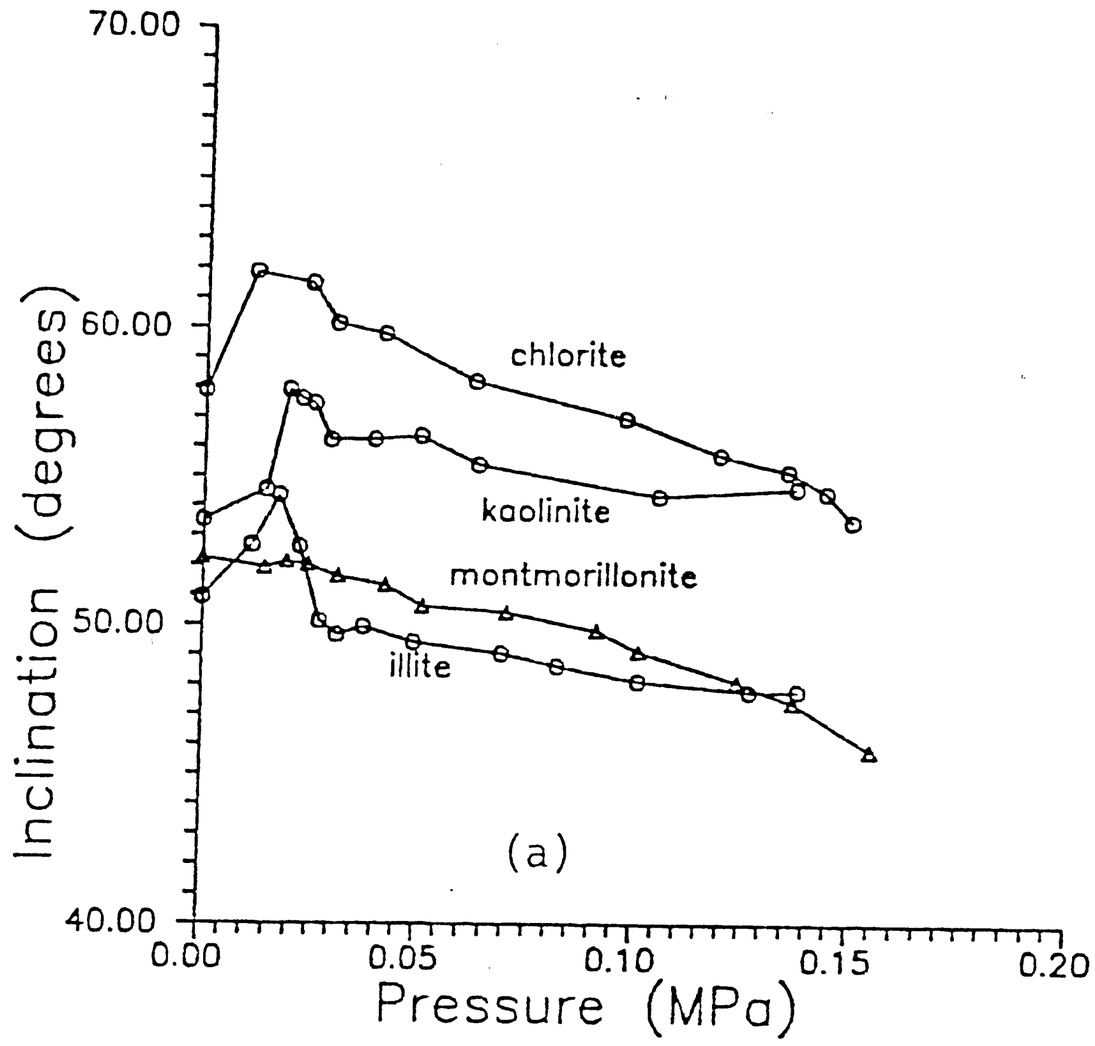

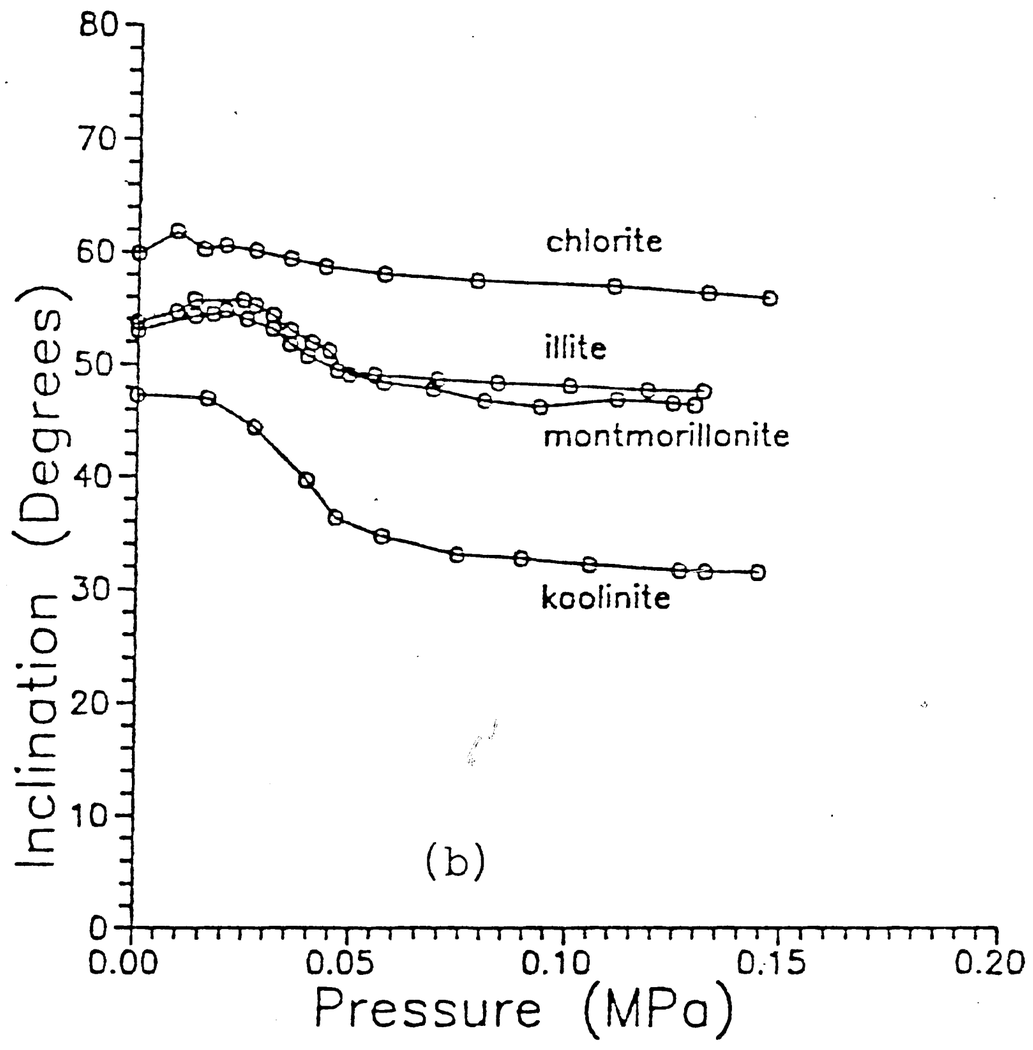

Figure 11. Plots of inclination versus pressure for clays with equidimensional magnetite in water (a) and instant ocean (b). Note the expanded Y-axis.

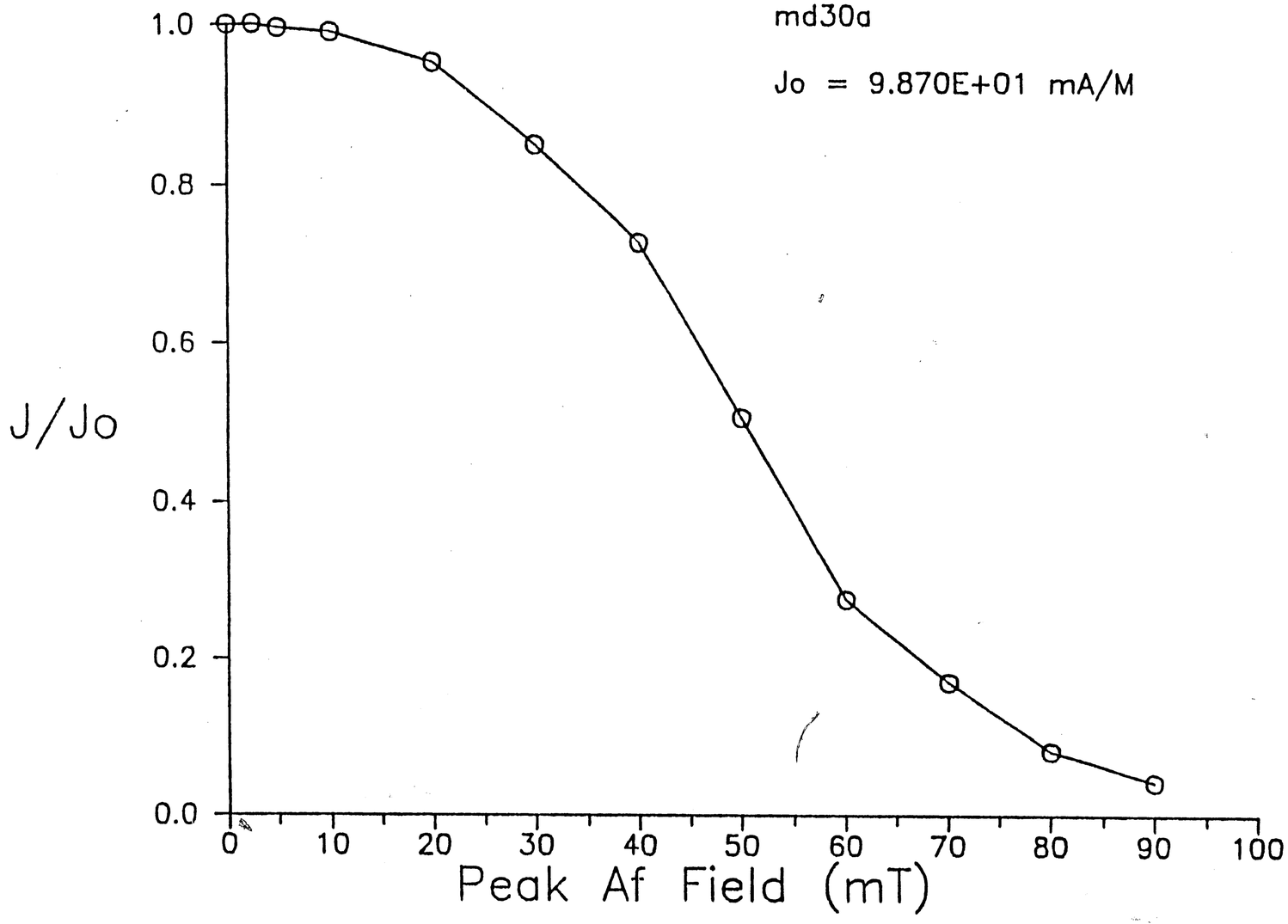

Figure 12. Representative intensity (J/Jo versus peak field) plot for montmorillonite in saline water with equi-dimensional magnetite. These clays generally show a wider range of coercivity than clays with acicular magnetite.

to those in figures 7-8 for acicular magnetite/saline experiments (figure 11b). Again, the montmorillonite curve has acquired the double-inflection shape more typical of illite and kaolinite, rather than having a uniform slope.

Demagnetization for these experiments showed a broad coercivity range, with intensity beginning to decrease at a lower field strength (about 20 mT). Three samples in this set were demagnetized; illite became steeper, montmorillonite maintained the same direction, and kaolinite had a variable response, first becoming steeper and then shallower. Representative intensity and orthogonal projection (Zidgerveld, 1967) plots are shown in figure 13.

V. Natural and Reconstructed Sediments

The two natural sediments exhibited inclination shallowing to different degrees. Sediment containing a higher proportion of clay shallowed more (5.1-12.4^{o}), and had a higher decrease in volume (mean = 55.8%) than the sediment containing more silt/sand. The latter shallowed between 3.3-9.5^{o}, and lost an average of 41.8% volume. The reconstructed sediment decreased in volume by an average of 40.0%, and in inclination angle by 5.1-6.0^{o}. The inclination versus pressure plots for this set of experiments are shown in figure 14. The plots all exhibit the characteristic double-inflection shape seen in most of the previous curves, with the steeper slope at about 0.05 MPa.

Demagnetization results for these samples showed either slight steepening (4 samples) or no change in direction (5 samples). One sample had mixed shallowing and steepening. Again, for the samples

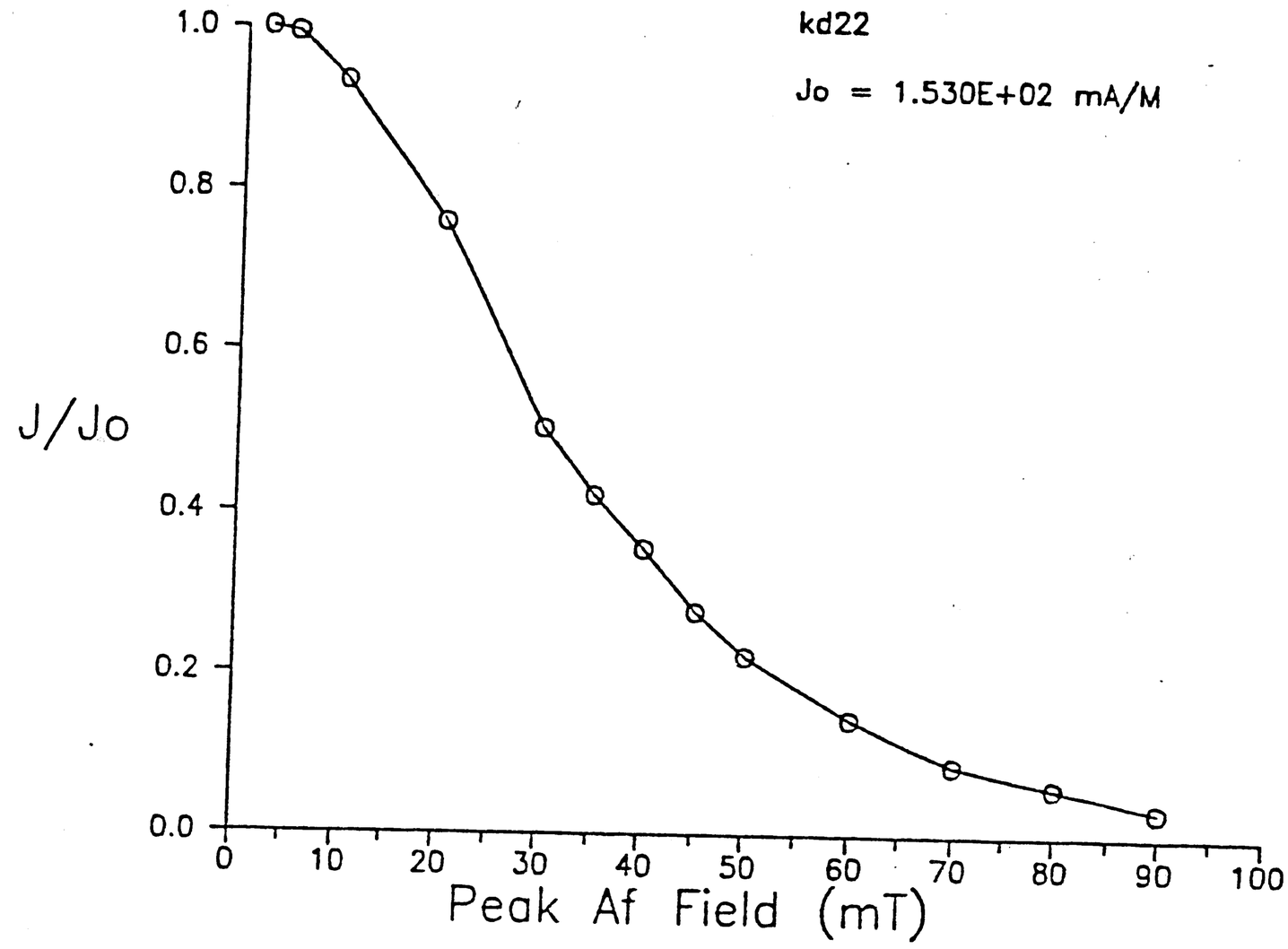

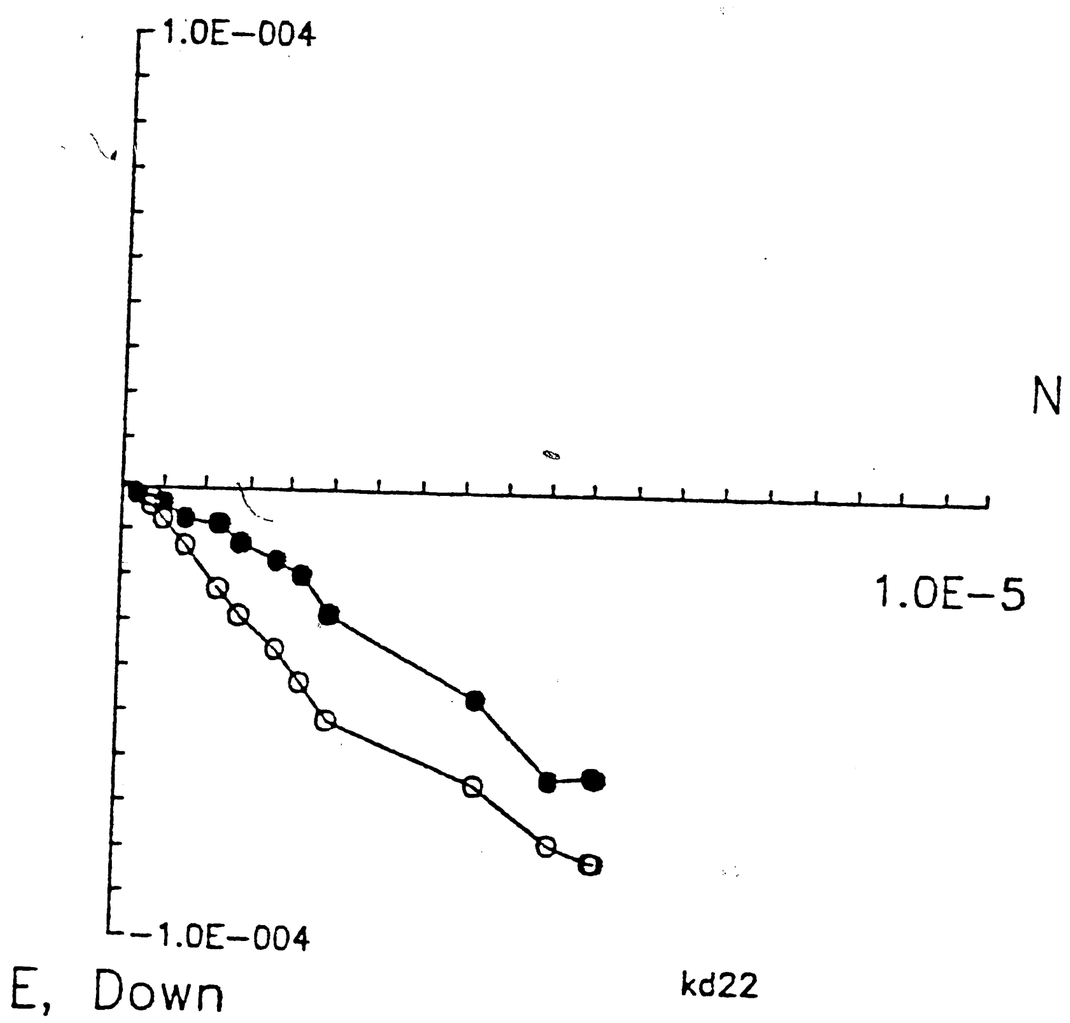

Figure 13. Representative Zijderveld and intensity plot for kaolinite in instant ocean with equi-dimensional magnetite. Kaolinite steepened during most steps, but then shallowed slightly during the last two steps.

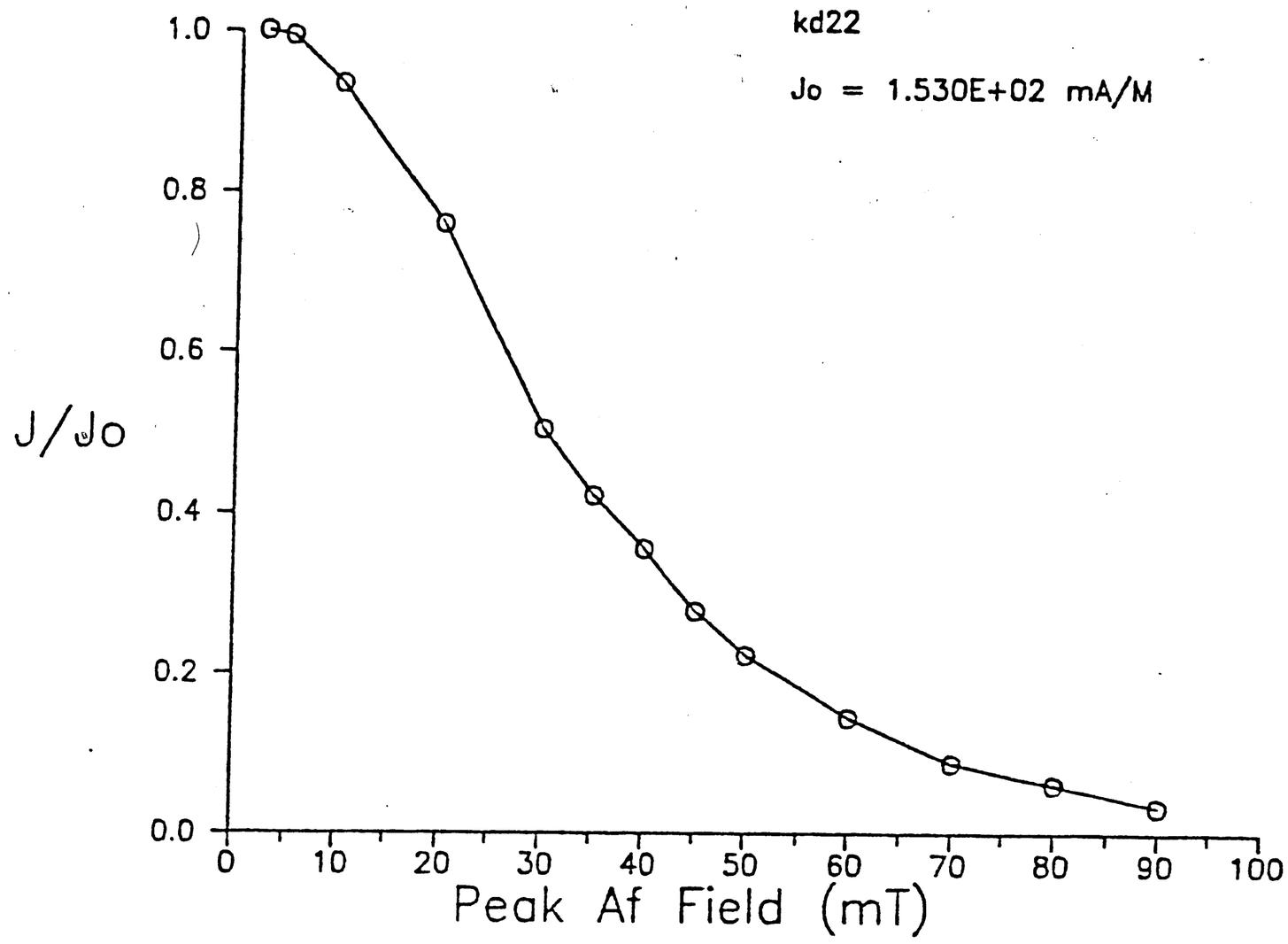

Figure 13. Representative Zijderveld and intensity plot for kaolinite in instant ocean with equi-dimensional magnetite. Kaolinite steepened during most steps, but then shallowed slightly during the last two steps.

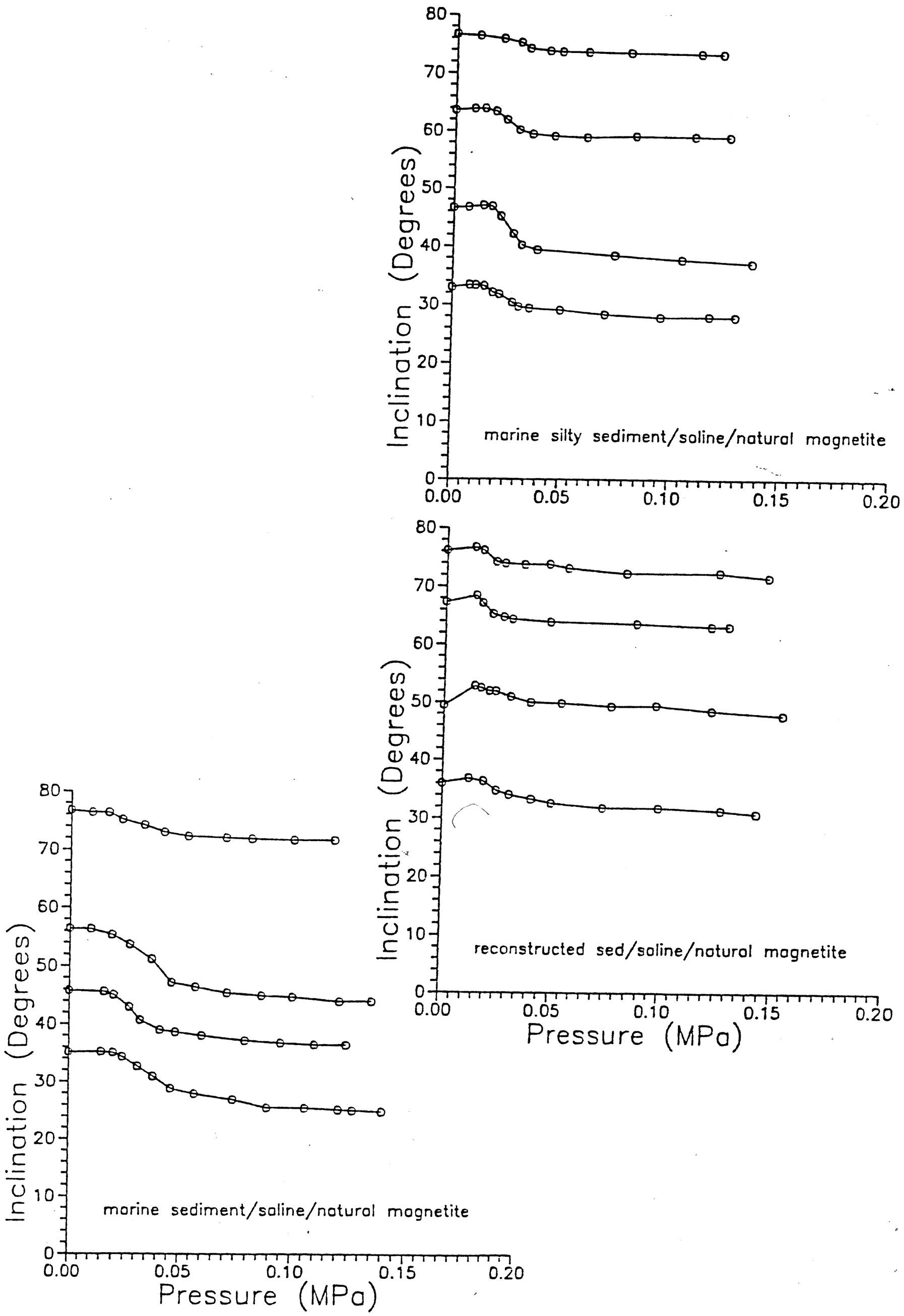

Figure 14. Inclination versus pressure for natural and reconstructed sediments. These all show the characteristic double-inflection curves.

which steepened, this behavior generally manifested itself in the last few steps of demagnetization. Representative Zidgerveld plots are shown in figures 15-16.

Demagnetization resulted in a different intensity curve since these samples all contained natural magnetite. The decrease in intensity began at very low field strengths (2.5-5.0 mT), and did not always proceed smoothly (see figures 17-18). For the natural sediments, 90% of the intensity was lost below 50 mT, and for the reconstructed sediment, 90% intensity was lost below 40 mT.

The magnetic grain size for these samples was estimated using the method of Banerjee, et. al. (1981). This method involves determining the slope of the line defined by the samples' ARM divided by their susceptibility values. The ARM values ranged from 4.8-13.9E-5 emu/g, and susceptibility values ranged from 2.9-8.2E-5 emu/Oe-g. These values resulted in a slope of approximately 1.75 Oe^{-1} for the natural sediment, and approximately 1.1 Oe^{-1} for the reconstructed sediment.

Water content, void ratio, and porosity values were determined for the two natural sediments. The clay-rich sediment slurry had a water content of 250%; using a bulk grain density of 2.66 g/cc (Hamilton, 1979), a void ratio of 6.7 and a porosity of 0.87 were calculated. After compaction,the water content was 80%, corresponding to a void ratio of 2.2 and a porosity of 0.69. The siltier sediment slurry began with a water content of 105%, and using a bulk density of 2.66 g/cc (Hamilton, 1979), a void ratio of 2.8 and a porosity of 0.73 was determined. After compaction, the water

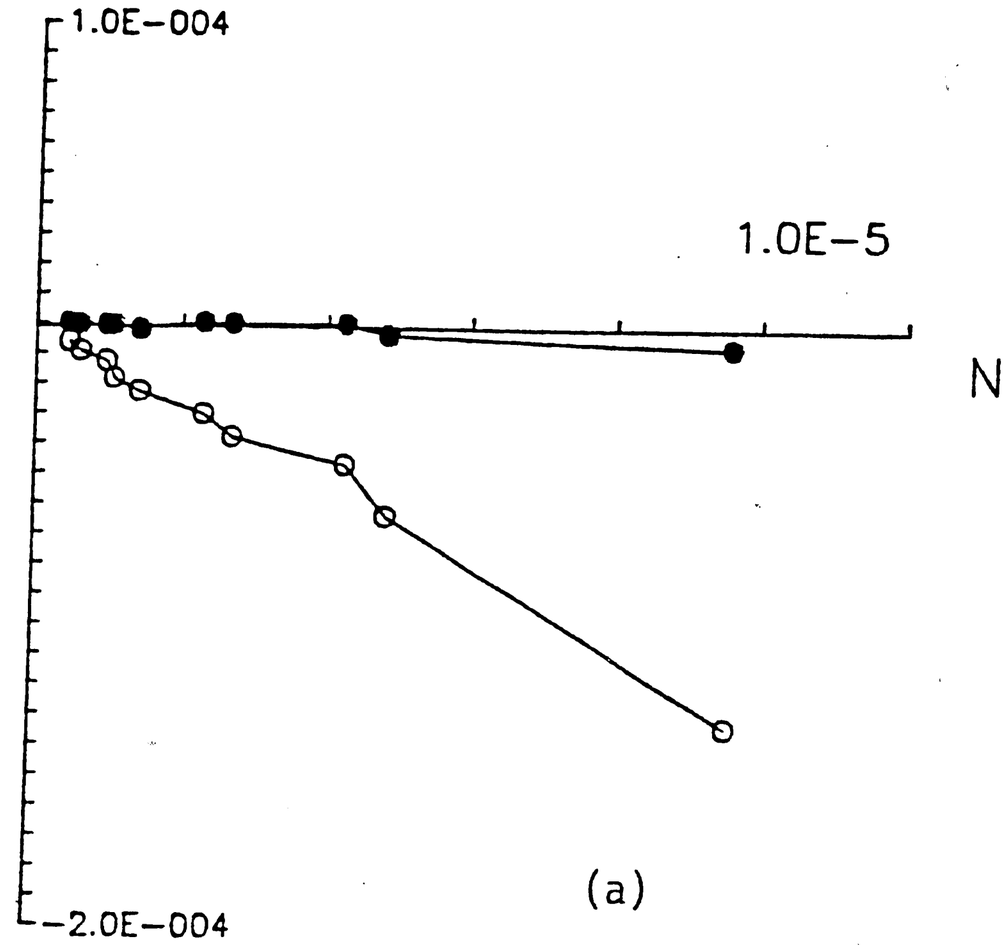

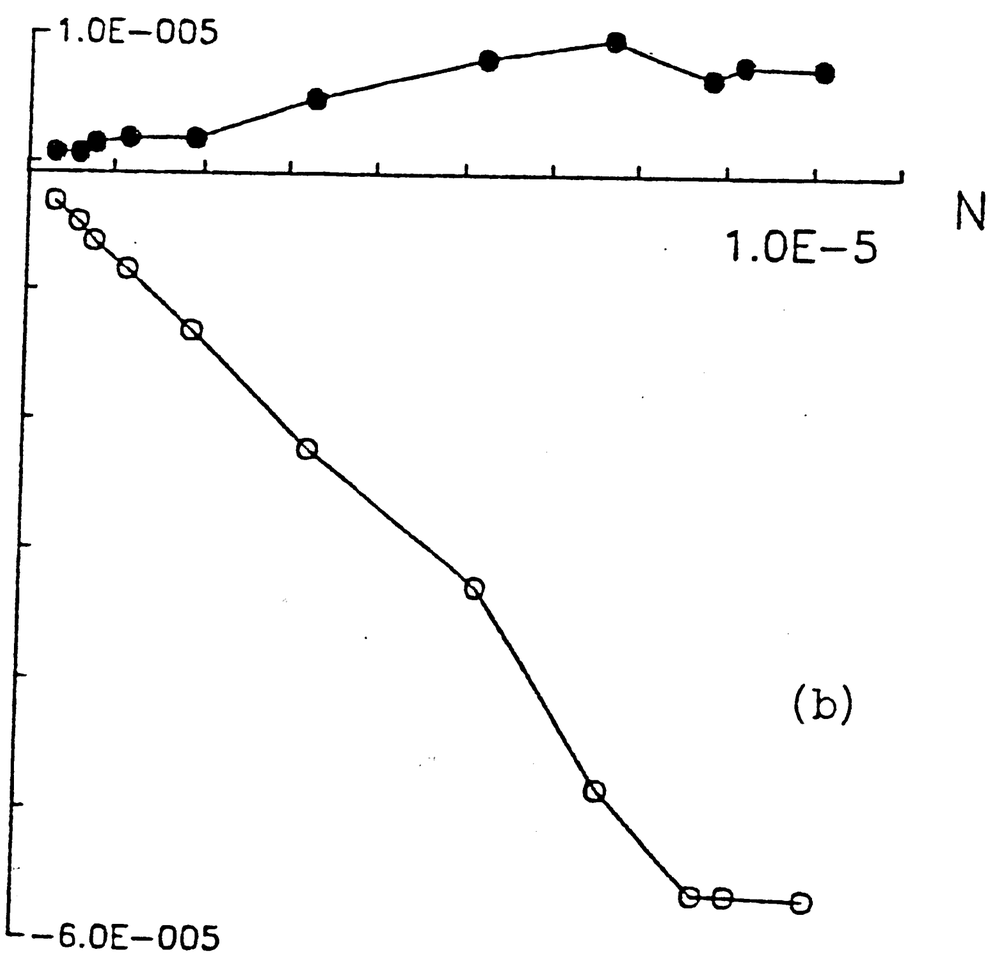

Figure 15. Representative Zijderveld plots for clay-rich natural sediment. Sample mmdl4b (a) steepened very slightly, and mmdllb (b) maintained its direction during demagnetization.

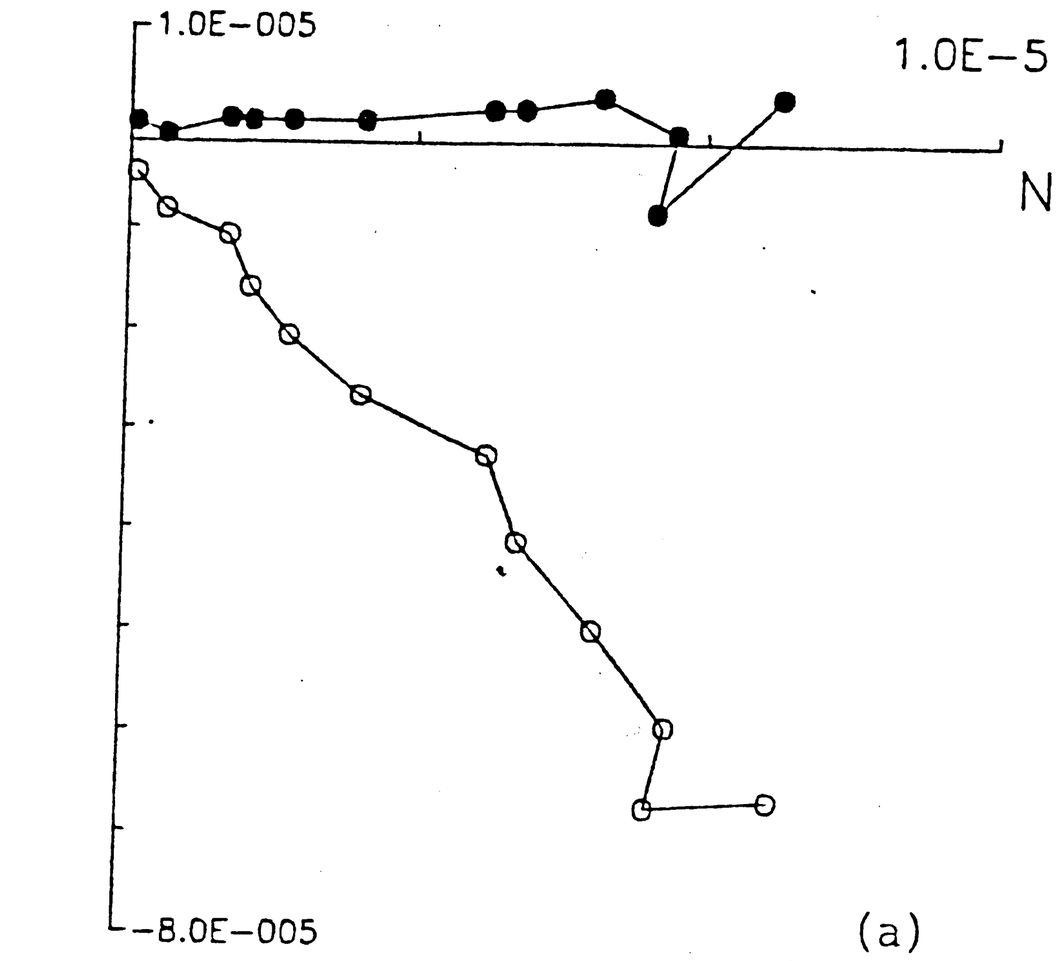

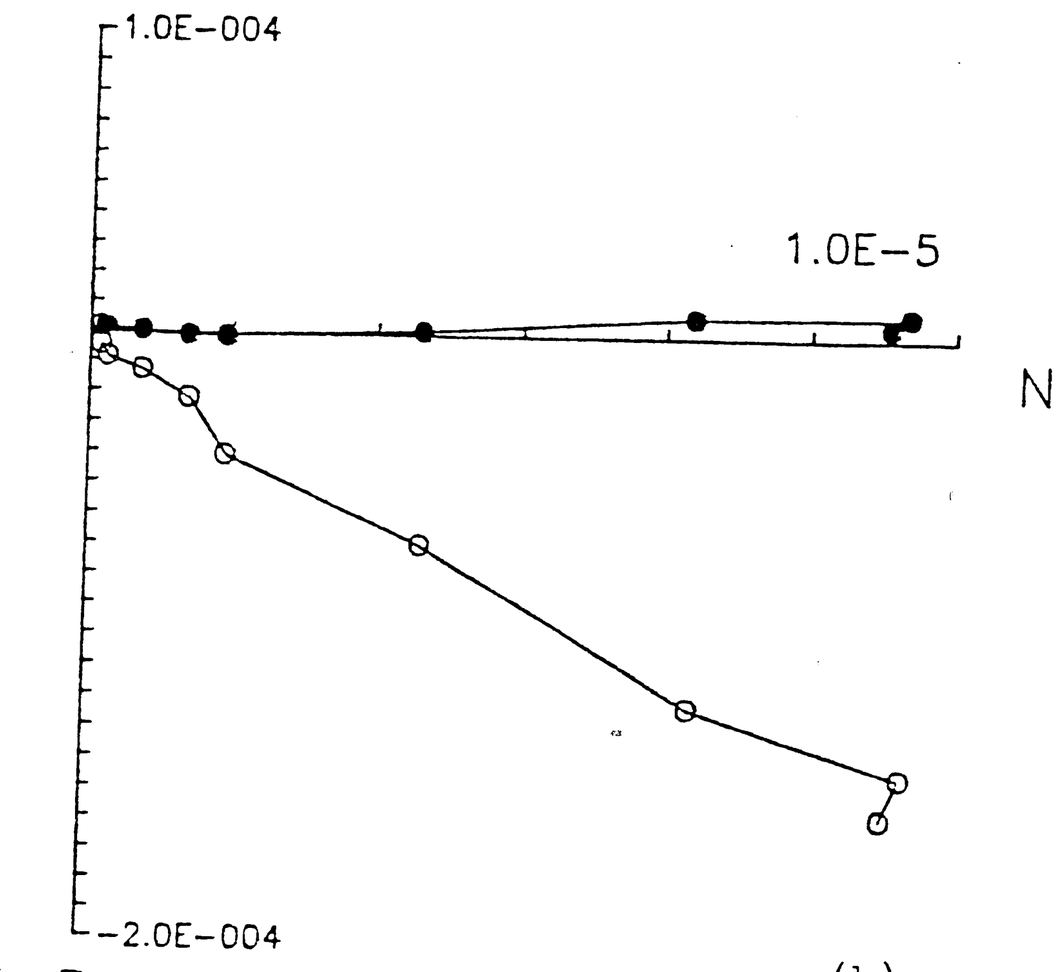

Figure 16. Representative Zijderveld plots for silty natural sediment and reconstructed sediment. The natural sediment (a) steepened slightly toward the end of demagnetization, and rej12 shallowed, then steepened.

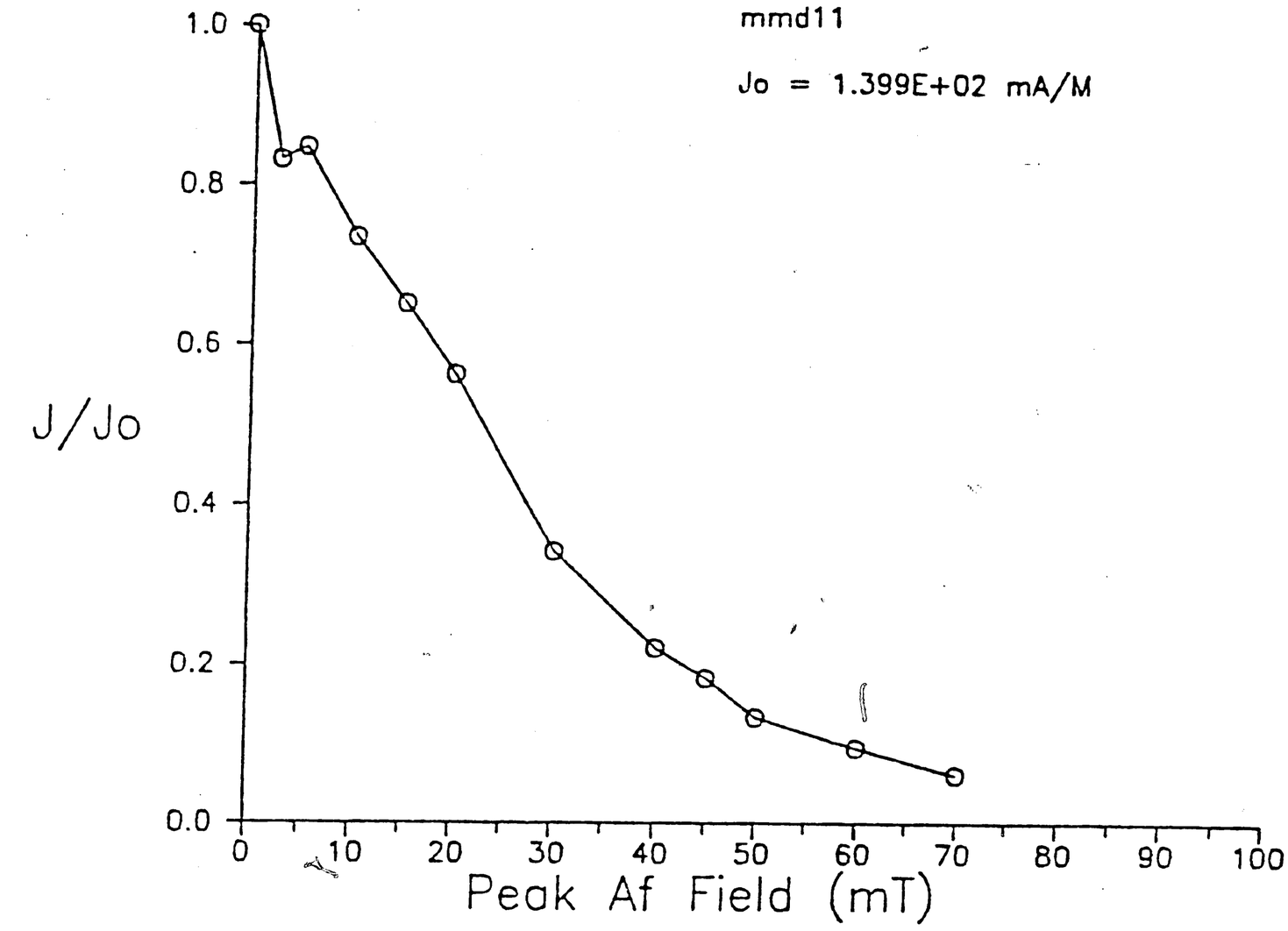

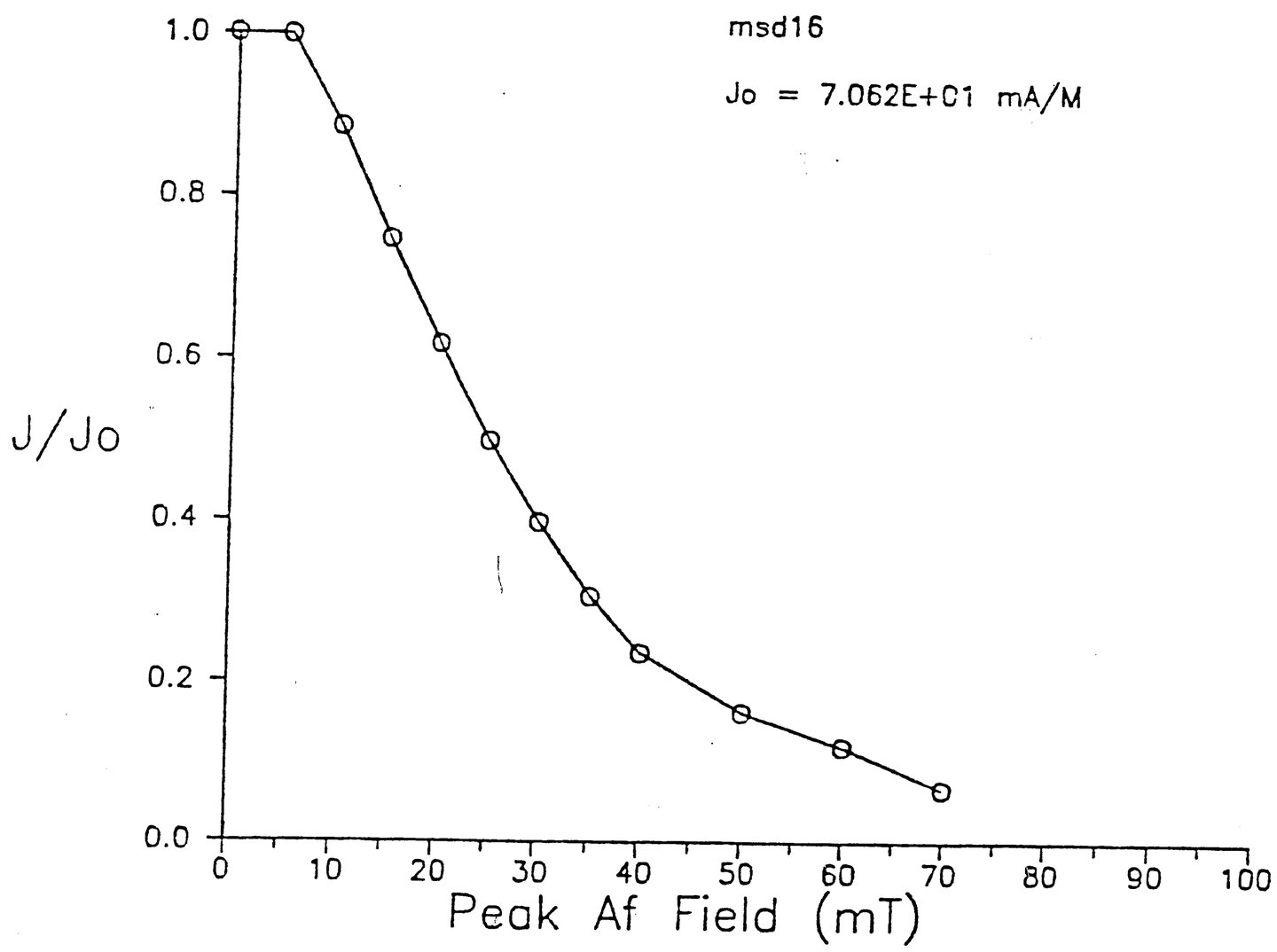

Figure 17: Plot of J/Jo versus peak af field for two natural marine sediments.

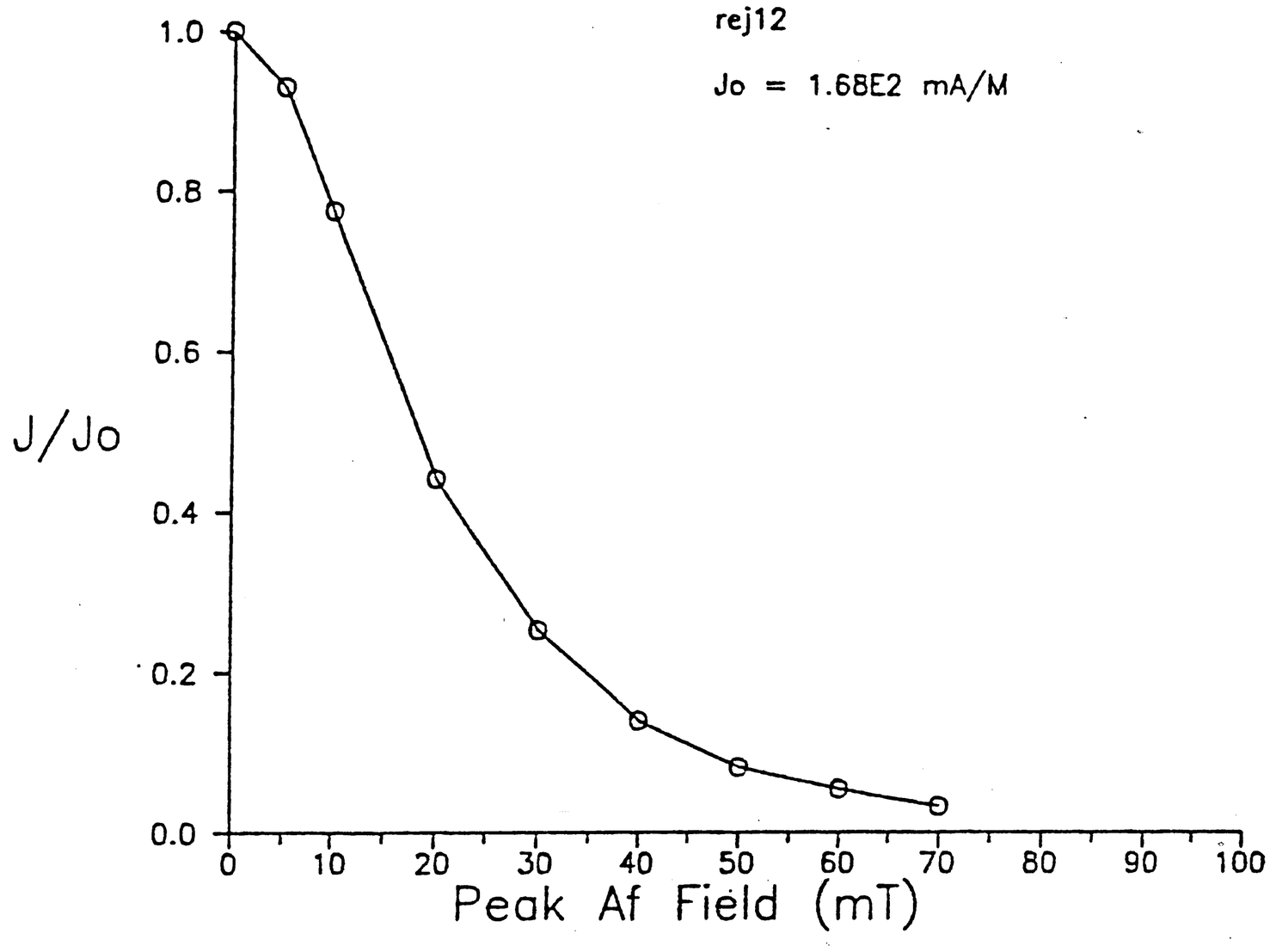

Figure 18: Plot of J/Jo versus peak af field for the reconstructed sediment using natural magnetite.

content was 40%, corresponding to a void ratio of 1.0 and a porosity of 0.5.

VI. Combination natural and equi-magnetite

The experiments in which natural and equi-dimensional magnetite were mixed showed no unusual results with respect to volume or inclination change. These values were comparable to the results for the same clays containing either acicular or equidimensional magnetite.

The demagnetization of these samples resulted in three maintaining their original inclination, and one becoming slightly steeper.

The combination of magnetite types did not affect the shape of the intensity curve drastically; intensity began to decrease immediately for all samples, although two of them (illite and kaolinite) lost intensity more rapidly, with 90% intensity lost below 40 mT. The other two (montmorillonite and kaolinite with NaOH added) exhibited a broader coercivity range, losing 90% intensity at about 70 mT (figure 19).

Effect of pH

The pH values for the clay slurries and natural and reconstructed sediments ranged from 4.1-9.5, and are listed in table 2. Chlorite and montmorillonite slurries had pH values above the zero point of charge (ZPC) of magnetite, kaolinite slurries were below the ZPC, and illite was very close to the ZPC. There was no correlation between the pH of the slurries and the amount of inclination shallowing. Chlorite and montmorillonite slurries, on

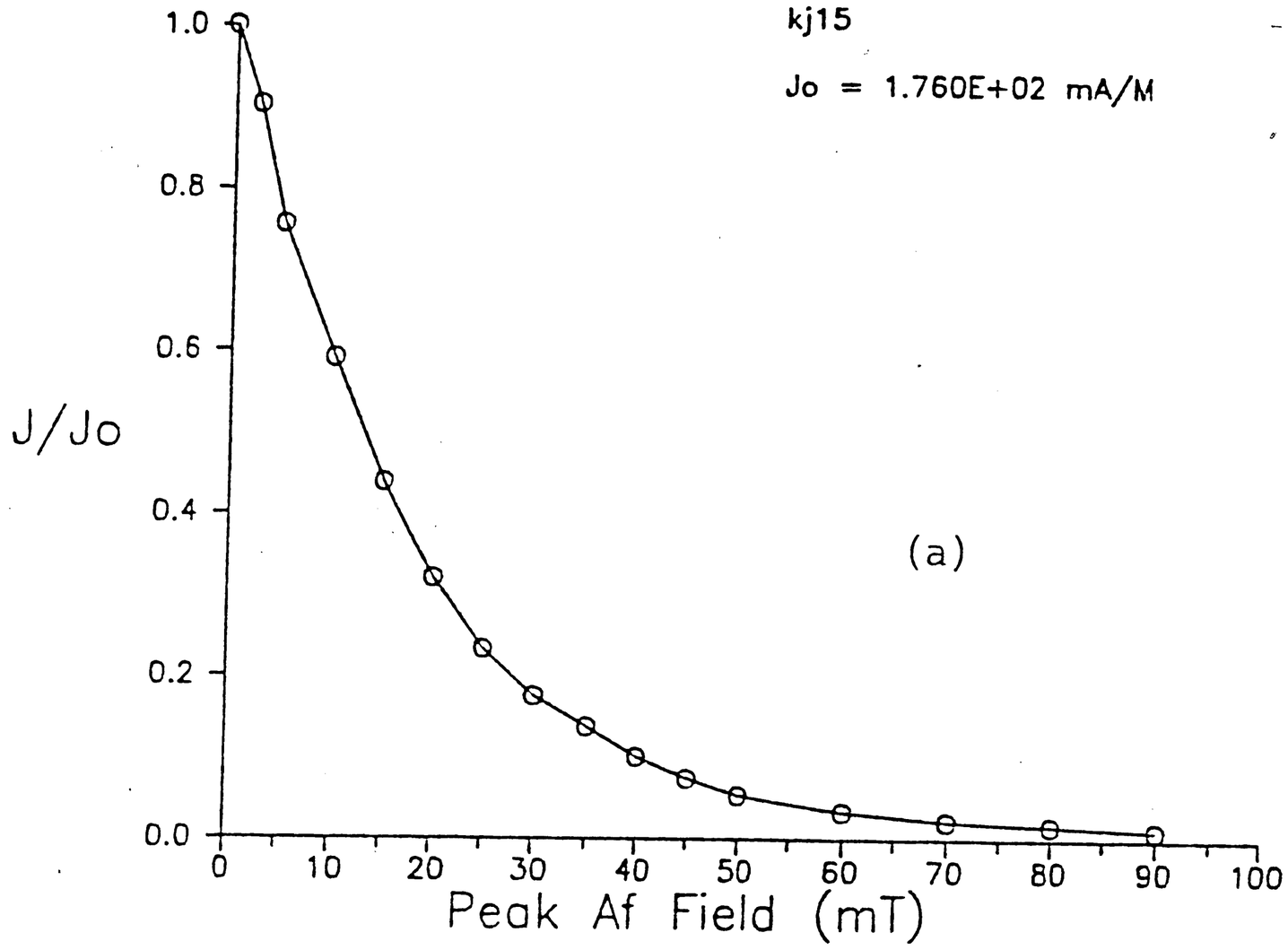

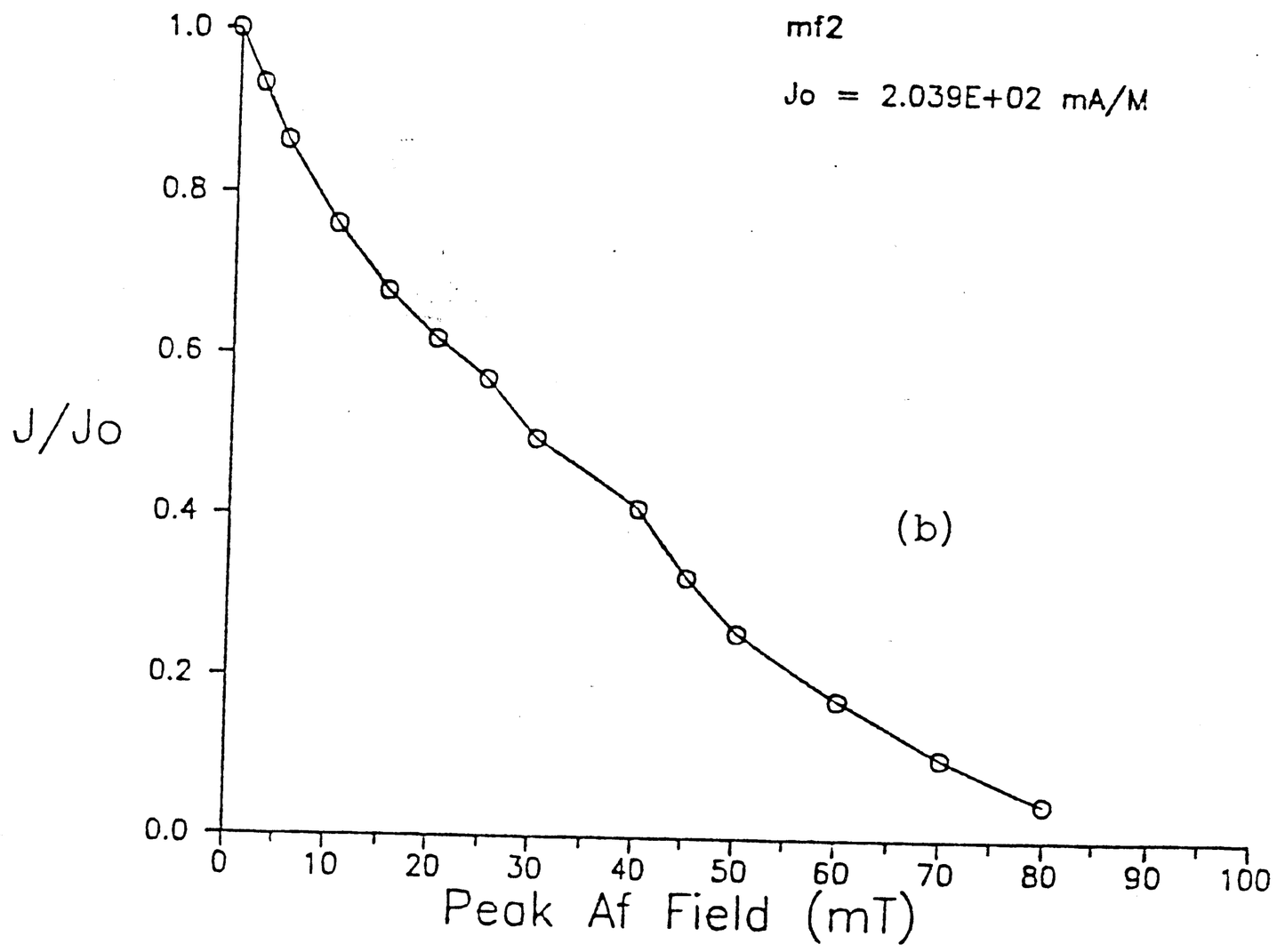

Figure 19. Intensity diagrams for clays containing a combination of natural and equidimensional magnetite. The kaolinite curve (a) is shaped like the intensity curves for clays containing all natural magnetite. The montmorillonite curve (b) has the appearance of a combination of natural and equi-dimensional intensity curves.

the average, showed the least and most amounts of shallowing, respectively, while kaolinite and illite tended to fall somewhere in between.

In the one kaolinite slurry in which the pH was forced to an abnormally high value (9.5) by the addition of NaOH, both the amount of inclination shallowing (4.2^{o}) and the volume loss (47.3%) were significantly smaller than similar values for other kaolinite slurries compacted in fields between 45^{o} and 60^{o}.

Inclination versus change in volume

Inclination versus volume change was plotted for each experiment in this study (figures 20-21). Most of the curves exhibited a similar pattern: an initial volume range in which the curve is either almost horizontal, or steepens slightly, and then, as the volume decrease becomes larger, there is a more rapid decrease in inclination angle. This pattern is not universally seen in all of the compaction experiments, but 48 out of 54 of the samples show this type of behavior. Chlorite samples were the ones most likely to show an initial steepening trend. Seven out of ten chlorite samples exhibited steepening during initial volume change steps.

The compaction experiment in which the vertical field was cancelled using a Helmholtz coil resulted in less steepening. With the vertical field cancelled, less than one degree of steepening occurred. An identical sample compacted in the steep field steepened 3.5 degrees.

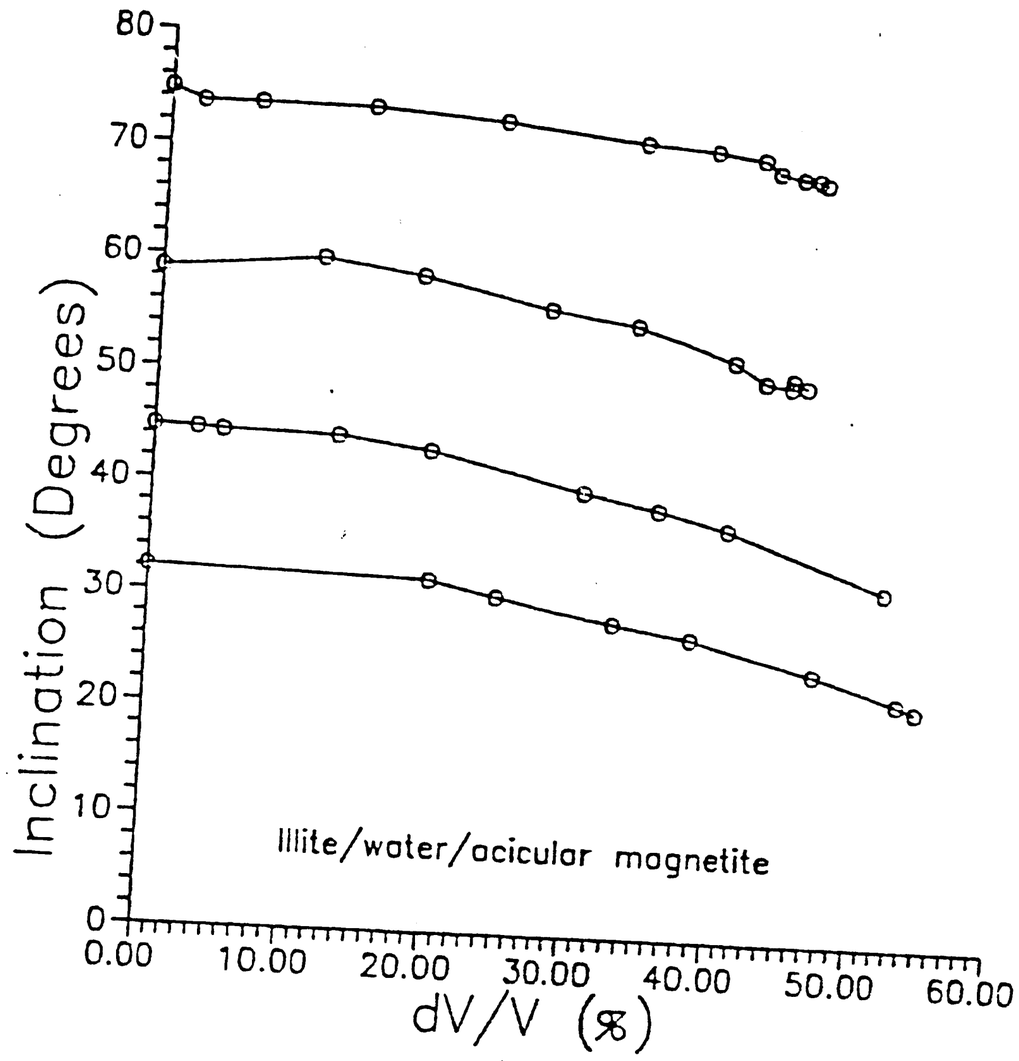

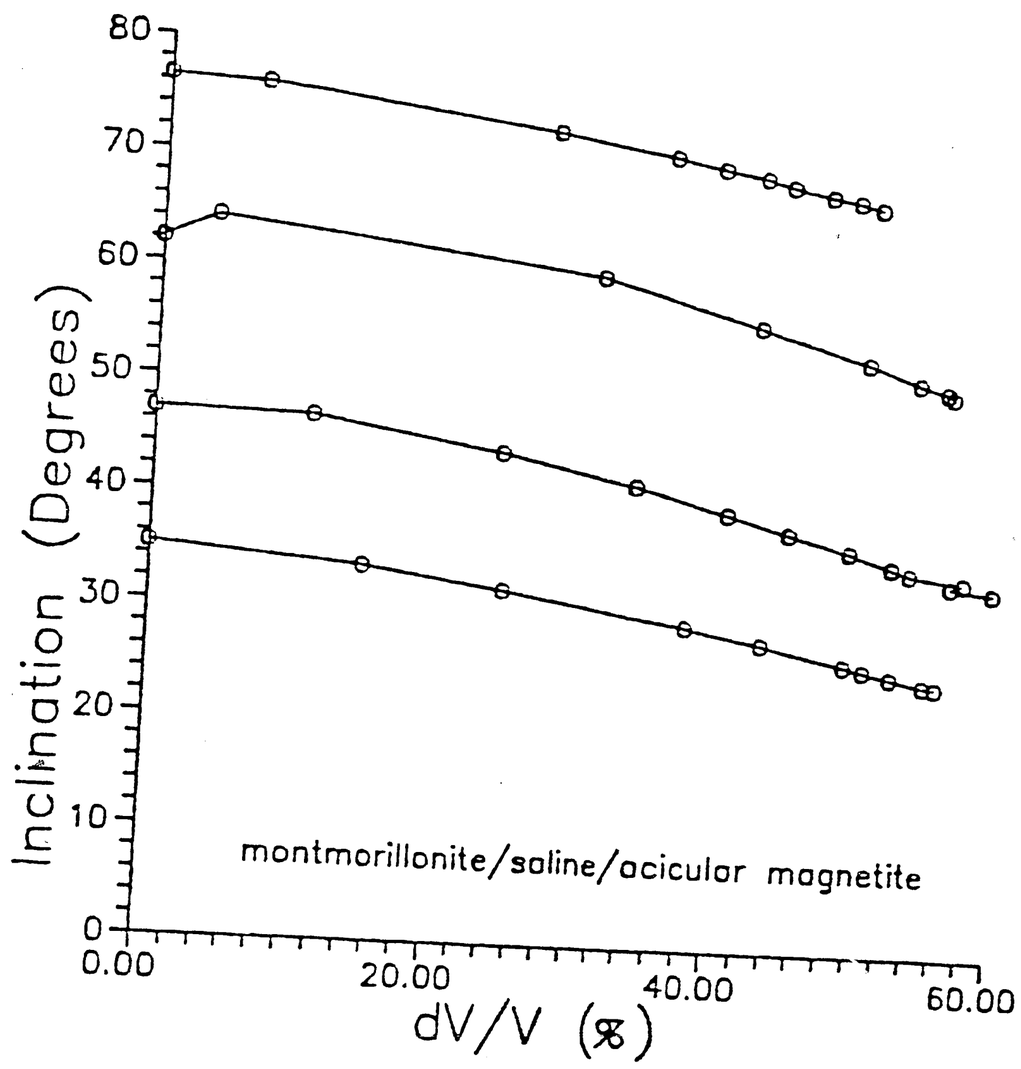

Figure 20. Inclination versus compaction (dV/V) curves for illite and montmorillonite. The decrease in inclination angle is more rapid at higher compaction for most curves.

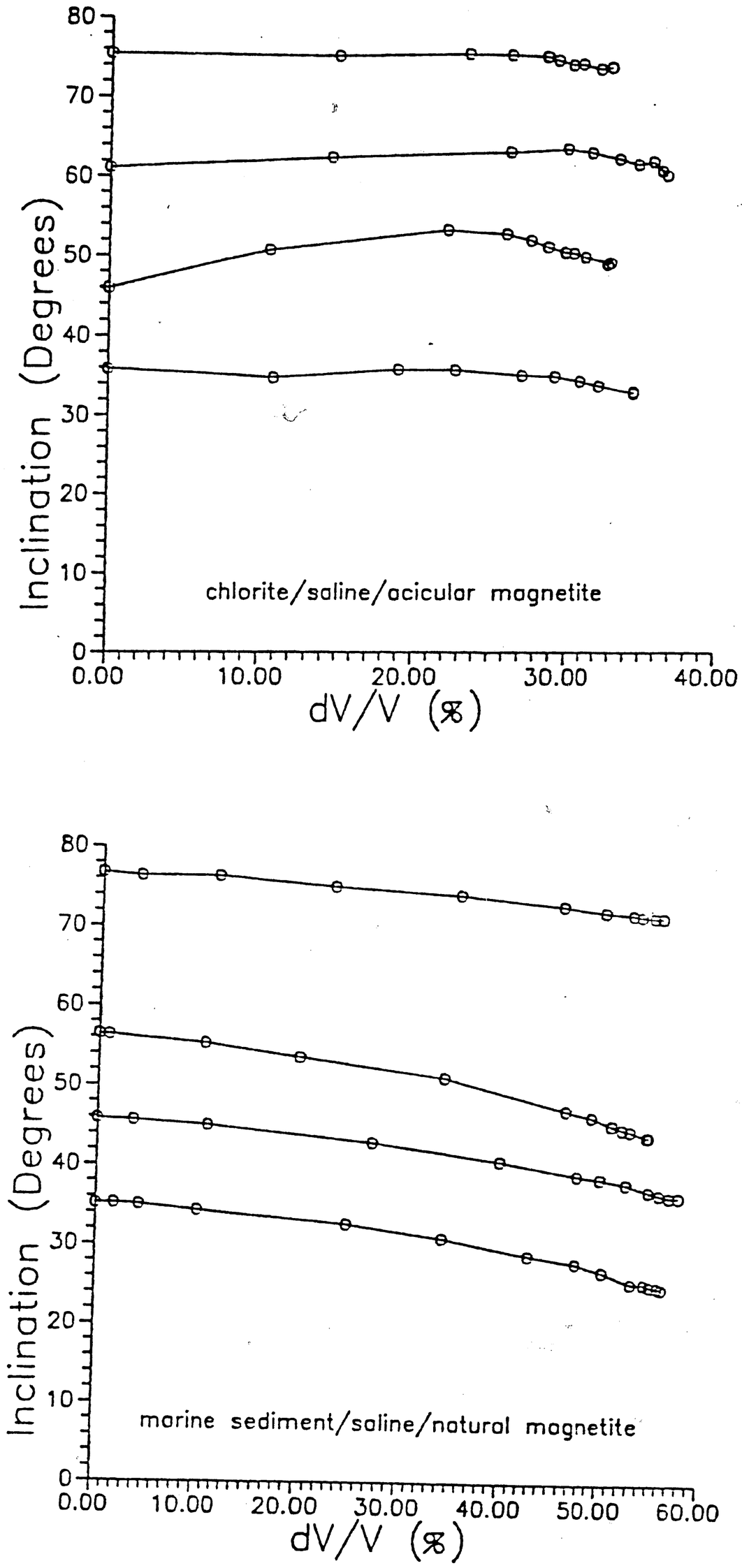

Figure 21. Inclination versus compaction (dV/V) curves for chlorite and a natural marine sediment. The decrease in inclination angle is more rapid at higher compaction for most curves.

Change in inclination versus initial inclination angle

Although a decrease in inclination angle was observed for each sample, there were unequal decreases depending on the original inclination angle of each sample (figure 22). In general, larger decreases in inclination occurred at the 45° and 60° field inclinations, and smaller decreases in the samples compacted in 30° and 75° fields, although this trend is most striking in the saline compaction experiments.

Magnetic Intensity

Magnetic intensity almost invariably decreased during compaction, and the intensity tended to vary with field inclination angle (figures 23-24). The amount of intensity loss was noticibly less for chlorite slurries. In most cases, the highest loss in intensity was observed at the highest field inclination angle (75°), and the intensity loss decreased continuously for the 60°, 45°, and 30° inclination angles. Intensity loss was observed during compaction at most compaction steps, although this was not always the case. Occasionally, increases in intensity were observed during the initial stages of compaction.

Error Analysis

Experiments to estimate measurement error and sample positioning error were performed with the cryogenic magnetometer. For the measurement error estimate, two samples, ones with a high water content and one partially consolidated with a low water content, were left in the magnetometer sample holder and remeasured ten consecutive times. The precision parameter, K_{meas}, value

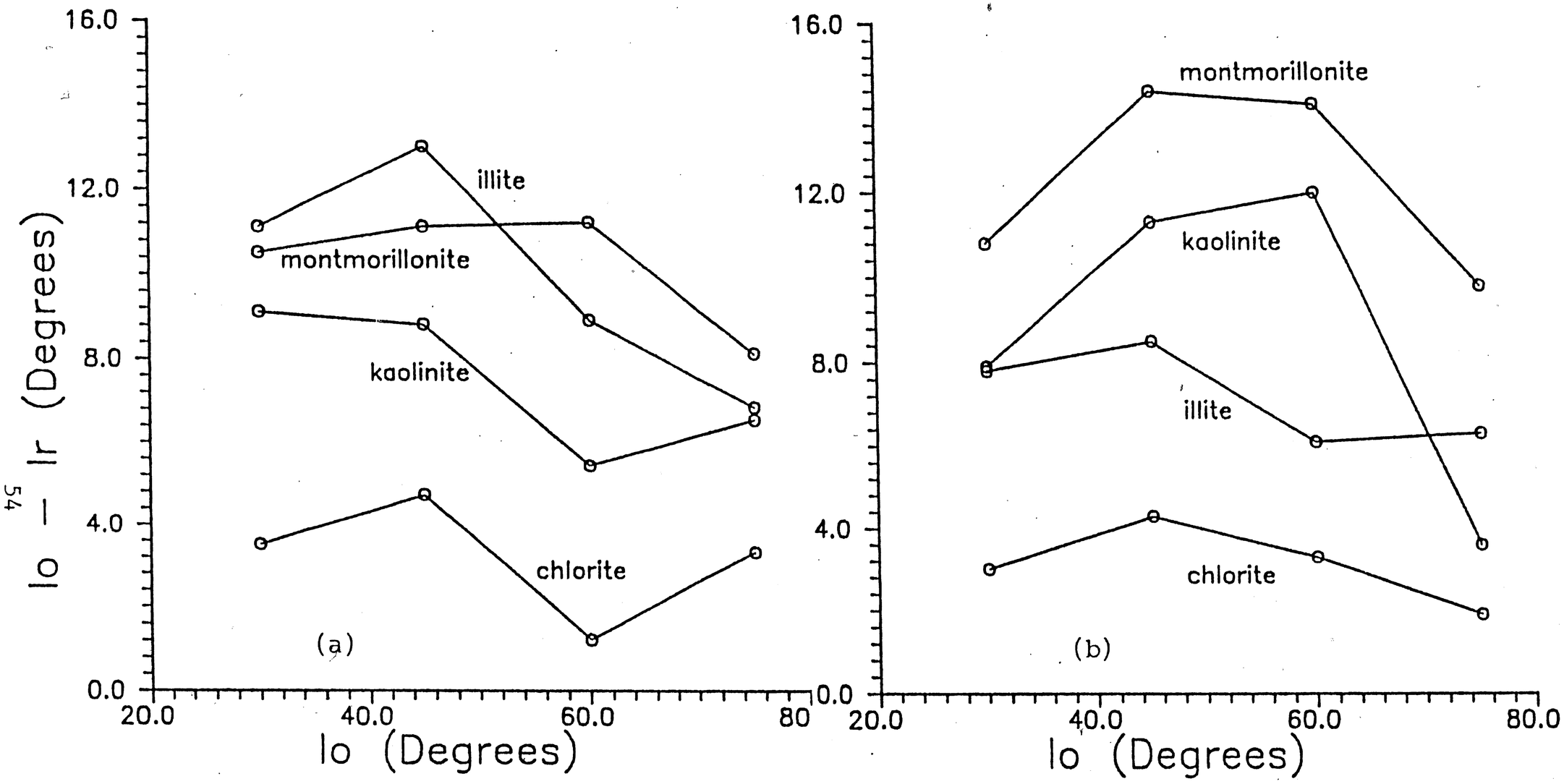

Figure 22. Change in inclination angle (Io - Ir) versus initial inclination angle for clays in water (a) and instant ocean (b). For most slurries, the inclination change is highest at 45° and 60° and lower at 30° and 75°.

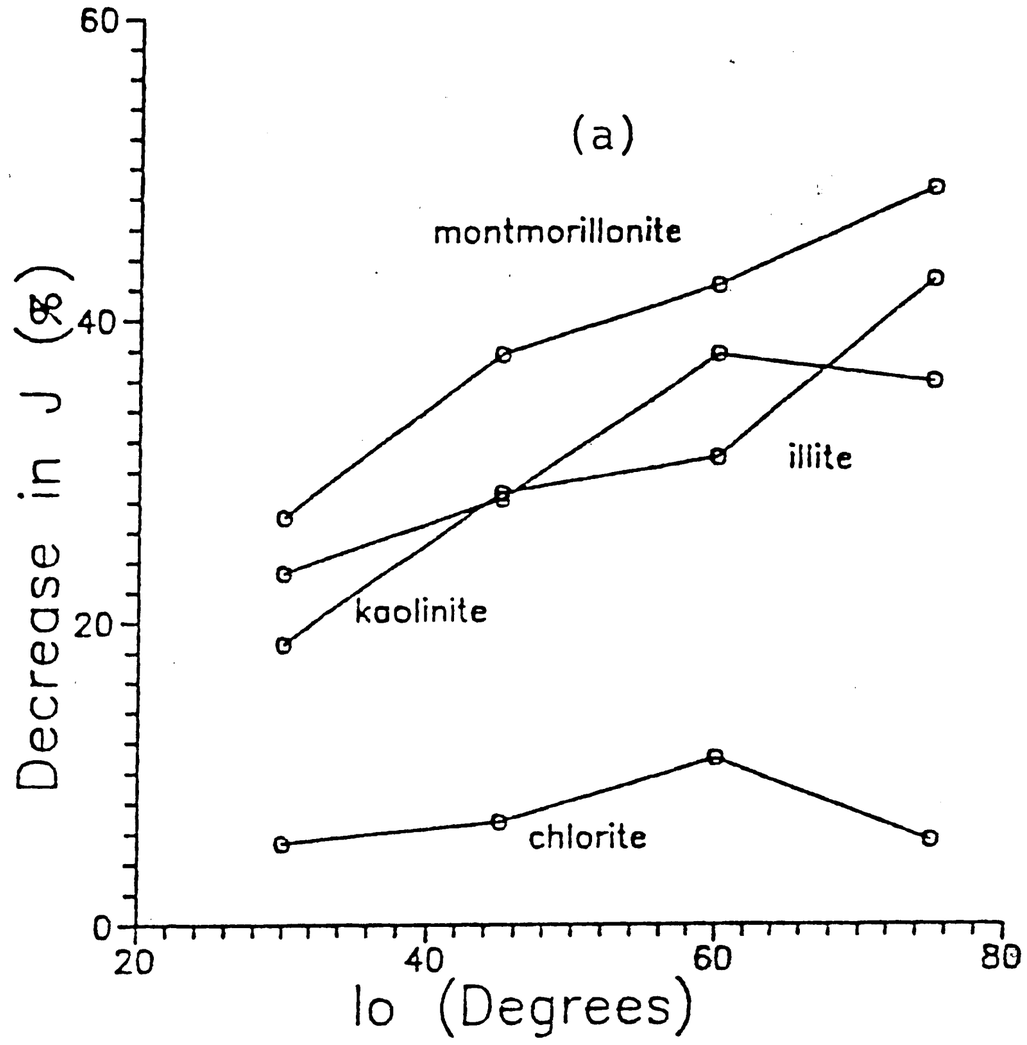

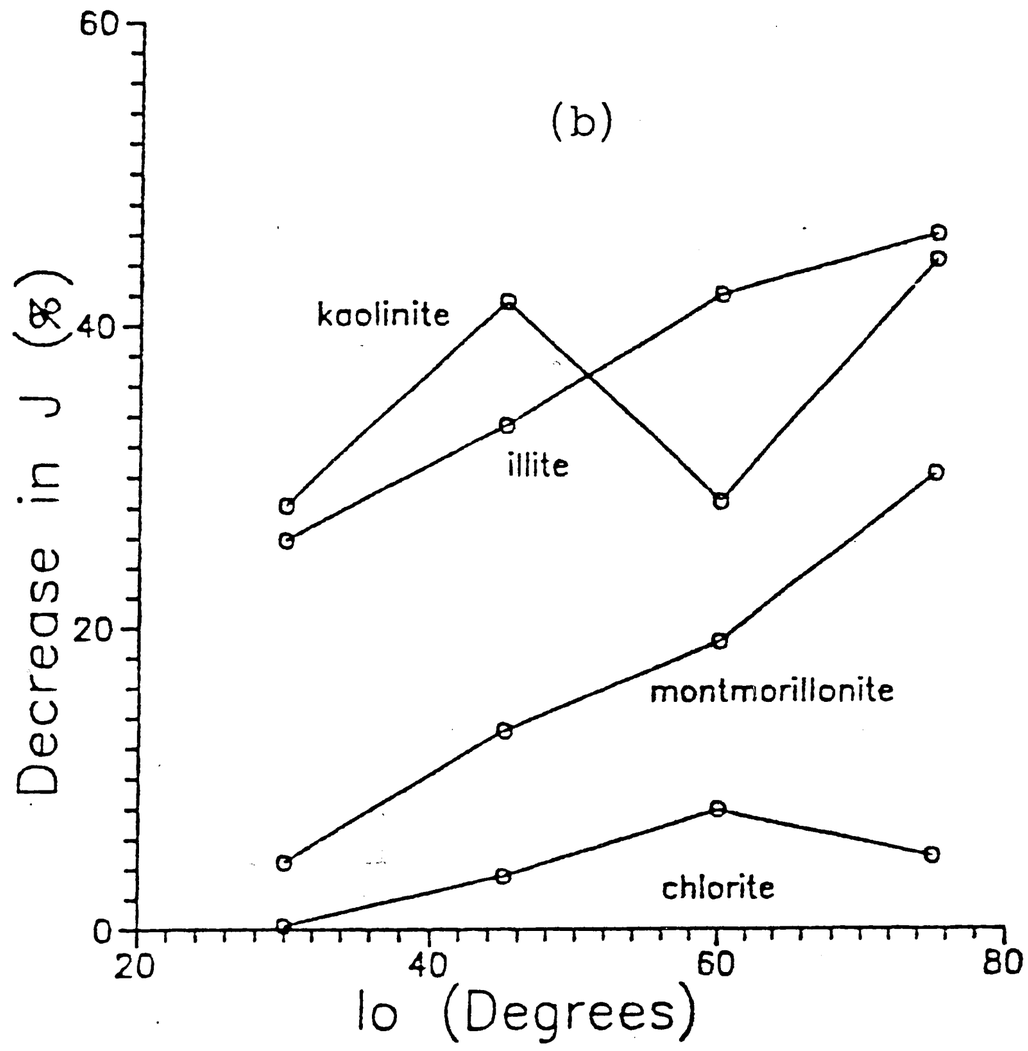

Figure 23. Decrease in magnetic intensity versus Io for clays in water (a) and instant ocean (b). In general, the decrease of intensity increases with Io.

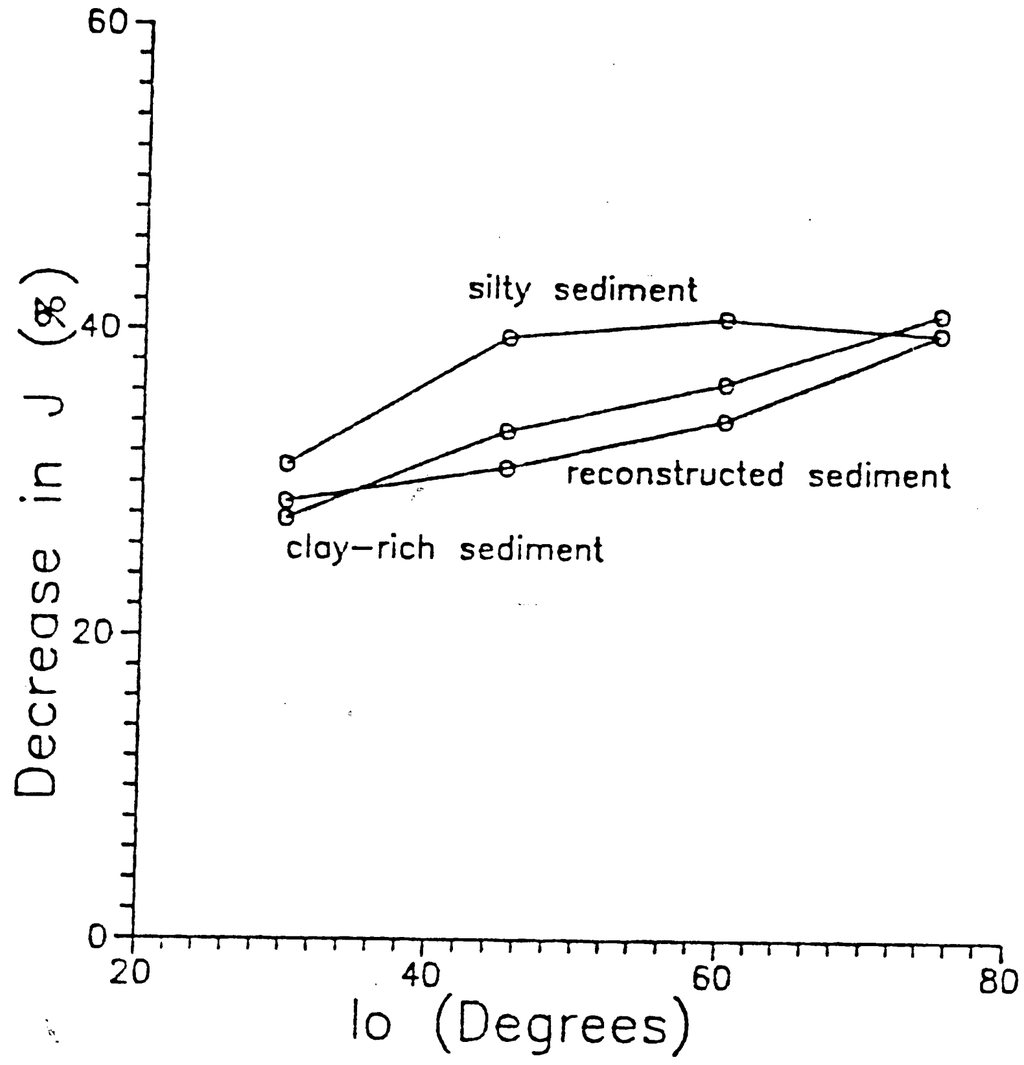

Figure 24. Decrease in magnetic intensity versus Io for natural and reconstructed sediments. The intensity decrease gets larger with Io.

obtained for the high water content sample was 1882 and for the low water content sample was 5,242,880. The total sample positioning error was measured by removing the two samples from the sample holder, then replacing them and remeasuring. The K_{total} value for the high water content was 138 and for the low water content was 55,168. The true positioning error, $K_{position}$, was then determined from the two K values already measured according to the equation:

$$1/K_{position} = 1/K_{total} - 1/K_{meas}$$

The true positioning K values were found to be 149 for high water content samples and 52,631 for low water content samples. For N=10 measurements, this gives a measurement alpha$_{95}$ (a_{95}) of 1.0° and positioning a_{95} of 3.6° for high water content samples, and a measurement a_{95} of 0.02° and positioning a_{95} of 0.19° for low water content samples.

DISCUSSION

Data from both Blow and Hamilton (1978) and Anson and Kodama (1987) suggest a linear relationship between the tangent of the remanence inclination angle (tan I_r) and the compaction of sediment (dV). Anson and Kodama based their observation on the fact that above dV values of 25%, the relationship was linear. They were able to perform only one compaction experiment using a cryogenic magnetometer, which allowed them to determine inclinations at very low dV values. Since this value also fell along the same linear function, they reasoned that the linear relationship could be extrapolated to all samples.

The data in this study do not confirm the linear relationship between tan I_r and dV at low values of compaction. In most samples, the early stages of compaction did not cause as rapid a decrease in inclination angle as later stages. Figures 20-21 demonstrate this trend. At low dV values, the curves are more nearly horizontal than at higher dV values. It is not difficult to imagine the physical reason for this behavior. Most soils compact first by expelling water from their pore spaces; at early stages of compaction, relatively small amounts of applied pressure cause a large decrease in volume. This behavior can be seen in figures 25-26, which plots pressure versus change in volume for several of the compacted slurries. It is likely that during this initial rapid volume loss, where the major effect is to expel water from the pore spaces, there is little physical rotation of clay grains, and so also little inclination change.

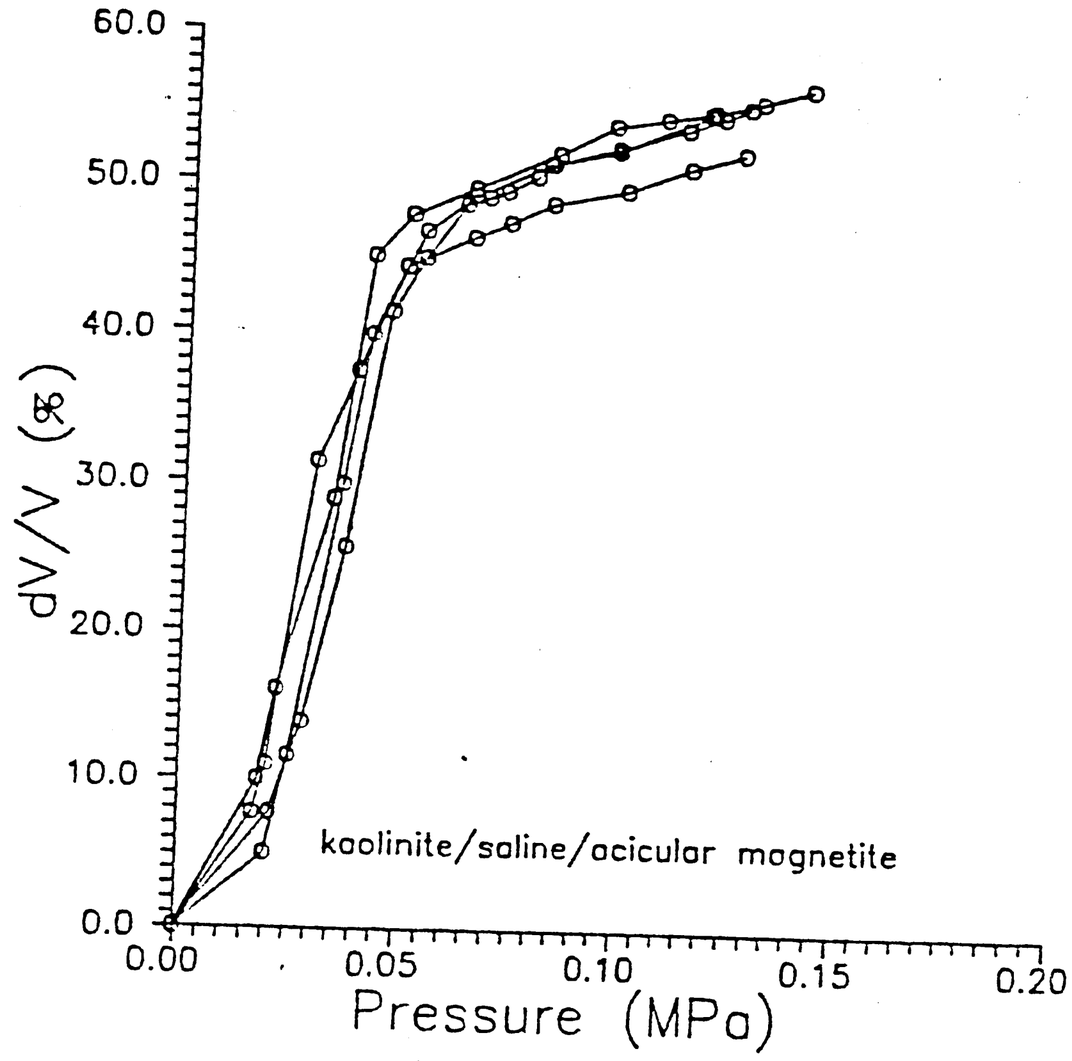

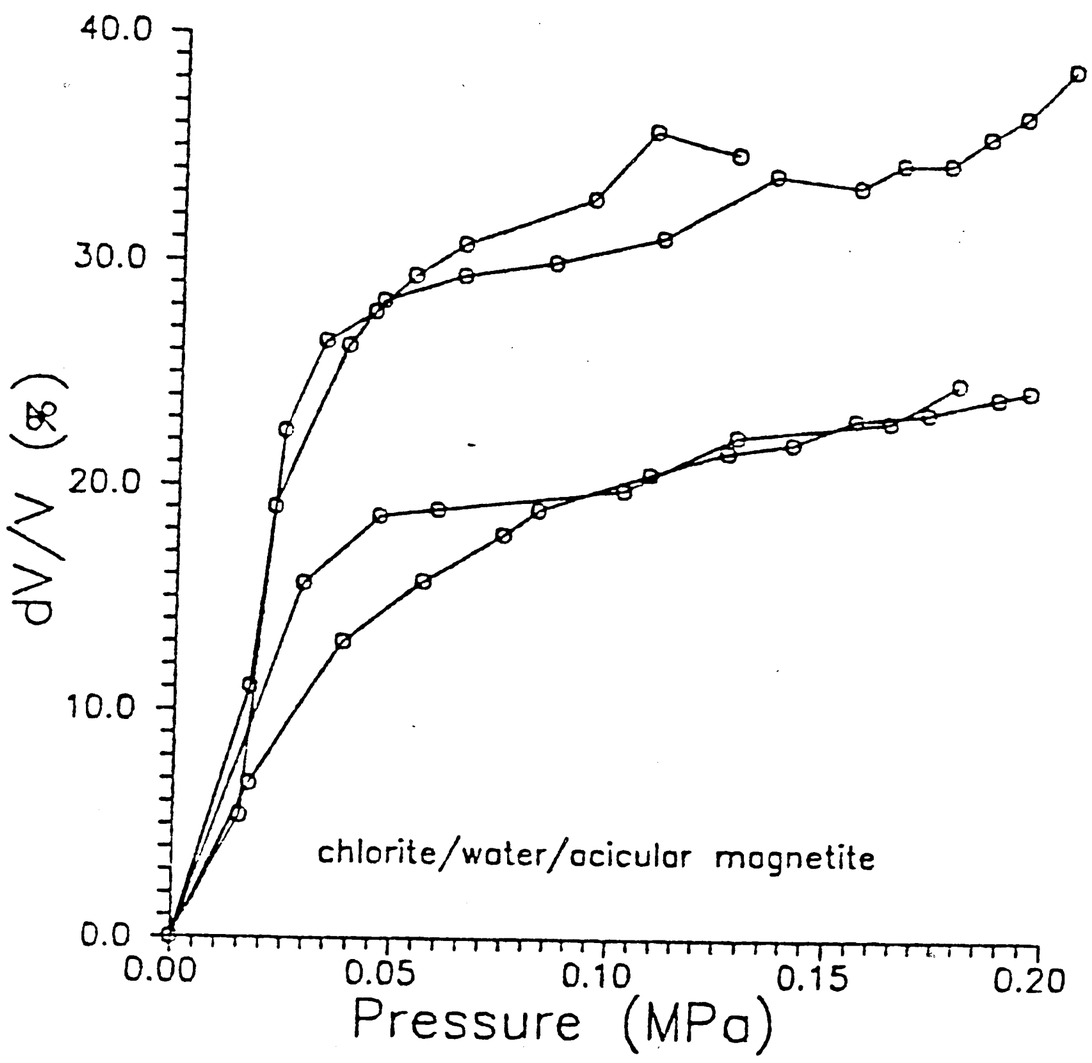

Figure 25. Representative compaction (dV/V) versus pressure plots for kaolinite in instant ocean and chlorite in water. Both exhibit an initial rapid volume decrease and an abrupt change in slope when compaction slows down.

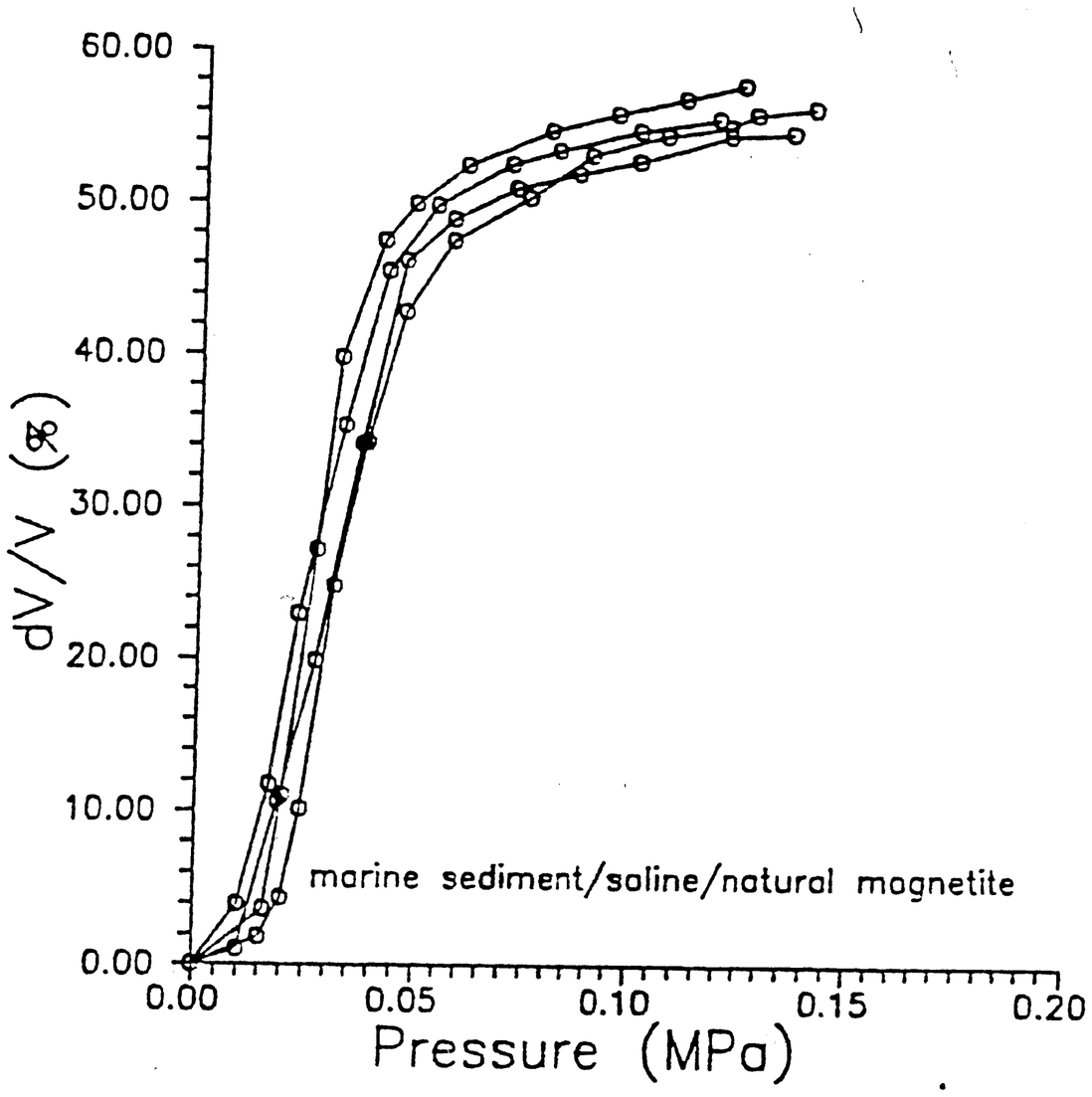

Figure 26. Compaction versus pressure for the natural clay-rich sediment.

The data collected in this study also suggest that the relationship between the change in inclination (dI) and the initial inclination angle determined by Anson and Kodama does not fall along a single curve as they suggest (see figure 8 of Anson and Kodama, 1987), although there is a relationship similar to the one they present. As in Anson and Kodama' study, it was found that higher dI values were obtained for the compaction experiments conducted in 45^{o} and 60^{o} fields, and lower dI values were observed when the field angle was 30^{o} or 75^{o}. This behavior is a result of the fact that a change in inclination affects only the vertical component of the remanent magnetization; the shortening of the vertical component has a greater effect at either a high or low inclination, resulting in a curve which follows a tan I function. Anson and Kodama's data also resulted in a tan I function curve. Figure 27 shows the comparison between the data obtained in this study and Anson and Kodama's results. Our data do not fall along the same line, but we did not expect it to, since Anson and Kodama linearly back extrapolated their data to zero compaction to obtain dI values. The data collected in this study indicate that this extrapolation would lead to an overestimate of dI. Figure 27 shows that, in fact, all of our data fall at or below their regression line. In general, however, our data also follow a tan I function, particularly for the saline experiments (figure 22).

The decrease in intensity observed for each compaction experiment is thought to be related to the dispersion of magnetite particles around the mean field inclination angle. As the slurry is

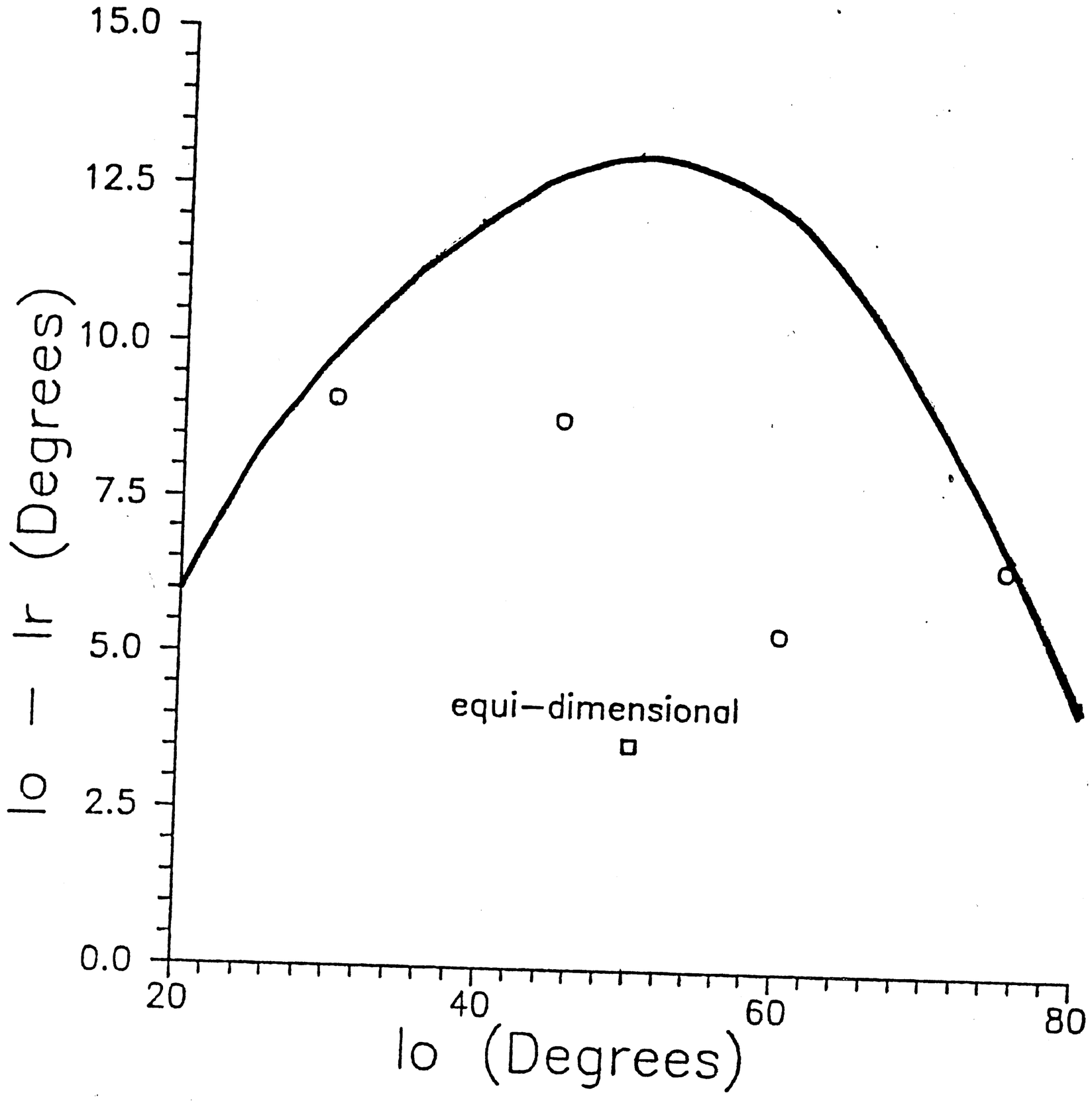

Figure 27. Data obtained in this study showing Io-Ir for kaolinite in water with acicular magnetite (circles) and equidimensional magnetite (square). The solid line shows the theoretical function presented by Anson and Kodama (1987) for inclination shallowing of clays.

compacted, the amount of dispersion of the magnetic grains increases, causing a loss of intensity. This effect is described by Cogne (1987). He conducted a series of experiments in which he applied uniaxial strain to samples of plasticene embedded with hematite particles. He found that when the angle between the direction of applied pressure and the direction of the magnetic signal was 0^{o}, there was a maximum decrease in magnetic intensity. As the angle increased, the magnetic intensity decrease became less pronounced, until at 90^{o}, the intensity actually increased slightly. The same trend was observed in these experiments; the intensity decrease was largest when the field inclination angle was 75^{o} (making a 15^{o} angle with the axis of compression) and intensity decrease lessened as the inclination angle decreased to 30^{o} (creating a 60^{o} angle with the axis of compression). Cogne's explanation for this behavior is that when the angle between the strain axis and the net magnetization direction is low, strain causes additional dispersion of particles which in turn causes a decrease in intensity. As the angle increases towards 90^{o}, strain causes rotation of more particles in line with the magnetization direction, causing an increasingly smaller intensity decrease.

The initial steepening effect exhibited by many samples during early stages of compaction is probably due to the strong vertical field present at the top of the magnetometer. It is suspected that the vertical field (75,000 nT) was strong enough to cause physical rotation of the magnetite grains while the sample was being placed in the magnetometer. The probability of physical rotation as the cause

of the steepening behavior is also suggested by two additional observations: 1) steepening was often accompanied by an intensity increase, implying that an increasing number of magnetite particles could be orienting themselves in the vertical field, and 2) samples were measured at least two times for one reading. During initial readings while the water content of the samples was high, the inclination angle invariably increased continuously for consecutive measurements, suggesting that steepening occurred even during the short period of time the sample was exposed to the higher field in the transfer tube. Viscous remanent magnetization is an unlikely explanation for the effect, because the behavior appears to be a function of sediment type, yet the same magnetite was used in each sample.

One experiment was performed with Helmholtz coils placed around the magnetometer to offset the vertical field. In this sample, the steepening was eliminated, although the coils apparently created a strong horizontal field which caused a continuous horizontal rotation of the sample's direction during compaction. Although there was some concern that the vertical field was also causing the unexpected flattening of the inclination versus volume change curve, the sample compacted with the vertical field canceled also showed this characteristic shape (figure 28). The behavior of the latter sample indicates that the flattening is probably not an artifact of the vertical field.

The amount of shallowing was also dependent on clay type, with chlorite exhibiting the least inclination, and montmorillonite

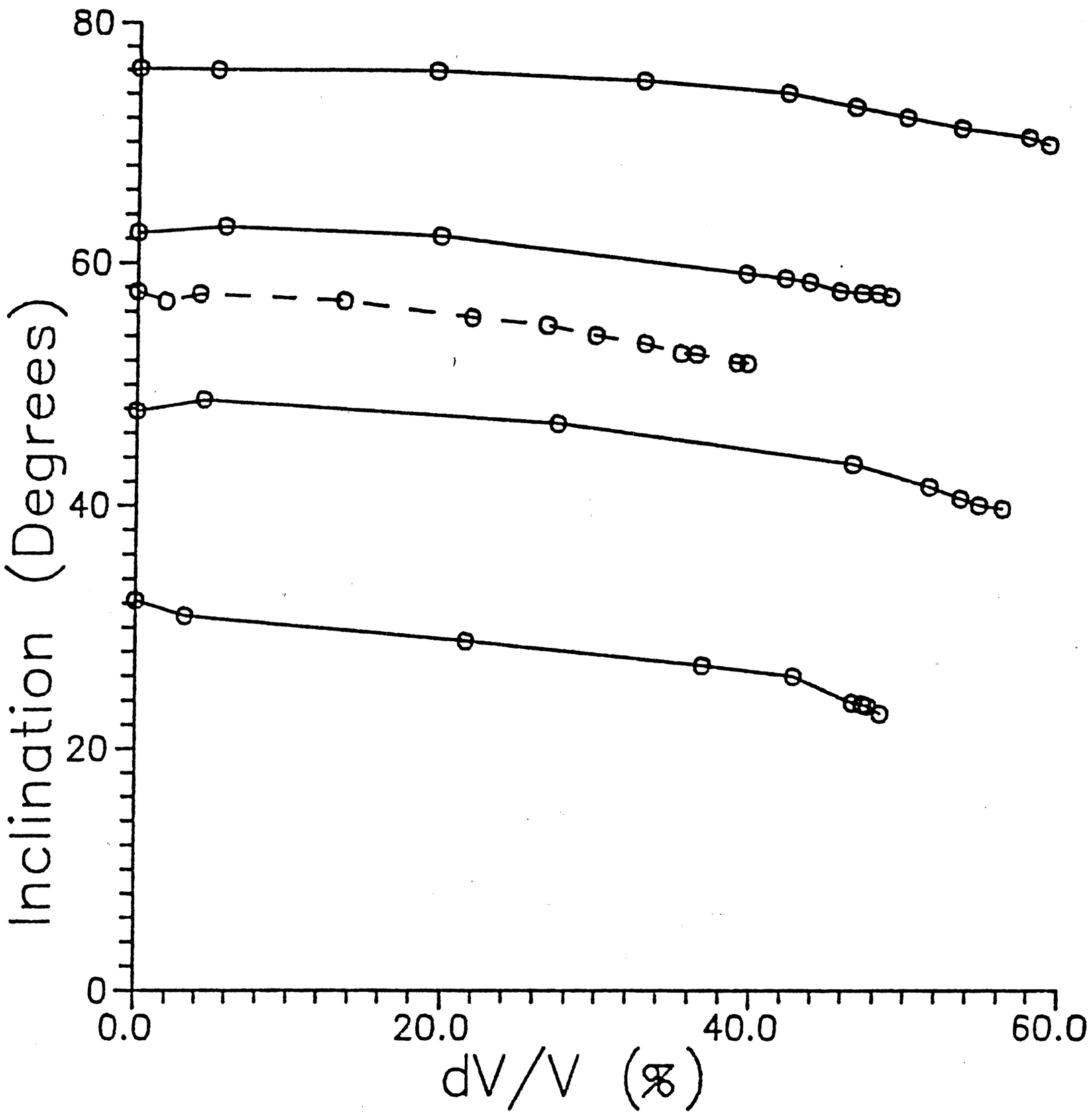

Figure 28. Inclination versus compaction for clays compacted in the strong vertical field (solid lines) and one compacted with Helmholtz coils offsetting the field (dashed line). The dashed line shows the same approximate shape as the solid lines and exhibits an initial horizontal slope at low compaction.

exhibiting the most. Since these two clays also contain the least and most water content respectively prior to compaction, it is reasonable to suggest that these data confirm earlier studies relating the alignment of sedimentary magnetite grains to water content of the sediment (Lovlie, 1974; Payne and Verosub, 1982). There are several cases, however, where slurries with higher water contents show less shallowing than ones with lower water contents. This somewhat contradictory behavior was observed primarily with kaolinite and illite; illite slurries have a lower water content than kaolinite, but frequently shallow more. This behavior suggests that water content alone does not explain the difference in inclination shallowing.

In the case of chlorite, the small amount of shallowing may also be partly due to its large grain size; Meade (1966) suggests that as the mean grain size of the clay particles increases, they are more likely to be deposited in parallel, horizontal arrangements. If Anson and Kodama (1987) are correct, and the magnetite particles are attached to clay particles, then the more horizontal chlorites will not rotate as much during compaction, and less inclination shallowing should occur. Horizontal deposition is therefore thought to be the reason for the small amount of shallowing observed in the chlorite experriments.

A comparison of results obtained from the pure clay experiments and the natural sediment experiments demonstrates the validity of using pure clay analogs for the compaction experiments. Natural sediments compacted in much the same way as both the pure clay

slurries and the sediment reconstructed from the pure clays to simulate the natural sediment, as indicated by both pressure versus inclination and volume change versus compaction. However, there are differences in the amount of compaction experienced by the natural sediments and the reconstructed analog, due primarily to the differences in the initial water content of the slurries. The natural sediment containing more mud had a much higher initial water content (250%) than the siltier sediment (105%). When the reconstructed sediment was formulated, the clay constituent was added using the pure clays obtained from Ward's. The chlorite, which comprised 64% of the clay component, had a mean grain size larger than that of clay-size (less than 2 microns). As a result, the reconstructed sediment tended to reflect the behavior of the siltier natural sediment, including its low initial water content. As a phyllosilicate mineral increases in size, its charge/unit volume decreases, and the amount of water it absorbs to offset its surface charge also decreases (Mitchell, 1976). With a larger grain size constituent, the reconstructed sediment more closely resembled the siltier sediment. In fact, the amount of shallowing exhibited by the reconstructed sediment closely approximated the amount experienced by the siltier natural sediment (see Table 3).

Test of the Electrostatic Model

The results of the compaction experiments performed in this study are not consistent with the Anson and Kodama (1987) model of electrostatic attraction. The inconsistencies are outlined below.

Effect of pH

The pH values for kaolinite slurries using deionized and saline water are both well below its ZPC, indicating a positive surface charge for magnetite. However, the pH for the two montmorillonite and two chlorite slurries are higher than the ZPC, suggesting that the magnetite surface in these slurries is negatively charged. If this is the case, there are repulsive electrostatic forces acting between the magnetite and clay particles. Nonetheless, shallowing occurred more extensively in montmorillonite than in kaolinite slurries. Illite, whose slurry pH values fell very close to the ZPC, would theoretically act as a nearly neutral particle, without attraction or repulsion to the clay. But illite also exhibited substantial shallowing.

The results of the experiment in which one kaolinite slurry was forced to a high pH by the addition of NaOH are also inconsistent with the electrostatic model. In this experiment, the kaolinite slurry had a pH of 9.5, and it shallowed 4.2^{o}. An identical sample without NaOH had a pH of 5.0, and shallowed 7.5^{o}. Although the amount of shallowing is less for the basic slurry, as predicted by the model, it is still within the range of dI values measured for other kaolinite samples (dI values for kaolinite ranged from 3.6-15.9^{o}). The smaller amount of shallowing can also be at least partly attributed to the smaller volume loss for the NaOH sample.

We also considered the possibility that the pH close to the clay flake would be low enough to change the surface charge of the magnetite particles to a positive value. A low pH near the clay

platelet would occur in the distilled water and the NaOH samples as H^+ ions are attracted to the negative surface of the clay flake. However, Stumm and Morgan (1981) estimate that for an average kaolinite, the pH will change only by a value of 2 pH units. For the NaOH sample with a pH of 9.5, this will not create positively charged magnetite particles. In addition, the effect should be reduced in saline water slurries, where ions other than hydrogen ions can offset the negative surface charge of the clay.

Demagnetization Results

Anson and Kodama (1987) observed that a statistically significant proportion of their samples exhibited progressive inclination shallowing during af demagnetization. The shallowing was attributed to smaller magnetite grains being most strongly affected by the electric fields of the clay flake, and thus closely following the reorientation of the clays. The larger magnetite grains, on the other hand, would have more difficulty in aligning themselves longitudinally to the clay surface, and would not experience as much shallowing. Demagnetization, then, would begin to remove the signal from the larger, more steeply inclined particles first, giving the sample a progressively shallow magnetization. These results were not observed our experiments. Almost equal numbers of samples exhibited steepening and shallowing, and some samples retained the same inclination angle through all demagnetization fields. In samples in which there was a significant change in inclination, the steepening or shallowing tended to occur after less than 20% of the original magnetization remained. The steepening or shallowing was not

consistent during demagnetization, which would be expected if differences in grain size were causing the effect. For example, a continuous decrease in pore size should cause a continuous rotation of decreasing-sized magnetite particles, which should be reflected during demagnetization.

In fact, Anson and Kodama's demagnetization results are surprising, since the synthetic magnetite grains have a nearly uniform size, as indicated by their narrow coercivity range. It seems unlikely that there would be a large enough range in magnetic grain size to cause any kind of systematic change in physical shallowing behavior which is based on grain size. It is not known why, then, this trend was observed in Anson and Kodama's study.

The samples containing natural magnetites in general exhibit the same type of behavior as the samples containing synthetic magnetite. The natural magnetites have a broad coercivity range, so it likely that the range in grain size is larger than in the synthetic magnetite. This behavior suggests that the effect of compaction is the same for both large and small magnetite grains. The samples containing both synthetic equidimensional and natural magnetite also did not exhibit any particular trend, again suggesting that all the grains are equally affected by compaction.

The unusual behavior of chlorite during af demagnetization was puzzling in two ways. First, demagnetization of chlorite in distilled water containing acicular magnetite exhibited a broader coercivity range than any of the other clay types containing acicular magnetite (figure 5). Since the same magnetite was used for every

experiment, it is not possible that the magnetic grain size for these samples is actually different from the others. Again there is no obvious explanation for this behavior.

In addition, chlorite in instant ocean could not be af demagnetized. When the samples were tumbled, the magnetization directions, both inclination and declination, fluctuated wildly. The only explanation for this behavior is that either the magnetite grains did not remain attached to the clay particles, or the clay particles themselves (with magnetite particles still attached) were loose in the matrix. The interesting aspect of this explanation is that the chlorite with its large grain size has the smallest surface charge, and with the instant ocean as the fluid, the surface charge is even more reduced. If anything, this behavior suggests that the magnetite is not attached because the surface charge is so small; this behavior could be construed as evidence for the electrostatic model.

Clay Types, Fluid Types, Magnetite Types

Using different clay types and fluid types resulted in different amounts of inclination shallowing in the compaction experiments, but the differences cannot be related to differences in the amount of attraction between the clay and magnetite. The evidence provided by the pH values of the slurries is a better indicator of attraction. The use of various clays and fluids did indicate that inclination shallowing would occur under different conditions using a variety of clay materials.

Anson and Kodama's model predicted less inclination shallowing for equidimensional magnetite than for acicular magnetite. The reason for the different amounts of shallowing is that the acicular magnetite grains have a more clearly defined long axis which is more readily affected by their proposed shallowing mechanism. The results of our study do not indicate different shallowing behavior between the two magnetite types. This was not expected, since even though this does not necessarily reflect on the validity of the electrostatic model, it does suggest that the two particle types are not attached. On the other hand, as long as it can be assumed that even the equidimensional and natural magnetites have a physical longitudinal axis along which they are magnetized, the shallowing can still be attributed to attachment of the magnetites and clays.

A New Model

Although the results of this study make it difficult to support the electrostatic model, there is evidence which suggests that some of the ideas presented by Anson and Kodama apply. Specifically, this evidence indicates that an interaction between the clay flakes and the magnetite grains, and suggests that the mechanism for magnetite rotation is still directly linked to the orientation of clays during compaction.

It has been pointed out (Verosub, 1987) that in a randomly oriented clay matrix in which the magnetite particles are attached to individual clay platelets, compaction of the clay fabric would cause no net change in inclination. Actually, the signal will not randomize as long as a certain condition is met. The magnetite

particles are aligned in the field as they fall through the water column (Collinson, 1965). If, as they are attached to the clay platelet they remain oriented with the field, and are also constrained to orient themselves along the long axis of the clay platelet, then compaction of the clay will not cause a random rotation of the magnetite particles.

Since this idea is dependent on the orientation of the clay fabric during compaction, it would be ideal to be able to associate changes in the clay fabric with changes in inclination angle during compaction. Direct measurement of clay fabric was not done in this study, but the literature contains many references to quantitative clay fabric studies.

In a study by McConnachie (1974), the orientation of kaolinite domains was measured using a vector sum method of orientation angles on sections of compacted samples cut along planes vertical and horizontal to the direction of applied pressure. His results indicate that kaolinite begins to orient at very low pressures, and the maximum amount of orientation is reached at 0.01 MPa (figure 29). Higher pressure did not increase the amount of orientation in his samples. He also measured the void ratio versus applied pressure and found that the slope of the curve changed abruptly at the same pressure at which the maximum amount of orientation was reached (fig. 30). At higher pressure, the void ratio continues to decrease, but the orientation does not change, suggesting that at some particular water content, the fabric elements no longer rotate to reorient, but simply move closer together.

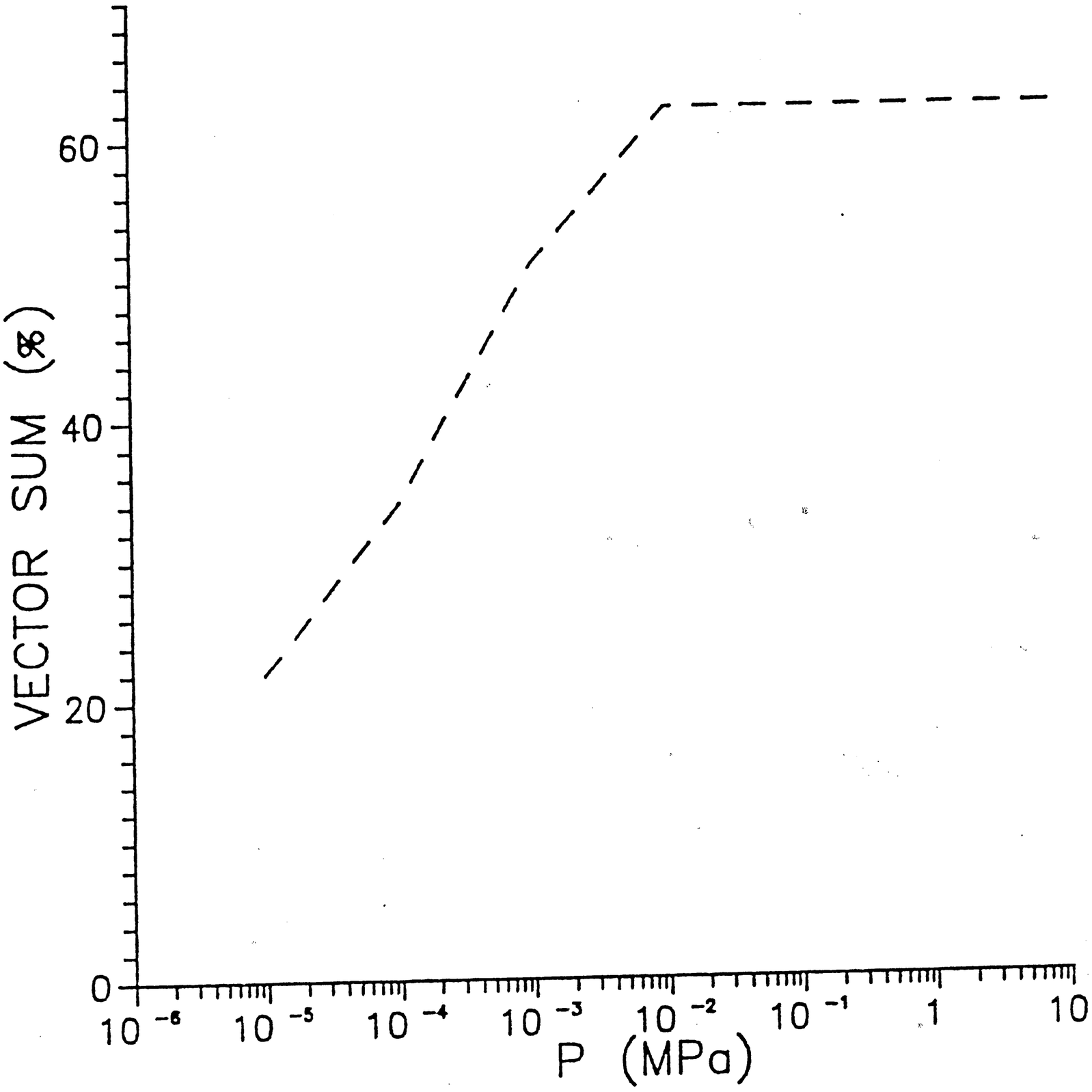

Figure 29. Plot of orientation of clay domains calculated using a vector sum method (McConnachie, 1974) versus pressure. The change in slope occurs at approximately 0.01 MPa.

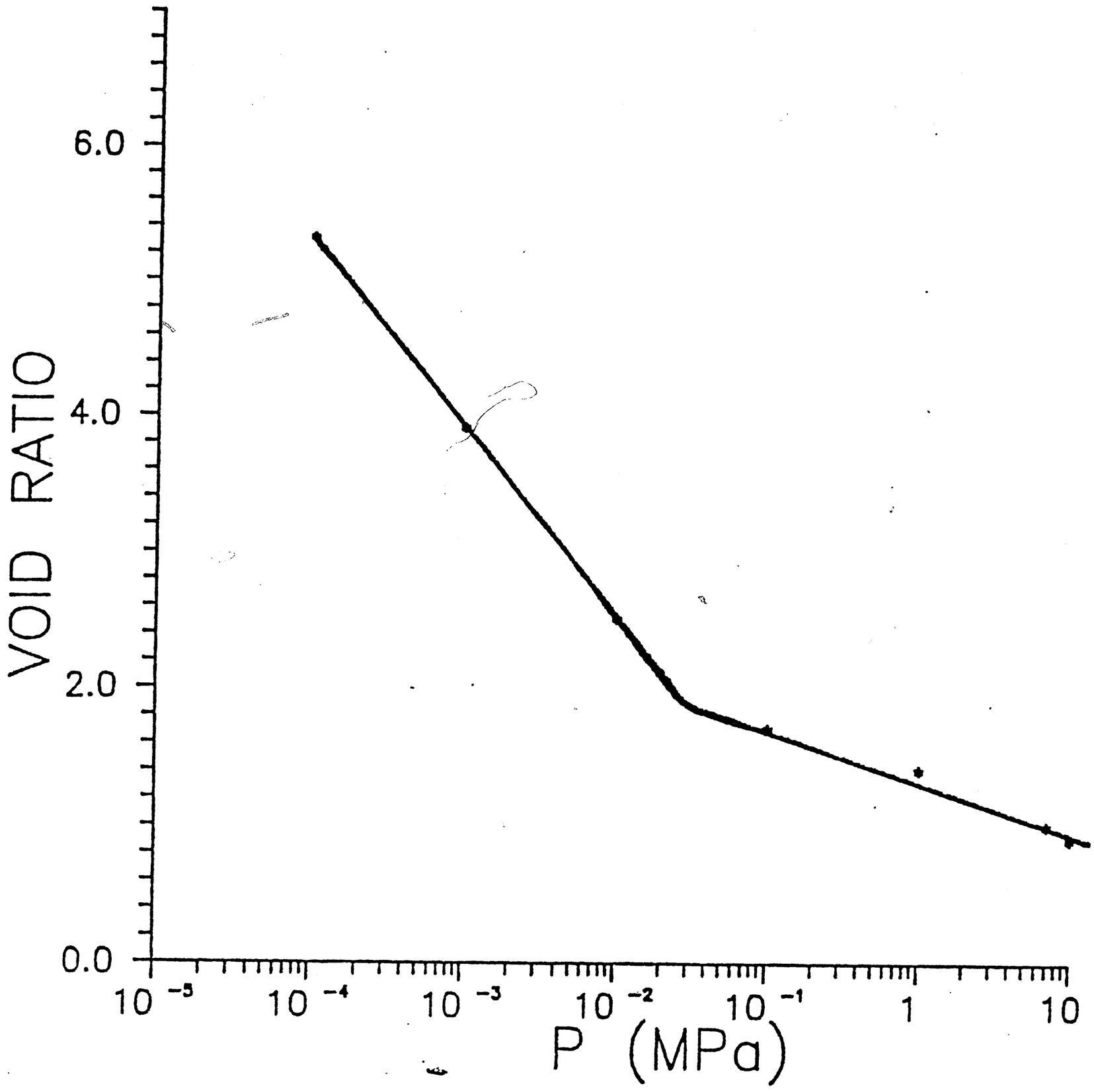

Figure 30. Plot of void ratio versus pressure, from McConnachie, 1974. The abrupt change in slope occurs at approximately 0.01 MPa.

Graphs of pressure versus inclination for the kaolinite samples show a curve shape very similar to McConnachie's results for pressure and orientation (fig. 31). Although there is an initial pressure interval over which the inclination remains fairly unchanged, further pressure increases cause a rapid decrease in inclination until the curve flattens out again at higher pressures. A series of curves plotting pressure versus dV/V for the same kaolinite samples show initially that there is a faster rate of volume loss until, at some pressure, this volume loss rate decreases considerably. The dV/V curves are analogous to McConnachie's void ratio curves, since changes in volume during compaction are directly related to the expulsion of pore water. In these graphs, it can be seen that, like McConnachie's results, the change in slope for both curve types occurred at approximately the same applied pressure (0.05 MPa). The similar shapes of the curves for both our data and McConnachie's data indicates that inclination shallowing of magnetite particles occurs at the same time as reorientation of the clay fabric; it seems likely that this happens because the particles are attached, or very closely associated. It should be pointed out that in figures 29 and 30, McConnachie has plotted pressure using a log scale, while in figure 31, we plotted pressure on an arithmetic scale since the range over which we applied pressure was much smaller than McConnachie's range.

McConnachie suggests that the pressure at which the plots change slope represents the point at which the effective stress (overburden) exceeds the physico-chemical forces due to electrostatic and van der Waal's bonds. At lower pressures, volume reduction

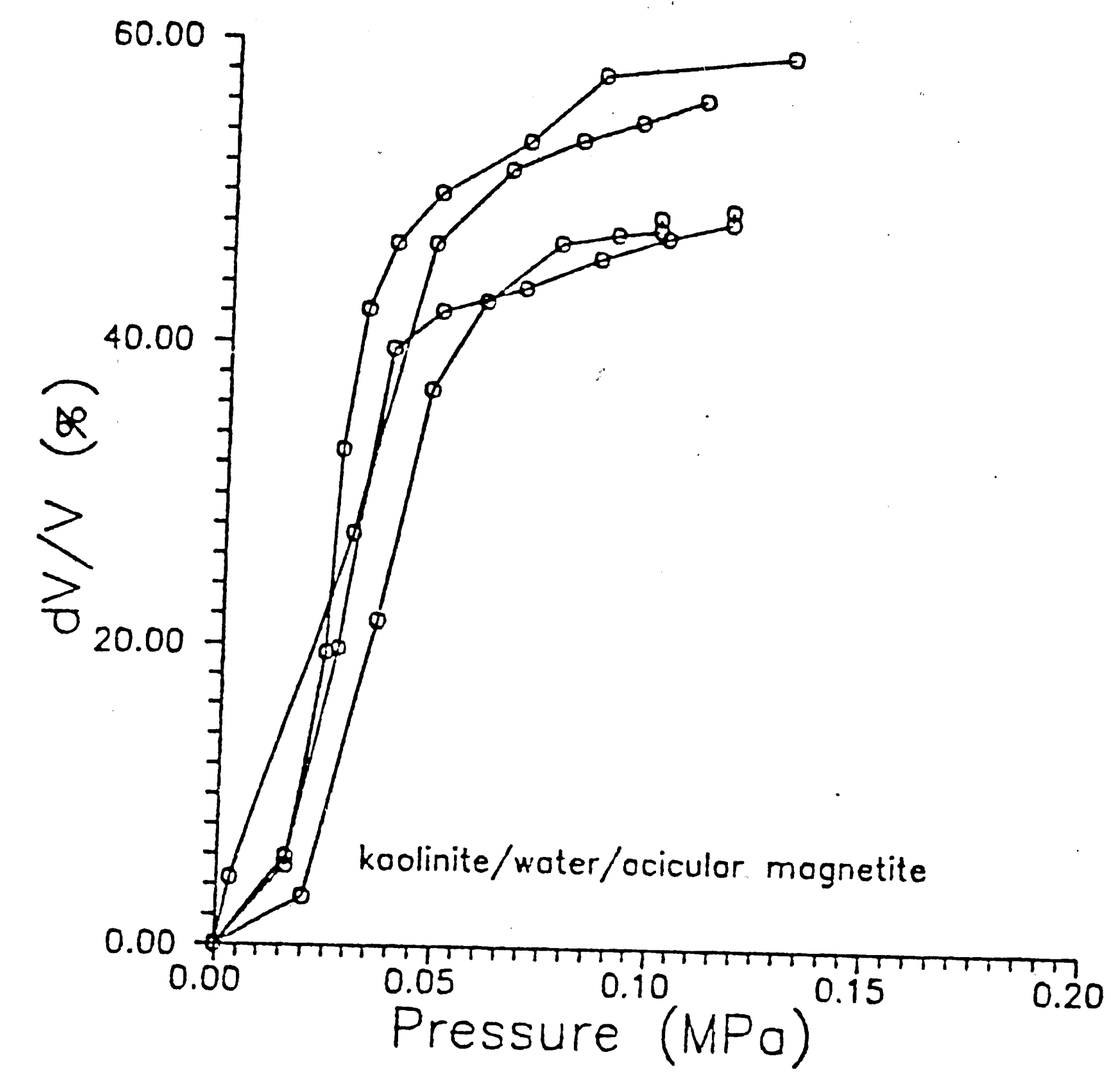

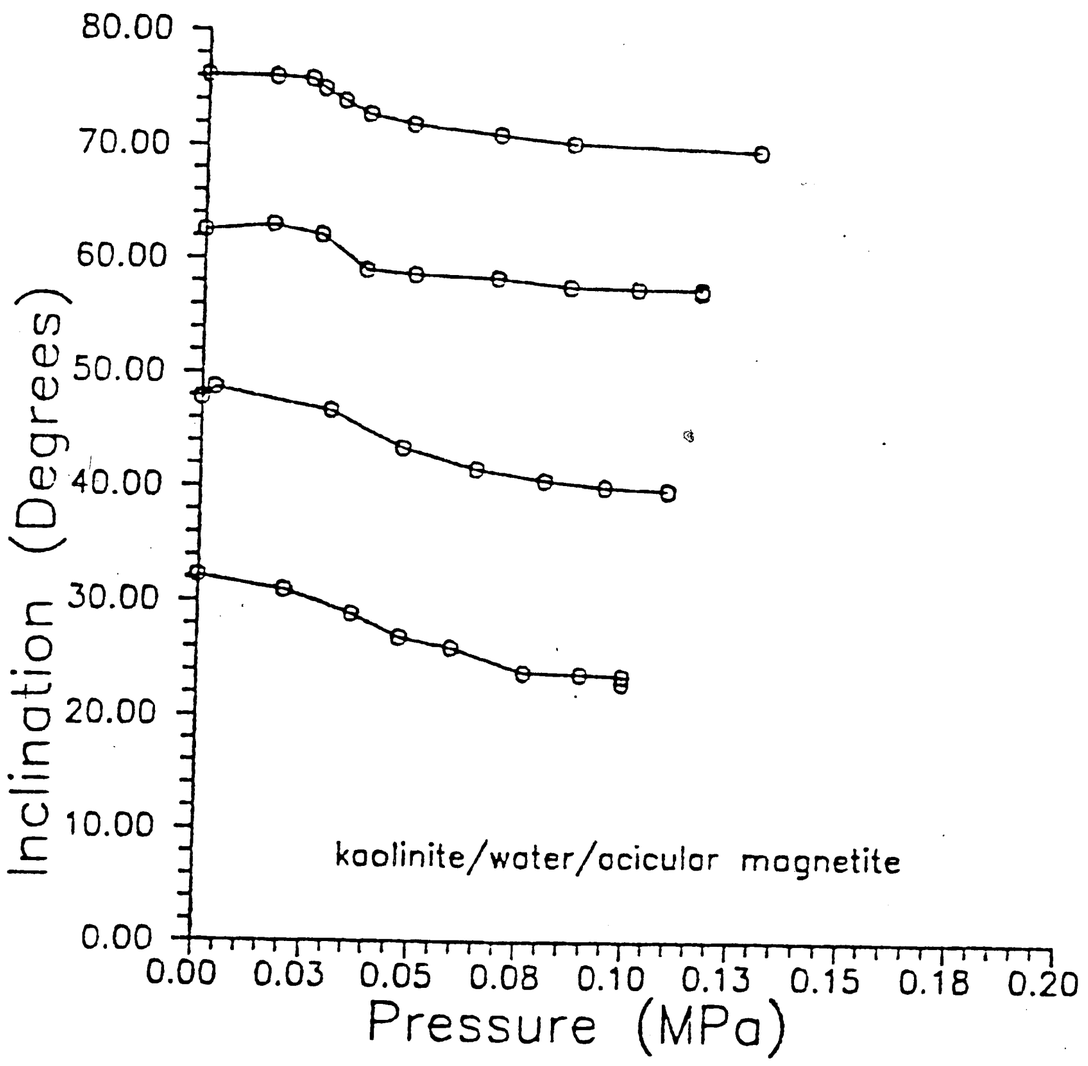

Figure 31. Plot of inclination and compaction versus pressure for kaolinite in water with acicular magnetite. The dV/V curve is analogous to McConnachie's void ratio plot. Both curves change slope at approximately the same pressure (0.04 MPa).

occurs due to water loss from pores, causing maximum reorientation of domains and particles. Compaction slows down when inter-domain and/or inter-particle forces begin to rupture in response to increased pressure. At this point, very little additional orientation occurs, presumably because there is less room for the fabric elements to rotate.

Since McConnachie worked only with kaolinite, it is not easy to make a direct correlation with the other clays in this experiment. However our results obtained from montmorillonite, illite and chlorite are in reasonable agreement with McConnachie's model. Plots for illite show similar trends to kaolinite, with the break in slope of the curves occurring at slightly higher pressures (0.055 MPa). Montmorillonite in water, however, never reaches a change in slope for either the inclination versus pressure or the dV versus pressure curve (figure 32). This lack of slope change in the compaction curve may be because the slurry has such a high water content initially, it never reaches the point where inter-particle or inter-domain bonds are ruptured; volume is lost only from pore water removal. When saline water is used as the slurry fluid with montmorillonite, however, the pressure versus inclination curves begin to flatten out at higher pressure, and the pressure versus dV/V shows a definite change in slope (figure 33). This may be due to the ions offsetting some of the high surface charge, since the curves show montmorillonite behaving more like kaolinite and illite.

The results for chlorite emphasize the effect that large grain size has on the clay's behavior. Although the samples still exhibit

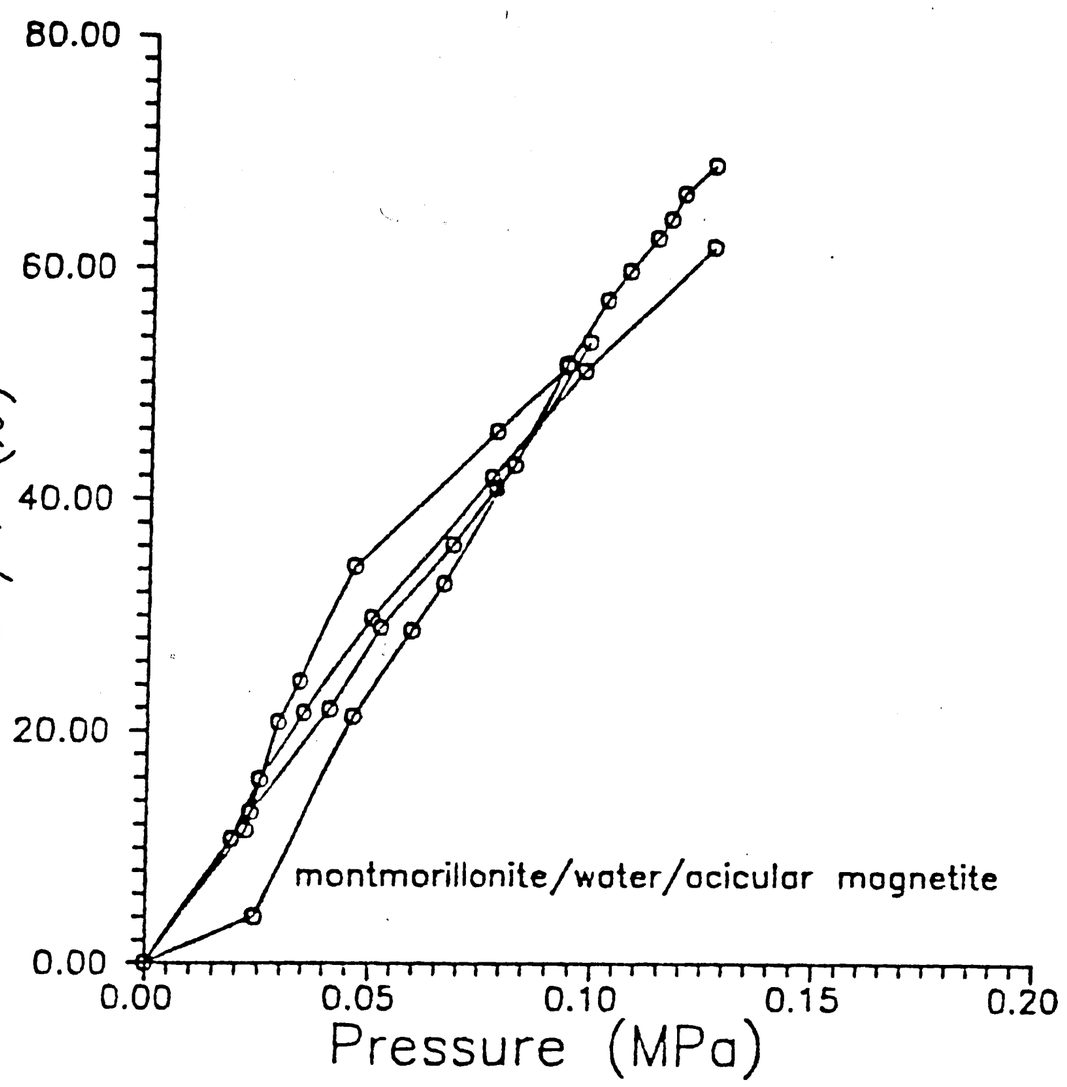

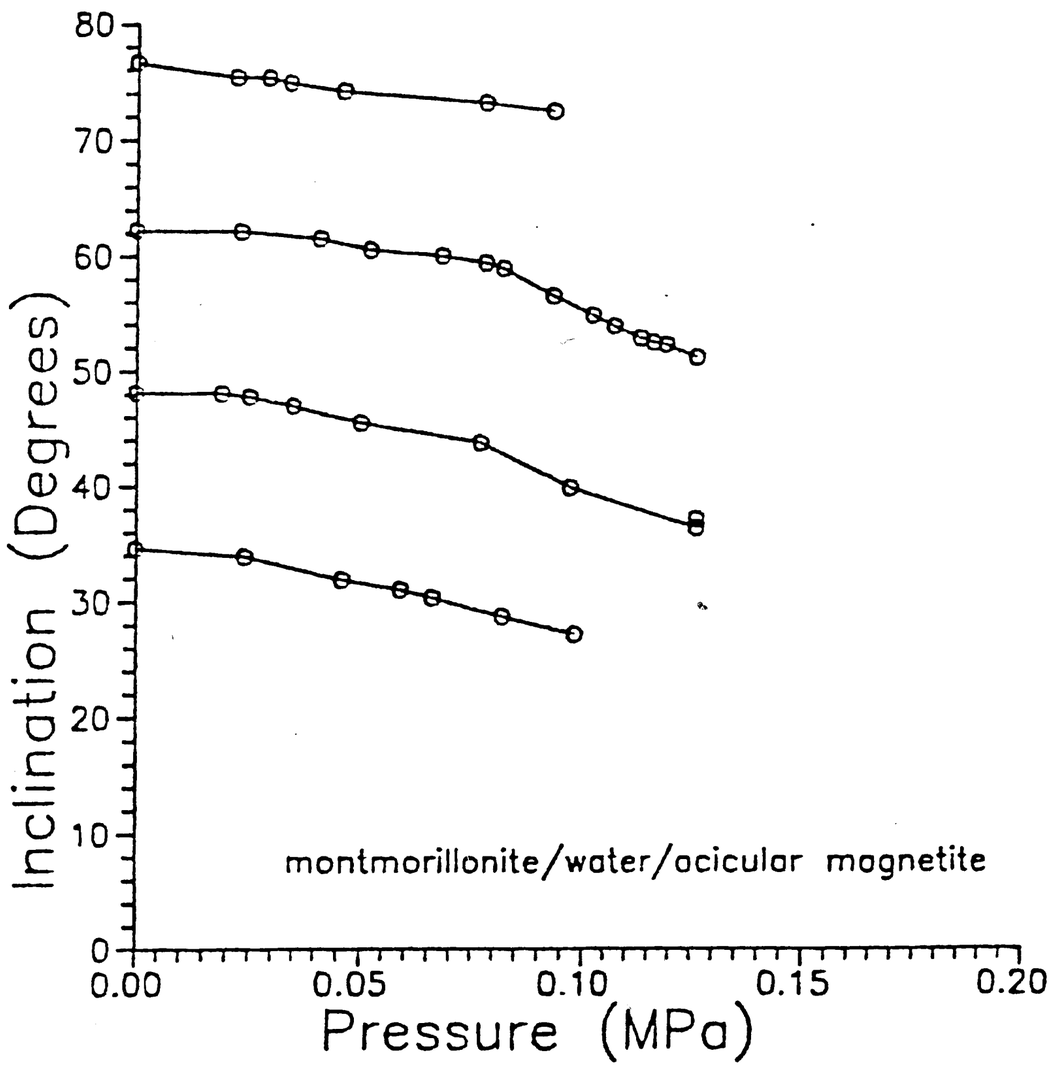

Figure 32. Plot of inclination and compaction versus pressure for montmorillonite in water with acicular magnetite. The compaction curve never changes slope, and the inclination curve likewise does not flatten out.

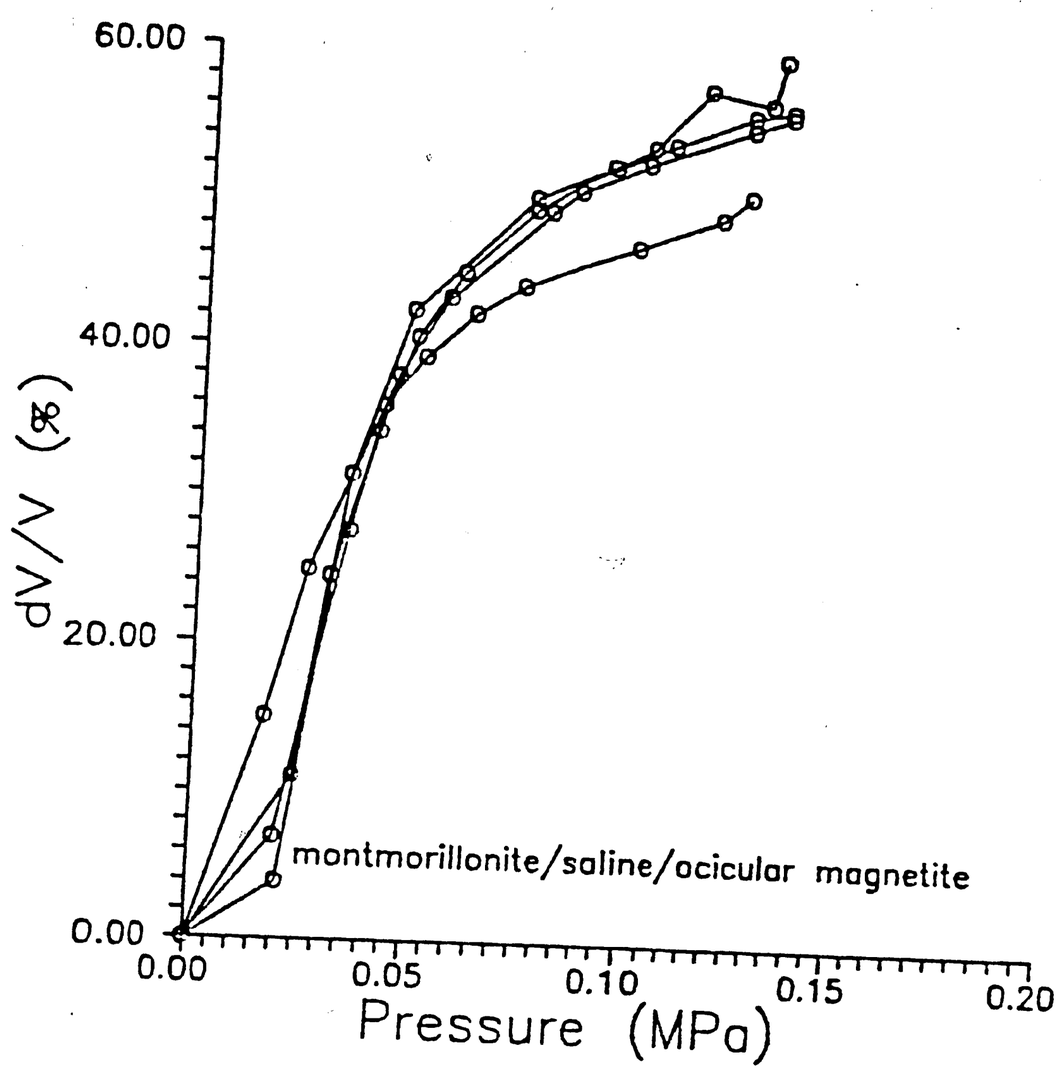

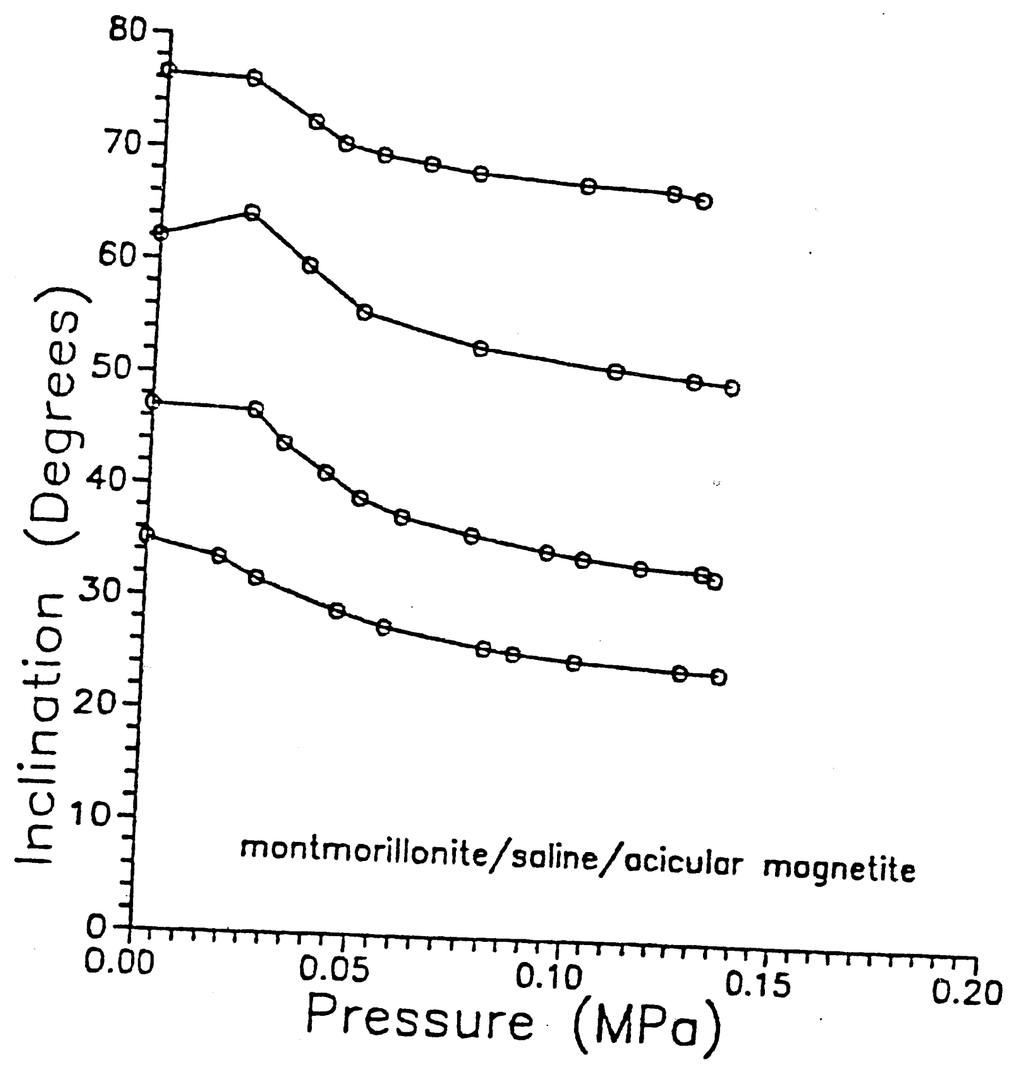

Figure 33. Plots of inclination and compaction versus pressure for montmorillonite in instant ocean. Both curves change slope at approximately the same location, 0.05 MPa.

the typical pressure versus dV/V curve, the curve changes slope at a much lower volume loss, reflecting the assumption that the smaller surface charge prevents the clay minerals from adsorbing as much water (figure 34). The pressure versus inclination plots (figure 34b) are nearly flat through the entire pressure range. This behavior could have several explanations, but it is suspected to result from the greater tendency of larger chlorite grains to attain a more horizontal orientation during deposition (Meade, 1966). If the grains are more nearly horizontal, they will obviously not experience as much rotation during compaction.

The natural sediments and reconstructed sediment also exhibit the characteristic pressure versus volume and inclination curves. The inflection points occur at approximately the same pressure for all three sediments (0.04-0.05 MPa).

A series of similar compaction experiments were performed by Stamatakos, et. al. (1988) with sediments containing primarily sand and silt particles from the Arkose Ridge Formation. In this study, rocks from this formation were disaggregated, and then redeposited and compacted to determine how redeposition and compaction affected inclination. The four samples exhibited very little inclination shallowing (figure 35). The results are similar to the chlorite plots (figure 34), with a nearly flat inclination curve. These results suggest that clay minerals are necessary in the sediment in fairly high proportions before inclination shallowing will occur. It is possible that without clay particles to adhere to, the magnetite particles do not have a coupled-mechanism of rotation.

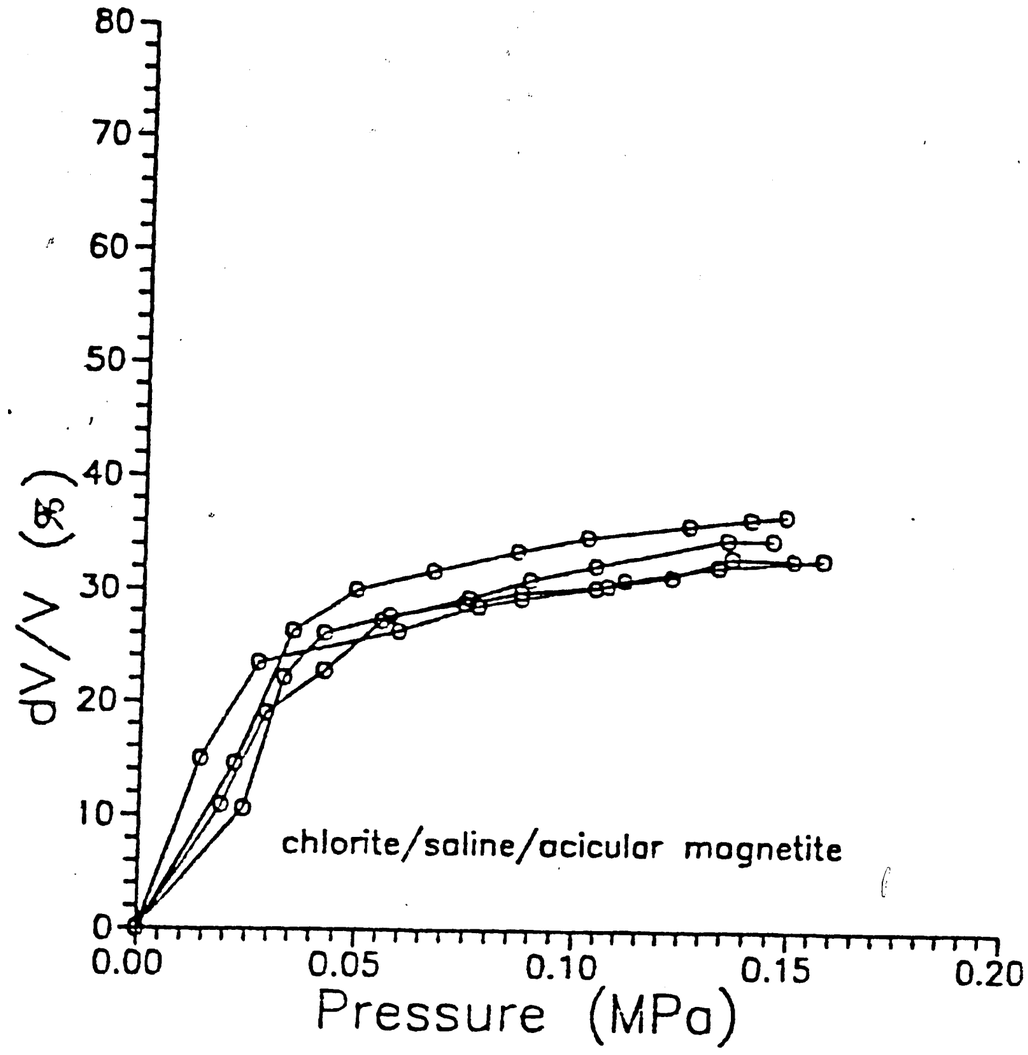

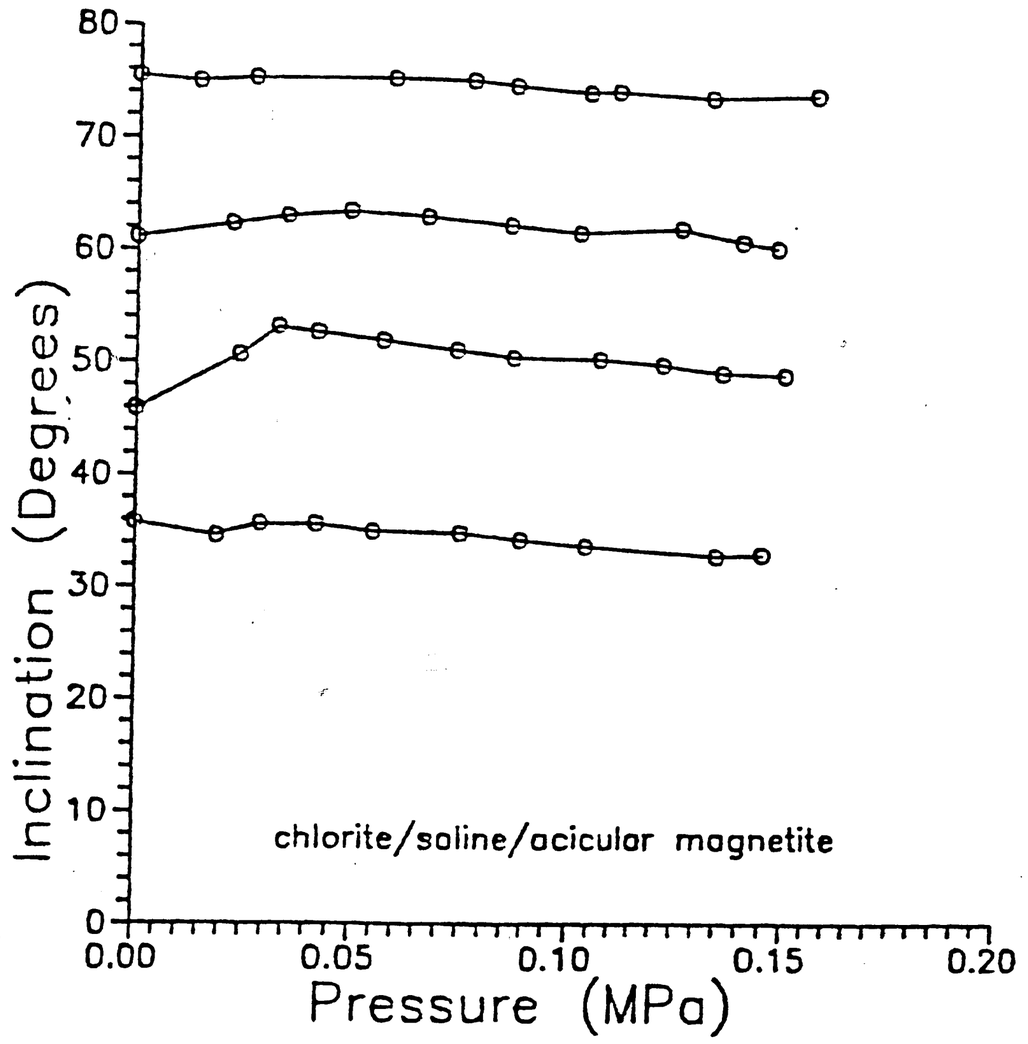

Figure 34. Plots of inclination and compaction for chlorite in instant ocean. Although chlorite exhibits the typical compaction curve, the inclination curve is almost flat.

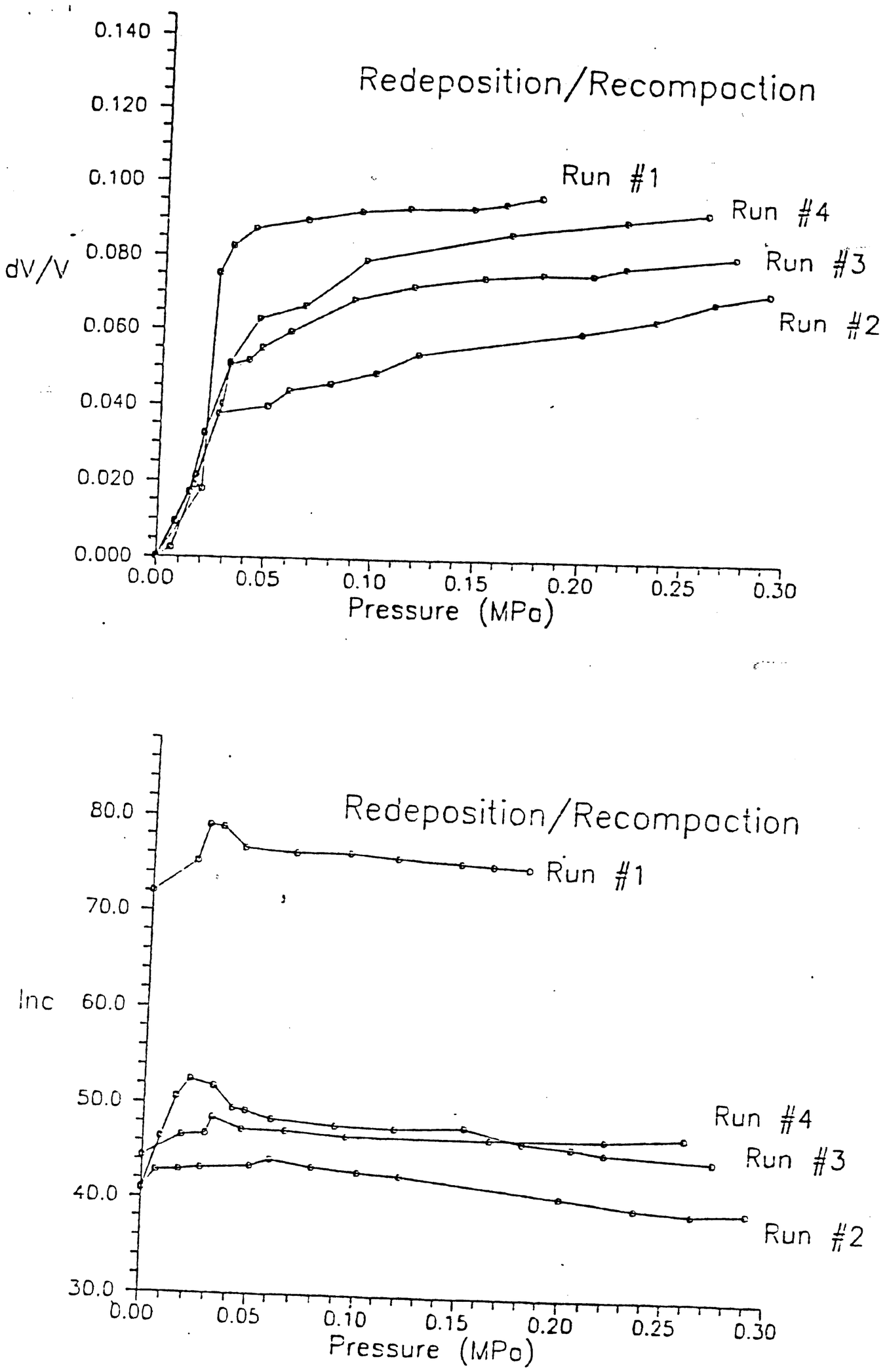

Figure 35. Plots of compaction and inclination for redeposited and compacted silty sediments (Stamatakos, 1988). These curves are similar to the chlorite curves (fig. 34). Although the sediments show the typical compaction curve, there is almost no change in inclination.

There is other evidence that clay platelets and magnetite particles may interact. A current study investigating the settling behavior of clay materials has shown that a slurry containing 0.1% magnetite which is allowed to settle through a column of water, the smallest clay size fraction settled out substantially faster than in a slurry not containing magnetite, but only pure kaolinite (Sibel Pamukcu, Lehigh University Civil Engineering Dept., pers. communication). One explanation for these results is that magnetite particles attached to clay platelets increase the particle density and size, thus increasing the settling velocity. Electrostatic attraction is possible in a kaolinite/water slurry where the surface of the magnetite may be positively charged. Clearly, however, if clay/magnetite interactions are found in other slurries where the pH is higher than 6.5, other types of attractive forces need to overcome net repulsive electrostatic forces.

A study by Payne and Verosub (1982) also provides some evidence for interaction of clays and magnetite by demonstrating a difference between the remagnetization behavior of sediments composed primarily of sand and those composed of clays. In their study, it was found that for a given water content below 50%, a sediment whose sand content exceeded 60% was able to remagnetize itself as the sample was rotated 90^{o} in a magnetic field. Samples whose sand fraction was less than 60% were not remagnetized. Payne and Verosub used the study to define a critical water content for sediments, below which magnetite carriers are not sufficiently mobile to remagnetize. However, their study also indirectly implies that the behavior of the

magnetic particles depends on whether the sediment is primarily sand or clay-sized particles.

Although the evidence discussed may indicate attraction between clays and magnetite, we have also found that the attraction is probably not due to electrostatic forces. This means that some other mechanism for attraction must be operating.

The primary attractive force present in clay systems is van der Waal's dispersive forces (Van Olphen, 1977; Yariv and Cross, 1979), and it is suggested that Van der Waal's forces are a more likely mechanism for the attraction between magnetite and clay because they do not depend on the surface charge on the particles. These forces are created because the charge distribution of nonpolar molecules over short periods of time (10^{-16} seconds) are not spherical, and this imposes a short-term dipolar character to the molecule. Although when averaged over longer time periods (10^{-14} seconds) the charge distribution is nearly spherical, the short-term dipoles exist long enough to induce distortions in the charge distributions of neighboring molecules. If two such nonpolar molecules approach each other closely enough, they can create a nonpolar character in each other, and the combined charge distribution will not average to zero over time, so that the dipoles of the molecules will exert an attraction between the molecules (Sposito, 1984, p.209). Although the attractive force between two individual molecules is fairly weak, Van Olphen (1977) points out that these forces are additive between atom pairs. This means that the total force between two particles containing many atoms will be the summation of every

attractive force of every atom in one particle for every atom in the other particle. Because of this additive effect, van der Waal's forces decay less rapidly with increasing distance than electrostatic forces. Van Olphen (1977) concludes that van der Waal's forces have a range and magnitude comparable to electrostatic forces.

The relative distances over which the electrostatic and van der Waal's forces are effective also would suggest that van der Waal's force are more important than electrostatic forces in clay-magnetite interactions. Mitchell (1976) indicates that electrostatic attractions may be important for particle distances up to 30 angstroms. However, the study by McConnachie (1974), suggests that pore sizes present in a kaolinitic slurry having 250% water content were approximately 0.75 microns by 0.4 microns at an applied pressure of 0.01 MPa. The pore size decreased to approximately 0.5 microns by 0.25 microns at a pressure of 0.15 MPa (approximately the maximum in this study). The 0.5 micron acicular magnetite particles in our study could easily be accommodated within the pore spaces suggested by McConnachie's work without approaching within 30 angstrom distance to the clay surface almost until the maximum pressure of our experiments was applied, suggesting that before any type of force can take effect, the particles must be brought close enough together by some other means. Yariv and Cross (1979, p.343) suggest that particles in a dispersed system will eventually collide due to Brownian motion for small particles, and due either to turbulent flow or settlement due to gravity for coarse particles. In clay/magnetite

systems, the possibility of collision is even greater due to the density difference between the two particle types. Once the surfaces of the particles can be brought close enough together, either van der Waal's or electrostatic forces can act to keep the particles together (Yariv and Cross, 1979, p. 348.)

Application to Natural Sediments

In these experiments, inclination shallowing occurred in a variety of clay and sediment types, and under various pH and salinity conditions. For most of the conditions, shallowing proceeded at a high rate at low pressures and continued at a very slow rate after a particular pressure had been reached (figures 31 and 33). The critical pressure fell in the range of 0.03-0.05 MPa for most sediment and clay mineral types. This pressure corresponds to extremely shallow depths of burial. Figure 36 shows the pressure vs. depth relationship developed by Hamilton (1976); a pressure of 0.05 MPa corresponds to only about 20 meters. Most paleomagnetic studies of sediments indicate that when inclination shallowing is observed in cores, it apparently occurs at depths of 150-250 meters (Celaya and Clement, 1988; Arason and Levi, 1986). The difference between depth suggested by Hamilton's overburden curve and the depth at which inclination shallowing is observed is an apparant discrepancy, but can explained by a closer examination of Hamilton's study.

Hamilton (1976) has compiled data from DSDP core samples to construct profiles of density and porosity variations for different sediment types with increasing overburden. These data can be used to compare pressures applied in the laboratory with depths in the

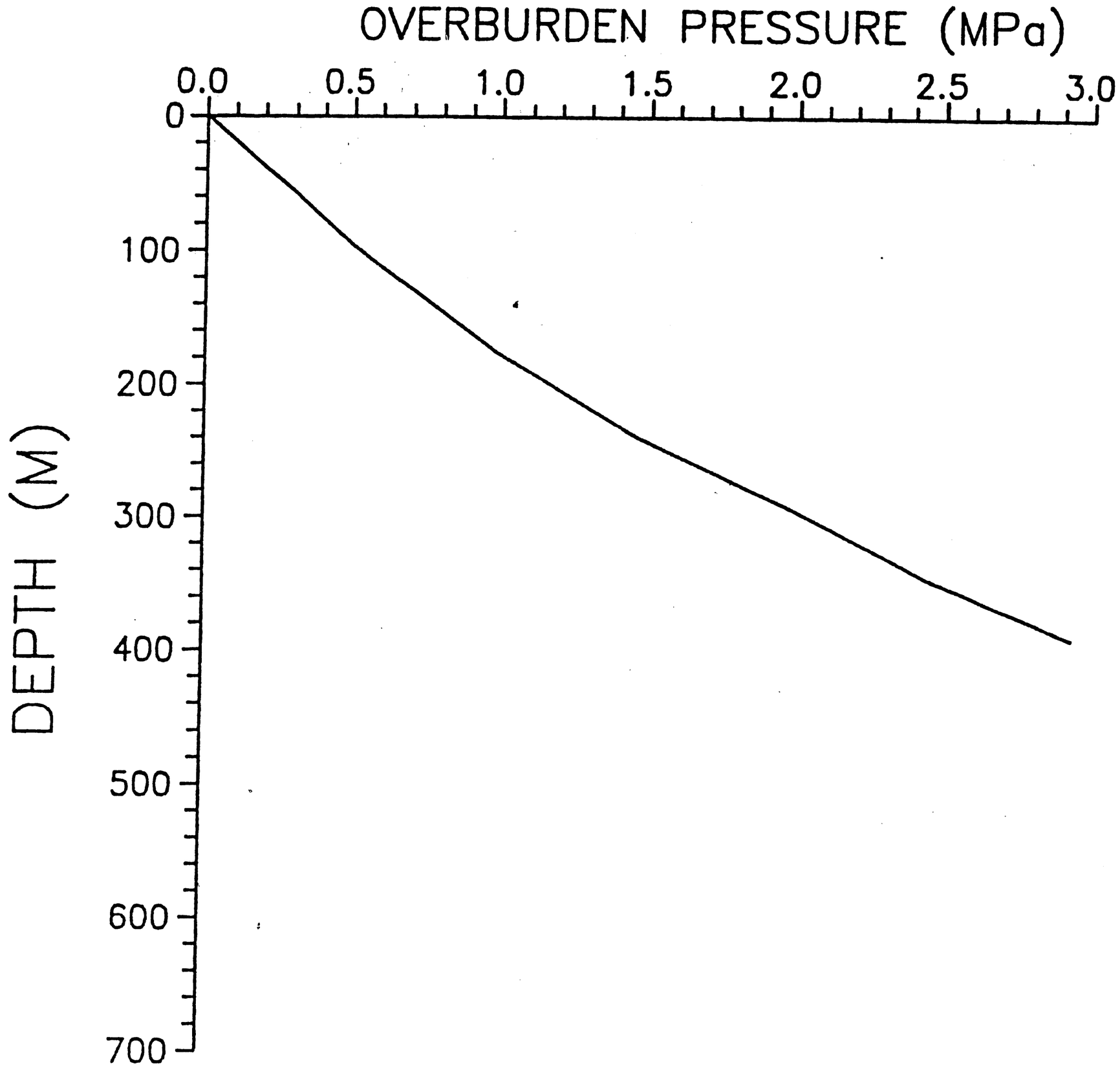

Figure 36. Plot of overburden pressure versus depth for terrigenous sediments (Hamilton, 1976).

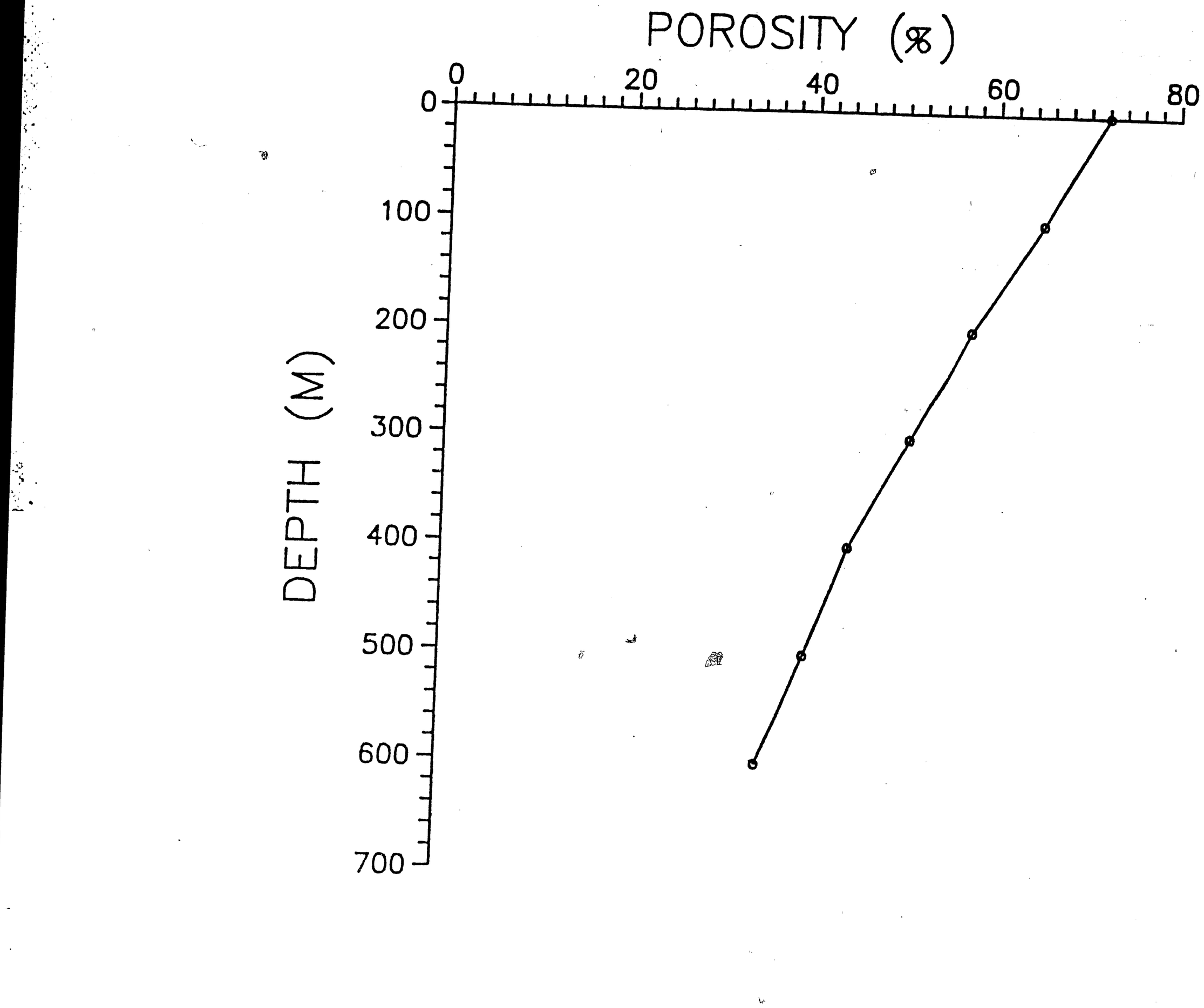

Figure 37. Plot of porosity versus depth for terrigenous sediments (from Faas and Crocket, 1983).

sediment column to predict actual density and porosities present at a particular depth. Hamilton's porosity vs. depth curve (figure 37) for terrigenous sediments shows that at 20 meters, only about 2% porosity has been lost. In comparison, the siltier natural sediment used in the current experiments, which starts with a porosity comparable to Hamilton's (73%), drops to a porosity of 55-60% at an applied pressure of 0.05 MPa (figure 38). In Hamilton's plot, this porosity would correspond to a depth of about 200 meters. Clearly, the sample measured in the lab compacts at much lower pressures than an in situ sediment. This phenomenon has long been recognized by soil scientists (ie, Mitchell, 1976), and is directly related to the way the sediment has been handled once it has been removed from its site of deposition.

Any type of mechanical working (remolding) of a natural sediment decreases its strength and it compacts at a lower pressure. The decrease in strength is probably to be due to breaking up of fabric structures and rupturing interparticle bonds which allow the sediment to compress further under increasing overburden pressures (Mitchell, 1976). Bennett, et.al. (1981) have compared the fabrics of two different sediment types (a Mississippi Delta sediment and a DSDP red clay from the equatorial Pacific Ocean), in the undisturbed and remolded states, and found that remolding creates completely different particle and domain associations.

In addition, many soft sediments experience delayed compression due to their flocculated structure, which allows increased resistance to overburden pressure. The effect of this clay structure is to make

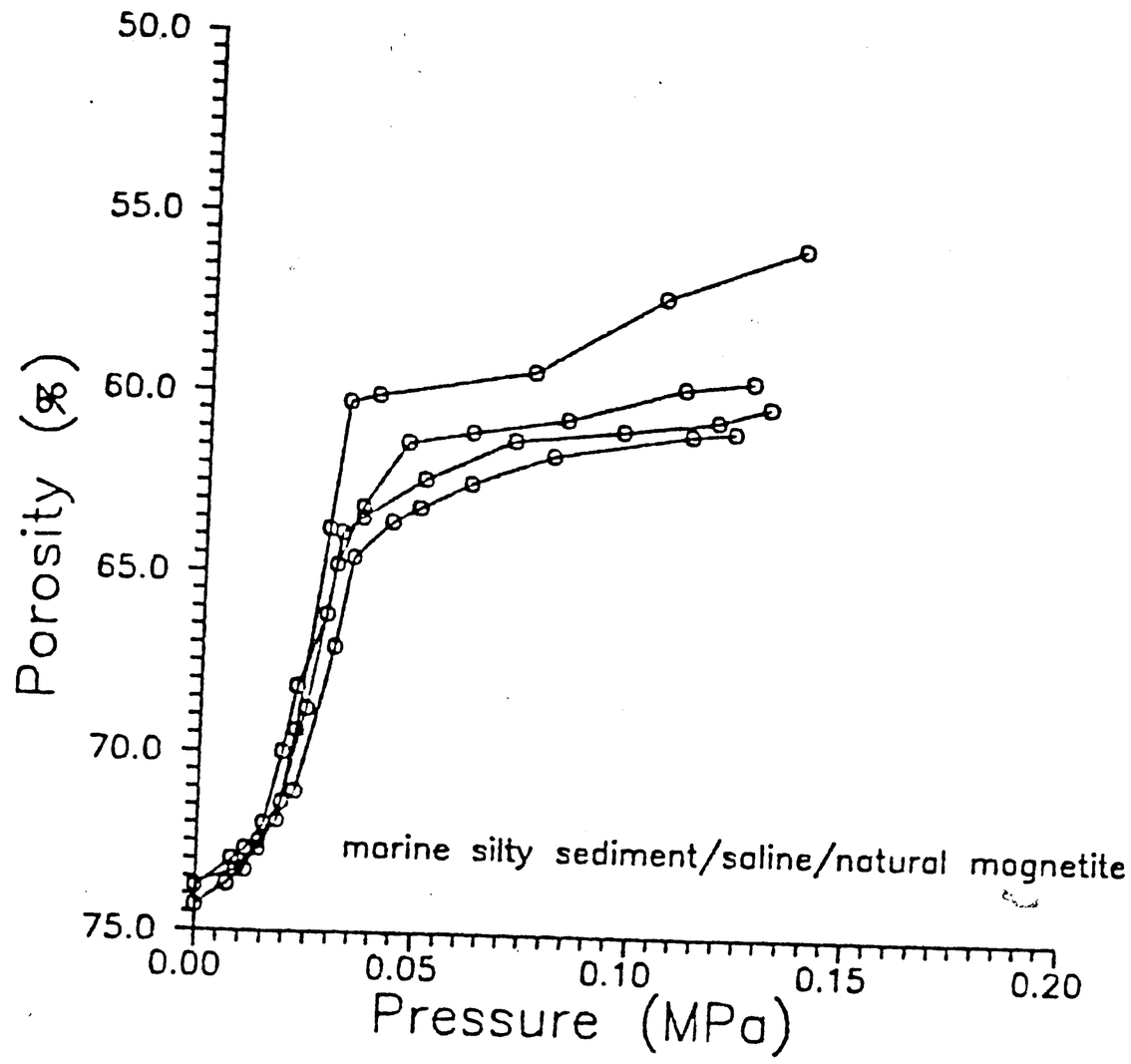

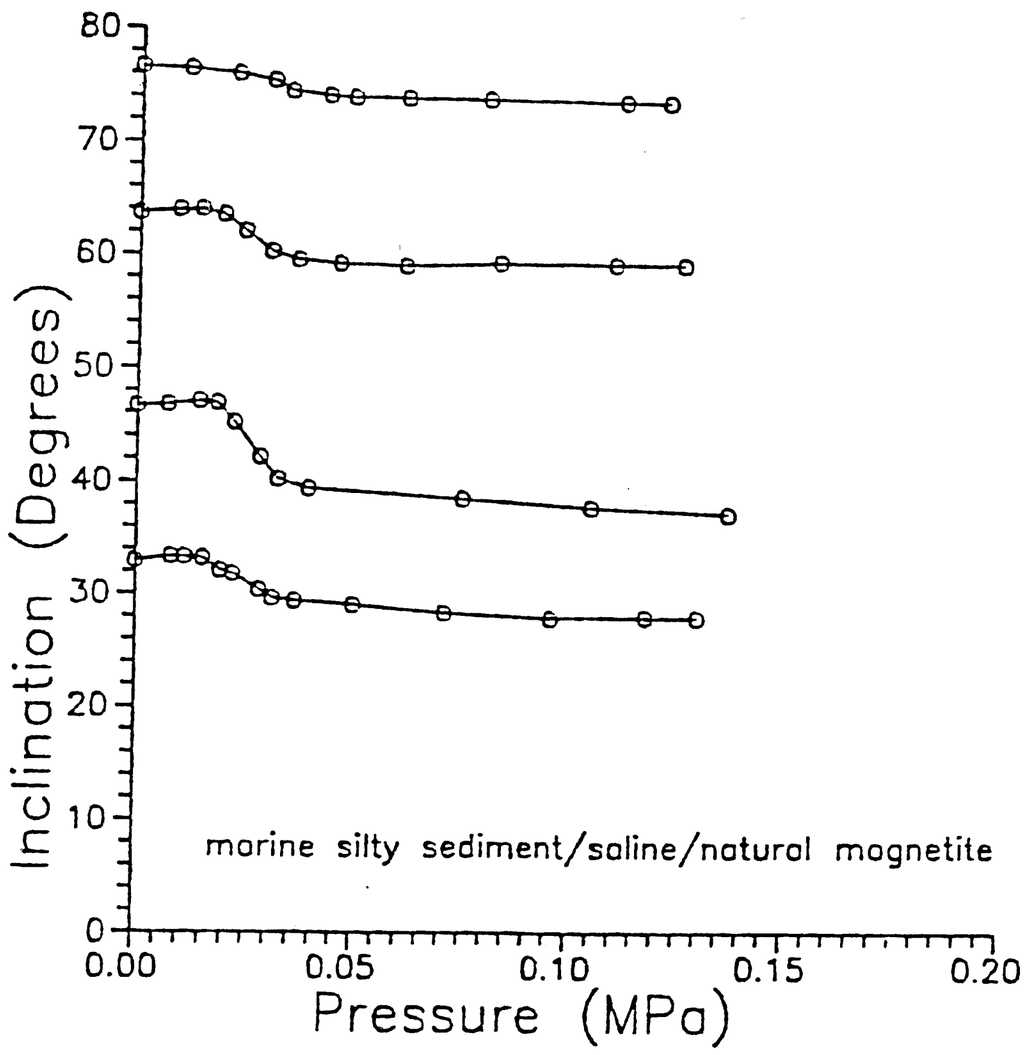

Figure 38. Plot of porosity and inclination versus compaction for silty natural sediment.

the sediment appear to be overconsolidated, so that it will not compress as readily in situ (Mitchell, 1976).

All of the slurries used in this study have been remolded. It is mixed first to make a slurry, and then again to orient the magnetite; the remolding causes the slurry sediment to compact and lose porosity at lower pressure than the in situ sediment. The effect of remolding indicates that the expected location for inclination shallowing should in fact be deeper than the pressures in our study would suggest. The pressure at which maximum compaction (dV/V) occurs for our remolded samples is therefore not a reliable indicator for predicting the depth at which inclination shallowing may occur for natural sediments. However, if the porosity of our samples is used, it may result in substantially more accurate depth predictions. The depth corresponding to the porosity marking the change in slope on the pressure versus volume (approximately 55% porosity) corresponds to a depth of about 250 meters, which is where Celeya and Clement (1988) found inclination shallowing.

CONCLUSIONS

1. The similar reaction of clay fabric orientation and inclination shallowing during compaction is evidence suggesting interaction between clay fabric units and magnetite particles. Under many conditions, the magnetite particles have a negative surface charge (as do clay minerals), indicating that the interaction is not due to electrostatic attraction. It is suggested that van der Waal's

forces may be a more likely mechanism for attraction between two particles having the same surface charge.

At some point during compaction, inclination shallowing will slow considerably. The decrease in shallowing is represented in clay-rich sediments by a change in slope on a compaction vs. pressure diagram. This is the volume change (30-60%) at which most interstitial water has been expelled, and interparticle or interdomain bonds begin to rupture.

2. Without clay minerals present in a sediment, very little inclination shallowing may occur, since clay minerals seem to be the mechanism for rotation of magnetic particles. Other studies using primarily non-clay sediments for compaction studies (Payne and Verosub, 1982, and Stamatakos, 1988) have also found these results.

3. Remolding a natural sediment causes the sediment to compact at pressures lower than an in situ sediment would. This would lead to an erroneously low depth estimate for the expected location for inclination shallowing in the sediment column. Using porosity values results in more reasonable depth estimates.

REFERENCES

Anson, G.L. and K.P. Kodama, Compaction-induced inclination shallowing of the post-depositional remanent magnetization in a synthetic sediment, Geophys. J. R. astr. Soc. 88, 673-692, 1987.

Arason, P. and S. Levi, Inclination shallowing recorded in some deep sea sediments, EOS Trans. A.G.U. 67 (64), p. 916, 1986.

Banerjee, S.K., J. King, and J. Marvin, A rapid method for magnetic granulometry with applications to environmental studies, Geophys. Res. Lett. 8 (4), 333-336, 1981.

Blow, R.A., and N. Hamilton, Effect of compaction on the acquisition of a detrital remanent magnetism in fine-grained sediments, Geophys. J. R. astr. Soc. 52, 13-23, 1978.

Bennett, R.H., W.R. Bryant, and G.H. Keller, Clay Fabric of selected submarine sediments: fundamental properties and models, J. Sed. Petrol. 51 (1), 217-232, 1981.

Celeya, M.A. and B.M. Clement, Inclination shallowing in deep-sea sediments from the North Atlantic, Geophys. Res. Lett. 15 (1), 52-55, 1988.

Collinson, D.W., Depositional remanent magnetism in sediments, J. Geophys. Res. 70, 4663-4668, 1965.

Cogne, J.P., Experimental and numerical modelling of IRM rotation in deformed synthetic samples, in Memoires et Documents du Centre Armoricain D'Etude Structurale des Socles, Rennes, France, 111-120, 1987.

Faas, R.W. and D.S. Crocket, Clay fabric development in a deep-sea core: site 515, deep sea drilling project leg 72, in Init. Repts. DSDP 72, Washington, (U.S. Government Printing Office), 519-534, 1983.

Hall, F., The effect of compaction on the magnetization of argillaceous sediments, Master's thesis, Lehigh University, 103p, 1982.

Hamano, Y., An experiment on the post-depositional remanent magnetization in artificial and natural sediments, Earth Planet. Sci. Lett. 51, 221-232, 1980.

Hamilton, E.L., Variation of density and porosity with depth in deep sea sediments, J. Sed. Petrol. 46 (2), 280-300, 1976.

Hammond, S.R., D. Epp and F. Theyer, Neogene relative motion between the Pacific plate, the mantle, and the Earth's spin axis, Nature 278, 309-312, 1979.

Irving, E., Origin of the paleomagnetism of the Torridonian sandstones of north-west Scotland, Phil. Trans. Roy. Soc. London, Ser. A, 250, 100-110, 1957.

Irving, E. and A. Major, Post-depositional remanent magnetization in a synthetic sediment, Sedimentology 3, 135-143, 1964.

King, R.F., Depositional remanent magnetization in sediments, Mon. Notic. Roy. Astron. Soc., Geophys. Suppl. 7, 115-134, 1955.

Kirschvink, J.L., The least-squares line and plane and the analysis of paleomagnetic data, Geophys. J.R. astr. Soc. 62, 699-718, 1980.

Lovlie, R., Post-depositional remanent magnetization in a re-deposited deep-sea sediment, Earth Planet. Sci. Lett. 21, 315-320, 1974.

Mayer, L.A., Physical properties of sediment recovered on DSDP leg 68 with the hydraulic piston corer, in Prell, et.al.,in Init. Repts. DSDP 68,: Washington (U.S. Govt. Printing Office), 365-382, 1982.

McConnachie, I., Fabric changes in consolidated kaolin, Geotechnique 24 (2), 207-222, 1974.

Meade, R.H., Factors influencing the early stages of the compaction of clays and sands-a review, J. Sed. Petrol. 36 (4), 1085-1101, 1965.

Mitchell, J.K., Fundamentals of Soil Behavior, Wiley and Sons, New York, 422p, 1976.

Noel, N., Surface tension phenomena in the magnetization of sediments, Geophys. J. R. astr. Soc. 62, 15-25, 1980.

Opdyke, N.D., and K.W. Henry, A test of the dipole hypothesis, Earth and Planet. Sci. Lett. 6, 139-151, 1969.

Otofuji, Y., and S. Sasajima, A magnetization process of sediments: laboratory experiments on post-depositional remanent magnetization, Geophys. J. R. astr. Soc. 66, 241-269, 1981.

Parks, G.H., The isoelectric points of solid oxides, solid hydroxides, and aqueous hydroxy complex systems, Chem. Rev. 65, 177-198, 1964.

Payne, M.A. and K.L. Verosub, The acquisition of post-depositional detrital remanent magnetism in a variety of natural sediments, Geophys. J. 68, 625-642, 1982.

Prince, R.A., G.R. Heath, and M. Kominz, Paleomagnetic studies of North Pacific sediment cores: stratigraphy, sedimentation rates, and the origin of magnetic instability, Bull. Geol. Soc. of America, Part II, 91, 1789-1835, 1980.

Quigley, R.M., and C.D. Thompson, The fabric of anisotropically sensitive marine clays, Can. Geotech. J. 3, 61-73, 1966.

Sposito, G., The Surface Chemistry of Soils, Oxford University Press, New York, 234p, 1984.

Stamatakos, J.A., K.P. Kodama, and T.L. Pavlis, EOS Trans.A.G.U., in press.

Stumm, W. and J.J.Morgan, Aquatic Chemistry, Wiley and Sons, New York, 780p, 1981.

Tauxe, L., P. Tucker, N.P. Petersen, and J.L. La Brecquc, Magnetostratigraphy of Leg 73 basalts, in Init. Repts. DSDP, 73, Washington (U.S. Gov't Printing Office), 609-621, 1984.

Tovey, N.K., and K.Y. Wong, The preparation of soils and other geological materials for the S.E.M., in Proceedings of the International Symposium on Soil Structure, Gothenburg, Sweden, 59-67, 1973.

Tucker, P., Stirred remanent magnetism: A laboratory analogue of post-depositional realignment, J. Geophys. 48, 153-157, 1980.

Van Olphen, H., An Introduction to Clay Colloid Chemistry, 2nd edition, Wiley and Sons, New York, 1977.

Verosub, K.L., Depositional and postdepositional processes in the magnetization of sediments, Rev. of Geophys. and Space Phys. 15 (2), 129-143, 1977.

Verosub, K.L., The effect of compaction on the magnetization of sediments, EOS Trans A.G.U. 68 (16), p296, 1987.

Von Englehardt, W. and K.H. Gaida, Concentration change of pore solutions during the compaction of clay sediments, J. Sed. Petrol. 33, 919-930, 1963.

Yariv, S. and H. Cross, Geochemistry of Colloid Systems, Springer-Verlag, New York, 1979.

Zidjerveld, J. D. A., Af demagnetization of rocks: analyses of results, in Methods in Paleomagnetism, ed. D.W. Collinson, K.M. Creer, and S.K.Runcorn, 254-286, Elsevier, New York, 1967.

Appendix 1

Summary of Compaction Experiments

PRESSURE (MPa)	dV/V (%)	INCLINATION (DEGREES)	INTENSITY (emu/vol)
CD1A:CHLORITE/ACICULAR MAGNETITE/SALINE/45			
0	0.00	45.90	3.300E-04
0.024	10.60	50.58	3.850E-04
0.033	22.10	53.05	4.320E-04
0.042	26.00	52.56	4.230E-04
0.057	27.60	51.78	4.180E-04
0.074	28.70	50.94	4.110E-04
0.087	29.80	50.26	4.100E-04
0.107	30.40	50.12	4.100E-04
0.122	31.20	49.64	4.030E-04
0.136	32.90	48.90	3.950E-04
0.15	32.70	48.71	4.030E-04
CD1B:CHLORITE/ACICULAR MAGNETITE/SALINE/60			
0	0.00	61.10	3.360E-04
0.022	14.50	62.25	3.480E-04
0.035	26.20	62.92	3.670E-04
0.049	29.90	63.31	3.660E-04
0.067	31.60	62.80	3.640E-04
0.086	33.40	62.01	3.590E-04
0.102	34.70	61.34	3.710E-04
0.126	35.70	61.73	3.450E-04
0.14	36.30	60.53	3.350E-04
0.148	36.60	59.98	3.270E-04
CD28:CHLORITE/ACICULAR MAGNETITE/SALINE/60			
0	0.00	75.41	4.820E-04
0.014	14.90	74.90	4.500E-04
0.027	23.40	75.17	4.600E-04
0.059	26.20	75.06	4.880E-04
0.077	28.50	74.86	4.830E-04
0.087	29.20	74.40	4.760E-04
0.104	30.20	73.80	4.840E-04
0.111	30.90	73.91	4.770E-04
0.133	32.10	73.30	4.610E-04
0.157	32.80	73.53	4.610E-04
CN30B:CHLORITE/ACICULAR MAGNETITE/SALINE/30			
0	0.00	35.81	4.030E-04
0.019	10.90	34.60	4.100E-04
0.029	19.00	35.64	4.650E-04
0.042	22.70	35.59	4.640E-04
0.055	27.10	34.89	4.560E-04
0.075	29.20	34.72	4.610E-04
0.089	30.90	34.14	4.650E-04
0.104	32.20	33.55	4.560E-04
0.135	34.50	32.69	4.430E-04
0.145	34.50	32.85	4.400E-04

PRESSURE (MPa)	dV/V (%)	INCLINATION (DEGREES)	INTENSITY (emu/vol)
MD3A:MONTMORILLONITE/ACICULAR/SALINE/75			
0	0.00	76.44	4.450E-04
0.02	6.90	75.97	4.390E-04
0.035	27.40	72.35	3.480E-04
0.042	35.80	70.48	3.000E-04
0.051	39.20	69.59	2.810E-04
0.062	42.20	68.89	2.680E-04
0.073	44.10	68.21	2.560E-04
0.099	46.80	67.44	2.400E-04
0.119	48.80	67.01	2.350E-04
0.126	50.30	66.47	2.260E-04
MD3B:MONTMORILLONITE/ACICULAR/SALINE/60			
0	0.00	62.01	3.280E-04
0.021	3.90	64.10	2.780E-04
0.035	31.20	59.60	2.400E-04
0.048	42.30	55.60	2.050E-04
0.075	50.00	52.70	1.790E-04
0.107	53.70	51.07	1.700E-04
0.126	55.70	50.37	1.640E-04
0.135	56.10	50.02	1.610E-04
MD4A:MONTMORILLONITE/ACICULAR/SALINE/45			
0	0.00	46.99	4.260E-04
0.024	11.00	46.62	4.200E-04
0.031	24.40	43.75	3.840E-04
0.041	34.10	41.16	3.520E-04
0.049	40.50	38.96	3.270E-04
0.059	44.90	37.40	3.130E-04
0.075	49.20	35.93	2.980E-04
0.093	52.20	34.65	2.840E-04
0.102	53.50	34.13	2.780E-04
0.115	57.40	33.47	2.720E-04
0.13	56.50	33.14	2.670E-04
0.133	59.50	32.63	2.620E-04
MD4B:MONTMORILLONITE/ACICULAR/SALINE/30			
0	0.00	35.02	6.500E-04
0.017	14.90	33.40	6.070E-04
0.026	24.80	31.56	5.580E-04
0.045	37.90	28.84	5.090E-04
0.056	43.20	27.51	4.530E-04
0.079	49.10	25.86	4.610E-04
0.086	50.50	25.46	4.540E-04
0.101	52.40	24.91	4.520E-04
0.126	54.80	24.30	4.490E-04
0.135	55.70	24.13	4.440E-04

PRESSURE (MPa)	dV/V (%)	INCLINATION (DEGREES)	INTENSITY (emu/vol)
MMD14B:MARINE SEDIMENT/NATURAL MAGNETITE/75			
0	0.00	76.72	2.050E-04
0.01	3.90	76.32	2.060E-04
0.017	11.70	76.30	1.970E-04
0.023	22.90	75.09	1.770E-04
0.033	35.20	74.15	1.610E-04
0.042	45.40	72.90	1.400E-04
0.053	49.70	72.20	1.310E-04
0.07	52.40	71.90	1.260E-04
0.081	53.30	71.75	1.250E-04
0.1	54.60	71.60	1.230E-04
0.118	55.40	71.60	1.210E-04
MMD14B:MARINE SEDIMENT/NATURAL MAGNETITE/60			
0	0.00	56.39	1.520E-04
0.01	1.00	56.29	1.540E-04
0.019	10.60	55.28	1.470E-04
0.027	19.80	53.61	1.410E-04
0.037	34.00	51.12	1.210E-04
0.046	46.10	47.12	1.090E-04
0.057	48.80	46.34	1.070E-04
0.071	50.80	45.34	9.870E-05
0.086	51.80	44.87	1.010E-04
0.1	52.60	44.65	1.000E-04
0.121	54.30	43.92	9.830E-05
0.135	54.50	43.95	9.830E-05
MMD11B:MARINE SEDIMENT NATURAL MAGNETITE/45			
0	0.00	45.80	1.680E-04
0.016	3.60	45.60	1.710E-04
0.02	11.00	45.03	1.650E-04
0.027	27.10	42.94	1.500E-05
0.032	39.70	40.66	1.370E-04
0.041	47.40	38.96	1.260E-04
0.048	49.80	38.58	1.230E-04
0.06	52.30	37.97	1.250E-04
0.079	54.60	37.07	1.170E-04
0.095	55.70	36.69	1.160E-04
0.11	56.70	36.39	1.150E-04
0.124	57.60	36.37	1.140E-04

MMD11:MARINE	SEDIMENT/NATURAL		MAGNETITE/30
0	0.00	35.11	1.870E-04
0.015	1.80	35.14	1.880E-04
0.02	4.30	34.99	1.870E-04
0.024	10.10	34.25	1.800E-04
0.031	24.70	32.61	1.660E-04
0.038	34.10	30.90	1.570E-04
0.046	42.70	28.78	1.480E-04
0.057	47.40	27.87	1.420E-04
0.074	50.20	26.85	1.380E-04
0.089	53.00	25.40	1.390E-04
0.106	54.30	25.38	1.380E-04
0.121	54.90	25.11	1.370E-04
0.127	55.70	24.97	1.360E-04
0.14	56.10	24.78	1.360E-04

PRESSURE (MPa)	dV/V (%)	INCLINATION (DEGREES)	INTENSITY (emu/vol)
MSD16:MARINE SILTY SEDIEMNT/NATURAL MAGNETI			
0	0.00	76.63	1.310E-04
0.011	2.00	76.37	1.320E-04
0.022	10.70	75.91	1.190E-04
0.03	23.70	75.29	1.070E-04
0.034	30.00	74.33	9.540E-05
0.043	32.90	73.94	9.890E-05
0.049	33.50	73.79	8.730E-05
0.061	35.10	73.74	8.510E-05
0.08	37.10	73.60	8.210E-05
0.112	38.60	73.33	8.010E-05
0.122	38.70	73.30	7.930E-05
MSD17:MARINE SILTY SEDIMENT/NATURAL MAGNETI			
0	0.00	63.59	1.080E-04
0.009	0.20	63.84	1.040E-04
0.014	2.40	63.88	1.000E-04
0.019	5.10	63.37	9.680E-05
0.024	9.40	61.91	8.760E-05
0.03	17.90	60.14	7.560E-05
0.036	29.10	59.38	7.080E-05
0.046	32.90	59.06	6.860E-05
0.061	37.00	58.88	6.700E-05
0.083	38.10	59.15	6.460E-05
0.11	39.60	58.98	6.340E-05
0.126	40.00	58.92	6.280E-05
MSD17B:MARINE SILTY SEDIMENT/NATURAL MAGNET			
0	0.00	46.59	9.610E-05
0.007	0.70	46.71	9.660E-05
0.014	4.30	46.97	9.430E-05
0.018	7.80	46.82	9.200E-05
0.022	16.40	45.10	8.810E-05
0.028	31.20	42.05	7.360E-05
0.032	38.60	40.11	6.770E-05
0.039	39.20	39.27	6.500E-05
0.075	40.40	38.39	6.220E-05
0.105	43.50	37.63	5.950E-05
0.137	45.90	37.04	5.820E-05

MSD18:MARINE	SILTY	SEDIMENT/NATURAL	MAGNETI
0	0.00	32.91	1.220E-04
0.008	3.10	33.31	1.260E-04
0.011	4.60	33.24	1.240E-04
0.015	7.60	33.11	1.220E-04
0.019	15.60	32.02	1.150E-04
0.022	21.90	31.69	1.110E-04
0.028	28.30	30.31	1.050E-04
0.031	34.40	29.55	9.820E-05
0.036	35.20	29.29	9.510E-05
0.05	38.10	28.95	9.280E-05
0.071	40.50	28.25	9.100E-05
0.096	41.30	27.79	8.970E-05
0.118	41.80	27.88	8.850E-05
0.13	42.50	27.82	8.760E-05

PRESSURE (MPa)	dV/V (%)	INCLINATION (DEGREES)	INTENSITY (EMU/VOL)
IL1030:ILLITE/ACICULAR MAGNETITE/WATER/60			
0.000	0.00	58.82	3.460E-04
0.026	11.20	59.84	3.390E-04
0.035	18.20	58.50	2.880E-04
0.047	27.40	55.96	2.630E-04
0.057	33.50	54.77	2.400E-04
0.067	40.50	51.87	2.170E-04
0.078	42.70	50.14	2.050E-04
0.093	44.50	49.83	2.040E-04
0.110	44.60	50.50	2.000E-04
0.110	45.60	49.89	1.970E-04
IL112:ILLITE/ACICULAR MAGNETITE/WATER/75			
0.000	0.00	74.83	6.760E-04
0.014	2.30	73.63	6.260E-04
0.022	6.20	73.64	6.400E-04
0.028	14.20	73.47	5.920E-04
0.038	23.40	72.56	5.390E-04
0.046	33.50	71.08	4.670E-04
0.060	38.50	70.62	4.330E-04
0.064	41.80	70.05	4.150E-04
0.079	42.90	68.96	4.090E-04
0.100	44.60	68.52	4.020E-04
0.116	45.70	68.43	4.020E-04
0.125	46.20	68.08	4.000E-04
IL113A:ILLITE/ACICULAR MANGETITE/WATER/45			
0.000	0.00	44.76	5.140E-04
0.013	3.00	44.59	4.980E-04
0.022	4.80	44.40	4.900E-04
0.032	12.80	44.14	4.840E-04
0.044	19.30	43.03	4.610E-04
0.058	30.30	39.77	4.470E-04
0.070	35.60	38.40	4.350E-04
0.081	40.60	36.85	4.290E-04
0.121	51.80	31.74	3.820E-04
IL113B:ILLITE/ACICULAR MAGNETITE/WATER/30			
0.000	0.00	32.10	8.200E-04
0.031	19.60	31.43	8.060E-04
0.042	24.30	30.11	7.600E-04
0.057	32.70	28.07	7.220E-04
0.066	38.20	26.95	7.140E-04
0.077	47.00	24.14	6.890E-04
0.091	53.10	21.75	6.590E-04
0.111	54.40	21.11	6.480E-04

PRESSURE (MPa)	dV/V (%)	INCLINATION (DEGREES)	INTENSITY (EMU/VOL)
CHLN15:CHLORITE/ACICULAR MAGNETITE/WATER/75			
0.000	0.00	76.92	5.170E-04
0.017	6.80	77.00	5.010E-04
0.038	13.00	75.95	4.900E-04
0.056	15.70	75.96	4.730E-04
0.074	17.80	75.57	4.710E-04
0.082	18.90	75.20	4.700E-04
0.108	20.50	74.88	4.740E-04
0.126	21.50	74.32	4.740E-04
0.141	21.90	74.45	4.740E-04
0.155	23.00	74.43	4.860E-04
0.172	23.30	74.04	4.900E-04
0.188	24.00	73.42	4.910E-04
0.195	24.30	73.68	5.000E-04
CHN4:CHLORITE/ACICULAR MAGNETITE/WATER/45			
0.000	0.00	47.61	4.520E-04
0.017	11.00	51.59	4.400E-04
0.022	19.00	54.32	4.040E-04
0.038	26.20	54.52	4.250E-04
0.046	28.20	54.44	4.230E-04
0.064	29.30	53.80	4.490E-04
0.085	29.90	53.12	4.440E-04
0.110	31.00	53.08	4.390E-04
0.136	33.80	52.15	4.310E-04
0.155	33.30	51.80	4.270E-04
0.165	34.30	51.13	4.400E-04
0.176	34.30	50.84	4.340E-04
0.185	35.50	50.89	4.450E-04
0.193	36.40	49.47	4.360E-04
0.204	38.50	49.78	4.330E-04
CHN14:CHLORITE/ACICULAR MAGNETITE/WATER/60			
0.000	0.00	62.48	4.130E-04
0.015	5.40	64.04	4.100E-04
0.024	22.40	66.04	3.940E-04
0.033	26.40	65.12	3.780E-04
0.044	27.70	64.90	3.980E-04
0.053	29.30	65.00	4.040E-04
0.064	30.70	65.46	3.950E-04
0.094	32.70	64.24	4.000E-04
0.108	35.70	65.15	4.000E-04
0.127	34.70	64.82	3.980E-04

CHN16:CHLORITE/ACICULAR MAGNETITE/WATER/30

0.000	0.00	33.64	6.560E-04
0.029	15.60	34.46	6.850E-04
0.046	18.60	33.77	6.760E-04
0.059	18.90	33.26	6.730E-04
0.102	19.80	31.92	6.980E-04
0.128	22.20	32.76	6.780E-04
0.163	22.90	32.18	6.860E-04
0.179	24.60	31.00	6.870E-04

PRESSURE (MPa)	dV/V (%)	INCLINATION (DEGREES)	INTENSITY (EMU/VOL)
KN17A:KAOLINITE/ACICULAR MAGNETITE/WATER/30			
0.000	0.00	32.18	9.120E-05
0.020	3.20	30.91	8.020E-05
0.036	21.50	28.78	7.420E-05
0.047	36.80	26.75	7.150E-05
0.059	42.70	25.85	6.890E-05
0.076	46.60	23.71	6.620E-05
0.089	47.20	23.60	6.550E-05
0.099	47.50	23.44	6.530E-05
0.099	48.30	22.83	6.490E-05
KN17B:KAOLINITE/ACICULAR MAGNETITE/WATER/45			
0.000	0.00	47.79	6.630E-05
0.003	4.40	48.68	5.560E-05
0.030	27.30	46.63	4.910E-05
0.047	46.50	43.29	4.290E-05
0.064	51.40	41.43	4.120E-05
0.080	53.40	40.45	4.000E-05
0.094	54.60	39.91	3.920E-05
0.109	56.10	39.63	3.870E-05
KN18A:KAOLINITE/ACICULAR MAGNETITE/WATER/60			
0.000	0.00	62.47	5.790E-05
0.016	5.80	62.93	6.080E-05
0.027	19.70	62.04	5.650E-05
0.038	39.50	58.93	5.020E-05
0.049	42.00	58.56	4.910E-05
0.068	43.60	58.24	4.810E-05
0.085	45.60	57.48	4.670E-05
0.101	47.00	57.33	4.790E-05
0.116	48.00	57.32	4.740E-05
0.116	48.80	57.03	4.740E-05
KN18B:KAOLINITE/ACICULAR MAGNETITE/WATER/75			
0.000	0.00	76.10	9.210E-05
0.016	5.20	75.92	8.400E-05
0.024	19.40	75.73	7.690E-05
0.027	32.80	74.90	7.130E-05
0.032	42.10	73.85	6.420E-05
0.038	46.50	72.69	6.090E-05
0.048	49.80	71.81	5.750E-05
0.068	53.30	70.94	5.580E-05
0.085	57.70	70.19	5.310E-05
0.129	59.00	69.56	5.140E-05

PRESSURE (MPa)	dV/V (%)	INCLINATION (DEGREES)	INTENSITY (EMU/VOL)
MN20A:MONTMORILLONITE/ACICULAR MAGNETITE/WATER/75			
0.000	0.00	76.60	2.160E-04
0.022	11.50	75.31	1.960E-04
0.029	20.70	75.25	1.870E-04
0.034	24.20	74.81	1.820E-04
0.046	34.20	74.09	1.800E-04
0.078	45.80	73.06	1.720E-04
0.093	51.40	72.34	1.690E-04
MN19B:MONTMORILLONITE/ACICULAR MAGNETITE/WATER/60			
0.000	0.00	62.20	1.840E-04
0.023	13.00	62.06	1.780E-04
0.041	21.80	61.44	1.740E-04
0.052	28.90	60.44	1.690E-04
0.068	36.10	59.91	1.660E-04
0.078	40.90	59.30	1.640E-04
0.082	42.90	58.82	1.630E-04
0.093	51.60	56.38	1.590E-04
0.102	57.10	54.71	1.560E-04
0.107	59.60	53.75	1.530E-04
0.113	62.40	52.73	1.570E-04
0.116	64.00	52.33	1.550E-04
0.119	66.20	52.12	1.510E-04
0.126	68.60	51.01	1.490E-04
MN21:MONTMORILLONITE/ACICULAR MAGNETITE/WATER/45			
0.000	0.00	48.09	1.860E-04
0.019	10.70	48.02	1.730E-04
0.025	15.80	47.70	1.690E-04
0.035	21.50	46.94	1.690E-04
0.050	29.70	45.46	1.650E-04
0.077	41.80	43.69	1.630E-04
0.097	51.00	39.78	1.590E-04
0.126	61.60	36.29	1.660E-04
0.126	61.60	37.05	1.650E-04
MN22:MONTMORILLONITE/ACICULAR MAGNETITE/WATER/30			
0.000	0.00	34.56	1.820E-04
0.024	4.00	33.83	1.760E-04
0.046	21.20	31.82	1.670E-04
0.059	28.60	30.93	1.610E-04
0.066	32.70	30.24	1.650E-04
0.082	42.90	28.66	1.660E-04
0.098	53.50	27.11	1.640E-04

PRESSURE (MPa)	dV/V (%)	INCLINATION (DEGREES)	INTENSITY (EMU/VOL)
IN24B:ILLITE/ACICULAR MAGNETITE/SALINE/75			
0.000	0.00	73.41	6.420E-04
0.036	25.60	74.85	5.250E-04
0.045	33.70	72.80	4.330E-04
0.053	36.80	70.50	4.170E-04
0.071	41.90	69.40	3.620E-04
0.080	43.30	68.30	3.550E-04
0.089	43.70	68.00	3.500E-04
0.103	44.60	67.30	3.430E-04
0.119	45.60	68.45	3.360E-04
0.141	46.70	68.55	3.370E-04
IN24A:ILLITE/ACICULAR MAGNETITE/SALINE/60			
0.000	0.00	64.47	5.180E-04
0.020	4.80	64.30	4.730E-04
0.030	13.10	64.20	4.390E-04
0.042	25.90	62.80	3.770E-04
0.053	31.50	61.05	3.290E-04
0.065	34.50	60.20	3.200E-04
0.075	35.30	60.10	3.120E-04
0.092	37.30	59.30	3.020E-04
0.110	37.90	59.00	3.000E-04
0.126	39.20	58.60	2.970E-04
0.137	39.70	58.20	2.950E-04
IN23B"ILLITE/ACICULAR MAGNETITE/SALINE/45			
0.000	0.00	47.53	8.060E-04
0.020	5.30	47.96	7.660E-04
0.027	17.40	46.45	6.710E-04
0.034	25.60	45.10	6.110E-04
0.042	32.20	43.30	5.760E-04
0.057	34.60	40.96	5.760E-04
0.078	36.00	40.36	5.690E-04
0.096	36.80	40.06	5.720E-04
0.107	37.90	39.98	5.630E-04
0.127	38.60	39.66	5.540E-04
0.127	39.30	39.43	5.500E-04
IN23:ILLITE/ACICULAR MAGNETITE/SALINE/30			
0.000	0.00	30.10	7.650E-04
0.017	3.63	33.95	7.030E-04
0.031	17.60	32.22	6.500E-04
0.041	30.10	28.48	5.890E-04
0.053	34.40	27.78	5.610E-04
0.082	34.70	27.05	5.430E-04
0.099	36.00	26.61	5.290E-04
0.114	36.70	26.46	5.440E-04
0.129	37.50	26.36	5.400E-04

PRESSURE (MPa)	dV/V (%)	INCLINATION (DEGREES)	INTENSITY (EMU/VOL)
KN25A:KAOLINITE/ACICULAR MAGNETITE/SALINE/75			
0.000	0.00	74.37	7.220E-04
0.021	7.70	74.96	7.480E-04
0.028	13.80	75.46	6.320E-04
0.037	25.60	75.76	5.810E-04
0.046	41.20	73.44	5.360E-04
0.053	44.80	73.10	5.110E-04
0.062	48.40	72.13	4.790E-04
0.067	48.90	72.37	4.810E-04
0.071	49.30	72.15	4.770E-04
0.078	50.30	71.84	4.710E-04
0.082	51.10	71.60	4.630E-04
0.097	52.00	71.55	4.480E-04
0.118	54.50	71.59	4.390E-04
0.118	54.60	71.35	4.300E-04
KN25B:KAOLINITE/ACICULAR MAGNETITE/SALINE/60			
0.000	0.00	65.84	6.290E-04
0.017	7.70	63.96	5.810E-04
0.020	10.90	63.31	5.310E-04
0.030	31.30	59.76	4.710E-04
0.039	37.30	57.02	4.400E-04
0.049	44.20	56.04	4.240E-04
0.064	46.20	55.70	4.120E-04
0.072	47.20	55.34	4.070E-04
0.082	48.50	55.29	4.090E-04
0.099	49.40	55.13	4.020E-04
0.114	50.90	54.32	4.060E-04
0.126	51.90	53.87	4.020E-04
KN26:KAOLINITE/ACICULAR MAGNETITE/SALINE/45			
0.000	0.00	42.20	8.420E-04
0.020	5.00	42.67	7.780E-04
0.025	11.50	41.80	6.900E-04
0.036	29.80	38.83	6.390E-04
0.042	39.70	37.23	6.040E-04
0.053	46.60	35.11	5.840E-04
0.064	49.00	34.50	5.700E-04
0.081	51.10	33.40	5.590E-04
0.097	52.20	32.72	5.650E-04
0.113	53.50	32.75	5.580E-04
0.121	54.30	31.88	5.780E-04
0.127	55.00	31.38	5.550E-04

KN30A:KAOLINITE/ACICULAR MAGNETITE/SALINE/30

0.000	0.00	30.23	9.810E-04
0.018	9.90	30.65	9.350E-04
0.022	16.00	29.80	9.050E-04
0.034	28.80	28.51	8.680E-04
0.042	44.90	25.56	8.210E-04
0.050	47.70	24.24	8.020E-04
0.064	49.50	24.09	8.040E-04
0.083	51.80	24.39	7.940E-04
0.096	53.70	23.92	7.850E-04
0.108	54.20	23.59	7.730E-04
0.119	54.70	23.34	7.740E-04
0.130	55.40	23.34	7.690E-04
0.141	56.30	22.71	7.630E-04

PRESSURE (MPa)	dV/V (%)	INCLINATION (DEGREES)	INTENSITY (EMU/VOL)
REJ112:RECONSTRUCTED SEDIMENT/NATURAL MAGNETITE/SALINE/75			
0	0.00	76.120	3.070E-04
0.013	3.30	76.680	3.020E-04
0.017	8.80	76.140	2.920E-04
0.023	23.50	74.190	2.440E-04
0.027	29.20	73.910	2.270E-04
0.036	35.20	73.690	2.100E-04
0.047	37.60	73.770	2.050E-04
0.056	38.40	73.080	2.020E-04
0.082	40.20	72.260	1.950E-04
0.124	43.90	72.360	1.880E-04
0.146	43.90	71.560	1.850E-04
REJ11A:RECONSTRUCTED SEDIMENT/NATURAL MAGNETITE/SALINE/60			
0	0.00	67.270	2.470E-04
0.014	7.80	68.430	2.420E-04
0.017	14.80	67.130	2.120E-04
0.022	31.00	65.200	1.920E-04
0.027	36.80	64.660	1.800E-04
0.031	37.90	64.310	1.780E-04
0.048	39.60	63.840	1.740E-04
0.087	42.30	63.590	1.680E-04
0.121	43.90	63.110	1.650E-04
0.129	44.80	63.120	1.630E-04
REJ11:RECONSTRUCTED SEDIMENT/NATURAL MAGNETITE/SALINE/45			
0	0.00	49.440	2.490E-04
0.014	4.60	52.810	2.520E-04
0.017	8.30	52.460	2.300E-04
0.021	15.10	51.920	2.110E-04
0.024	19.20	51.880	1.980E-04
0.031	21.70	50.920	1.960E-04
0.04	24.40	49.930	1.910E-04
0.054	25.60	49.820	1.890E-04
0.077	28.10	49.310	1.860E-04
0.097	30.10	49.460	1.800E-04
0.122	31.20	48.550	1.770E-04
0.154	33.20	47.760	1.720E-04

REJ13:RECONSTRUCTED SEDIMENT/NATURAL SEDIMMENT/SALINE/30

0	0.00	35.960	3.070E-04
0.012	2.10	36.780	3.040E-04
0.019	6.10	36.290	2.940E-04
0.025	13.10	34.690	2.830E-04
0.031	23.90	33.990	2.560E-04
0.041	29.10	33.220	2.400E-04
0.05	32.10	32.560	2.320E-04
0.074	33.90	31.770	2.280E-04
0.099	35.50	31.780	2.240E-04
0.127	37.20	31.340	2.200E-04
0.143	37.90	30.800	2.190E-04

PRESSURE (MPa)	dV/V (%)	INCLINATION (DEGREES)	INTENSITY (EMU/VOL)
CD29:CHLORITE/EQUI-MAGNETITE/WATER/50			
0	0.00	57.880	1.240E-04
0.011	4.10	61.820	1.340E-04
0.024	10.30	61.430	1.330E-04
0.03	13.30	60.100	1.320E-04
0.041	15.70	59.740	1.320E-04
0.062	18.40	58.170	1.290E-04
0.097	23.60	56.930	1.260E-04
0.119	26.70	55.710	1.220E-04
0.135	27.30	55.150	1.200E-04
0.144	28.30	54.430	1.170E-04
0.15	29.60	53.470	1.160E-04
ID28:ILLITE/EQUI-MAGNETITE/WATER/50			
0	0.00	50.910	1.760E-04
0.011	1.10	52.650	1.670E-04
0.017	2.30	54.340	1.520E-04
0.022	6.30	52.600	1.350E-04
0.027	15.80	50.110	1.080E-04
0.031	24.10	49.650	9.520E-05
0.037	32.70	49.910	9.030E-05
0.049	34.80	49.400	8.630E-05
0.069	36.30	49.030	8.290E-05
0.082	38.20	48.620	8.100E-05
0.101	38.60	48.110	7.790E-05
0.127	39.40	47.770	7.560E-05
0.138	40.50	47.800	7.400E-05
KD29:KAOLINITE/EQUI-MAGNETITE/WATER/50			
0	0.00	53.500	2.000E-05
0.014	2.70	54.530	1.910E-05
0.019	10.60	57.900	1.720E-05
0.022	18.60	57.600	1.620E-05
0.025	25.10	57.440	1.530E-05
0.029	31.30	56.200	1.440E-05
0.039	38.90	56.230	1.390E-05
0.05	42.90	56.340	1.340E-05
0.063	45.30	55.370	1.310E-05
0.105	49.30	54.310	1.250E-05
0.137	53.50	54.580	1.200E-05

MD30:MONTMORILLONITE/EQUI-MAGNETITE/WATER/50

0	0.00	52.230	1.650E-04
0.014	1.10	51.900	1.640E-04
0.019	2.10	52.100	1.620E-04
0.024	6.20	52.000	1.570E-04
0.031	9.60	51.600	1.530E-04
0.042	14.60	51.300	1.490E-04
0.051	19.00	50.600	1.440E-04
0.07	25.30	50.400	1.380E-04
0.091	31.20	49.800	1.320E-04
0.101	37.30	49.100	1.280E-04
0.124	42.60	48.100	1.220E-04
0.137	47.10	47.400	1.180E-04
0.155	54.40	45.800	1.120E-04
0.155	61.40	43.200	1.070E-04

PRESSURE (MPa)	dV/V (%)	INCLINATION (DEGREES)	INTENSITY (EMU/VOL)
CD26:CHLORITE/EQUI-MAGNETITE/SALINE/50			
0	0.00	59.840	1.280E-04
0.009	3.20	61.740	1.430E-04
0.015	15.10	60.190	1.300E-04
0.02	20.30	60.490	1.450E-04
0.027	26.20	60.030	1.470E-04
0.035	29.50	59.290	1.470E-04
0.043	31.90	58.600	1.470E-04
0.057	33.70	57.940	1.470E-04
0.078	35.80	57.340	1.430E-04
0.194	36.30	56.850	1.380E-04
0.132	37.40	56.240	1.340E-04
0.146	38.50	55.790	1.290E-04
ID22:ILLITE/EQUI-MAGNETITE/SALINE/50			
0	0.00	52.980	1.900E-04
0.013	1.90	54.240	1.910E-04
0.017	6.20	54.410	1.910E-04
0.02	10.20	54.720	1.800E-04
0.025	19.10	53.920	1.650E-04
0.031	25.90	53.100	1.490E-04
0.035	30.90	51.700	1.400E-04
0.039	34.60	50.690	1.300E-04
0.046	38.40	49.380	1.190E-04
0.055	40.10	48.970	1.140E-04
0.069	41.50	48.590	1.100E-04
0.083	42.30	48.290	1.070E-04
0.1	43.20	48.020	1.050E-04
0.118	43.90	47.650	1.020E-04
0.131	44.60	47.540	1.000E-04
KD22B:KAOLINITE/EQUI-MAGNETITE/SALINE/50			
0	0.00	47.250	2.040E-04
0.016	2.30	46.920	2.000E-04
0.027	13.20	44.300	1.870E-04
0.039	38.20	39.620	1.680E-04
0.046	41.50	36.260	1.710E-04
0.057	46.20	34.620	1.650E-04
0.074	49.10	32.950	1.640E-04
0.089	50.70	32.610	1.610E-04
0.105	50.80	32.070	1.600E-04
0.126	52.80	31.550	1.580E-04
0.132	53.70	31.440	1.570E-04
0.144	53.70	31.370	1.570E-04

MD23:MONTMORILLONITE/EQUI-MAGNETITE/SALINE/50

0	0.00	53.720	1.820E-04
0.009	1.60	54.630	1.740E-04
0.013	4.10	55.710	1.690E-04
0.024	10.70	55.650	1.600E-04
0.027	16.30	55.160	1.520E-04
0.035	25.90	52.950	1.340E-04
0.04	30.80	51.840	1.220E-04
0.044	34.10	51.130	1.140E-04
0.049	38.30	49.030	1.050E-04
0.057	40.80	48.330	9.910E-05
0.068	42.90	47.750	9.470E-05
0.08	46.50	46.710	8.710E-05
0.093	48.60	46.160	8.290E-05
0.111	50.30	46.830	7.750E-05
0.124	51.40	46.500	7.520E-05
0.129	52.20	46.290	7.420E-05

PRESSURE (MPa)	dV/V (%)	INCLINATION (DEGREES)	INTENSITY (EMU/VOL)
IF2:ILLITE/NATURAL+EQUI-MAGNETITE/WATER/60			
0	0.00	57.600	2.650E-04
0.013	1.80	56.770	2.560E-04
0.016	4.10	57.380	2.480E-04
0.02	13.50	56.750	2.420E-04
0.024	21.80	55,360	2.300E-04
0.027	26.60	54.750	2.210E-04
0.031	29.80	53.900	2.140E-04
0.039	33.00	53.210	2.080E-04
0.055	35.30	52.420	2.050E-05
0.069	36.30	52.350	2.020E-05
0.119	38.90	51.630	1.980E-05
0.137	39.60	51.590	1.970E-05
KJ15:KAOLINITE/NATURAL +EQUI-MAGNETITE/WATER/60			
0	0.00	64.610	2.410E-04
0.019	8.80	65.230	2.370E-04
0.025	32.20	63.910	2.190E-04
0.031	45.00	62.140	2.030E-04
0.04	49.90	60.970	1.970E-04
0.054	53.10	60.380	1.920E-04
0.067	55.20	60.080	1.890E-04
0.083	56.40	59.510	1.870E-04
0.108	58.30	58.570	1.840E-04
0.135	58.80	57.770	1.830E-04
KJ15A:KAOLINITE/NATURAL+EQUI-MAGNETITE/NaOH+WATER/60			
0	0.00	65.120	2.300E-04
0.016	4.30	65.090	2.300E-04
0.022	8.60	65.160	2.270E-04
0.03	16.40	64.730	2.160E-04
0.035	22.80	64.300	2.070E-04
0.042	28.40	63.120	1.990E-04
0.055	38.60	63.310	1.850E-04
0.068	39.20	62.360	1.760E-04
0.08	42.50	61.820	1.720E+00
0.108	43.30	61.460	1.670E-04
0.122	44.80	61.780	1.630E-04
0.137	47.10	61.210	1.610E-04
0.137	47.30	60.960	1.610E-04

MF1:MONTMORILLONITE/NATURAL+EQUI-MAGNETITE/WATER/60

0	0.00	61.780	3.030E-04
0.015	1.30	61.500	3.010E-04
0.02	3.00	61.200	2.970E-04
0.025	5.40	61.410	2.940E-04
0.031	13.70	61.370	2.850E-04
0.036	16.70	61.120	2.800E-04
0.044	21.30	60.800	2.750E-04
0.049	24.40	60.660	2.690E-04
0.055	28.00	60.390	2.650E-04
0.068	34.50	60.120	2.570E-04
0.093	43.70	58.570	2.470E-04
0.107	48.10	58.270	2.400E-04
0.119	52.70	57.790	2.350E-04
0.119	67.30	55.000	2.160E-05

Appendix 2

Demagnetization Results

Demagnetization

Step (mT)	Inc	Dec	J (mA/m)
il113a:illite/acicular magnetite/water/45°			
0.0	35.9	100.3	1.466E+02
2.5	35.6	89.9	1.504E+02
5.0	34.9	92.0	1.503E+02
10.0	35.9	91.1	1.490E+02
20.0	35.3	89.3	1.475E+02
30.0	35.9	93.6	1.427E+02
40.0	35.9	94.6	1.393E+02
50.0	34.4	92.4	1.144E+02
60.0	37.6	88.8	7.330E+01
70.0	26.7	88.8	4.023E+01
80.0	34.6	105.7	1.029E+01
90.0	27.3	140.7	3.910E+00
99.9	69.8	163.0	5.990E-01

Demagnetization

Step (mT)	Inc	Dec	J (mA/m)
ill112:illite/acicular magnetite/water/75°			
0.0	-68.2	99.0	1.650E+03
2.5	-69.2	98.4	1.650E+03
5.0	-67.9	92.2	1.650E+03
10.0	-69.8	99.9	1.650E+03
20.0	-68.7	95.2	1.650E+03
30.0	-69.5	97.9	1.620E+03
40.0	-68.3	96.1	1.520E+03
50.0	-70.3	97.4	1.320E+03
60.0	-65.9	94.3	8.400E+02
70.0	-73.3	79.4	3.620E+02
80.0	-66.9	146.7	1.210E+02
90.0	-42.2	136.1	5.660E+01
99.9	-14.8	201.9	2.900E+01

Demagnetization

Step (mT)	Inc	Dec	J (mA/m)
il113b:illite/acicular magnetite/water/30°			
0.0	23.9	130.2	2.457E+02
2.5	23.8	123.8	2.459E+02
5.0	24.2	123.6	2.432E+02
10.0	24.2	124.3	2.424E+02
20.0	23.5	124.6	2.444E+02
30.0	23.7	123.8	2.416E+02
40.0	23.8	123.9	2.339E+02
50.0	23.9	123.6	1.910E+02
60.0	26.8	128.8	1.423E+02
70.0	32.3	120.4	6.964E+01
80.0	28.5	133.4	1.433E+01
90.0	29.8	154.2	4.416E+00
99.9	18.7	94.1	1.654E+00

Demagnetization

Step (mT)	Inc	Dec	J (mA/m)
chl114:chlorite/acicular magnetite/water/60°			
0.0	54.5	4.9	1.057E+02
2.5	53.3	3.6	1.038E+02
5.0	56.4	5.4	1.017E+02
10.0	54.7	3.5	9.719E+01
20.0	54.9	359.2	8.512E+01
30.0	59.9	3.1	7.520E+01
40.0	59.1	2.4	6.165E+01
50.0	38.5	353.8	2.792E+01
60.0	47.1	367.0	1.898E+01
70.0	21.2	2.2	4.871E+00

Demagnetization

Step (mT)	Inc	Dec	J (mA/m)
chl1114:chlorite/acicular magnetite/water/45°			
0.0	45.7	120.2	1.980E+02
2.5	46.2	117.2	1.879E+02
5.0	44.3	117.0	1.792E+02
10.0	45.7	118.4	1.675E+02
20.0	46.7	117.4	1.470E+02
30.0	47.5	116.1	1.270E+02
40.0	47.4	117.4	1.030E+02
50.0	47.2	117.9	6.590E+01
60.0	59.4	121.8	3.059E+01
70.0	75.1	170.3	1.327E+01
80.0	-77.6	3.0	1.830E+01
90.0	30.6	68.4	3.880E+01
99.9	77.6	229.3	2.507E+01

Demagnetization

Step (mT)	Inc	Dec	J (mA/m)
kn17a:kaolinite/acicular magnetite/water/30°			
0.0	25.7	358.5	7.750E+01
2.5	26.0	359.9	7.740E+01
5.0	26.0	1.1	7.720E+01
10.0	26.2	355.7	7.540E+01
20.0	25.8	358.7	7.650E+01
30.0	27.0	360.0	7.410E+01
40.0	25.8	4.6	6.850E+01
50.0	28.4	353.4	4.570E+01
60.0	33.8	357.7	2.730E+01
70.0	37.3	356.8	8.270E+00
80.0	27.4	318.7	3.480E+00
90.0	54.2	25.1	1.000E+00
99.9	44.2	43.2	9.960E-01

Demagnetization Step (mT)	Inc	Dec	J (mA/m)
kn18b:kaolinite/acicular magnetite/water/75°			
0.0	70.6	345.6	4.610E+01
2.5	72.7	354.7	4.750E+01
5.0	70.4	13.6	4.865E+01
10.0	68.3	9.2	4.820E+01
15.0	69.5	1.6	4.740E+01
20.0	73.4	348.7	4.653E+01
30.0	73.1	350.5	4.447E+01
40.0	71.8	0.5	4.140E+01
50.0	76.5	0.6	3.060E+01
60.0	65.7	10.2	1.730E+01
70.0	43.2	26.5	7.910E+00
80.0	25.7	80.7	6.203E+00
90.0	7.5	134.0	5.218E+00
99.9	-18.8	334.0	4.300E+00

Demagnetization Step (mT)	Inc	Dec	J (mA/m)
kn18a:kaolinite/acicular magnetite/water/60°			
0.0	58.1	3.9	4.054E+01
2.5	55.7	7.3	3.650E+01
5.0	56.3	5.7	3.643E+01
10.0	55.6	6.1	3.650E+01
20.0	30.0	20.2	4.103E+01
25.0	35.1	18.6	3.890E+01
30.0	38.2	18.1	3.824E+01
35.0	44.1	13.0	3.530E+01
40.0	51.1	16.2	3.323E+01
50.0	57.1	13.9	2.561E+01
60.0	57.5	1.7	1.463E+01
70.0	65.2	353.7	4.400E+00
80.0	23.5	240.4	4.476E+00
85.0	13.6	224.9	4.920E+00
90.0	58.3	112.8	1.310E+00

Demagnetization Step (mT)	Inc	Dec	J (mA/m)
mn19b:montmorillonite/acicular magnetite/water/60°			
0.0	53.3	3.9	1.490E+02
2.5	53.5	7.3	1.480E+02
5.0	53.4	6.7	1.484E+02
10.0	53.3	6.2	1.482E+02

20.0	53.2	4.1	1.476E+02
30.0	53.1	4.8	1.461E+02
40.0	52.7	7.1	1.377E+02
50.0	54.2	358.9	1.113E+02
60.0	53.3	355.3	7.060E+01
70.0	46.8	13.7	3.081E+01
80.0	57.8	351.9	1.829E+01
90.0	64.4	36.0	2.189E+00
99.9	77.6	16.3	1.734E+00

Demagnetization

Step (mT)	Inc	Dec	J (mA/m)
mn21:montmorillonite/acicular magnetite/water/45°			
0.0	36.8	346.0	2.128E+02
2.5	37.6	351.0	2.124E+02
5.0	37.7	348.5	2.121E+02
10.0	37.2	351.6	2.120E+02
20.0	37.1	349.2	2.108E+02
30.0	37.0	347.6	2.089E+02
40.0	37.5	350.1	1.946E+02
50.0	37.7	351.6	1.554E+02
60.0	40.1	353.4	9.517E+01
70.0	37.5	345.4	4.516E+01
80.0	33.4	336.7	1.646E+01
90.0	42.7	332.6	5.646E+00
99.9	64.2	18.6	1.596E+00

Demagnetization

Step (mT)	Inc	Dec	J (mA/m)
mn22:montmorillonite/acicular magnetite/water/30°			
0.0	25.1	358.4	2.188E+02
2.5	26.6	354.1	2.193E+02
5.0	27.2	358.7	2.185E+02
10.0	26.7	355.7	2.192E+02
20.0	26.1	357.9	2.184E+02
30.0	26.0	358.3	2.155E+02
40.0	25.9	355.6	2.057E+02
50.0	25.4	359.3	1.697E+02
60.0	22.1	1.7	1.205E+02
70.0	20.2	356.7	6.175E+01
80.0	30.2	13.7	1.061E+01
90.0	56.6	2.0	2.070E+00
99.9	53.7	72.9	1.860E+00

Demagnetization

Step (mT)	Inc	Dec	J (mA/m)
ln23:illite/acicular magnetite/saline/30°			
0.0	30.6	359.3	4.735E+02
2.5	35.3	1.3	4.748E+02
5.0	30.8	358.8	4.723E+02
10.0	30.6	2.0	4.712E+02
20.0	30.2	359.6	4.673E+02
30.0	30.2	358.4	4.750E+02
40.0	30.6	1.4	4.310E+02
50.0	28.8	2.7	3.740E+02
60.0	24.5	6.9	2.491E+02
70.0	34.1	350.3	8.505E+01
80.0	27.7	10.1	2.490E+01
90.0	32.5	13.3	9.730E+00
99.9	51.2	14.1	4.227E+00

Demagnetization

Step (mT)	Inc	Dec	J (mA/m)
in24a:illite/acicular magnetite/saline/60°			
0.0	57.1	0.8	2.916E+02
2.5	57.7	1.2	2.920E+02
5.0	58.9	359.2	2.920E+02
10.0	59.8	1.1	2.919E+02
20.0	57.6	1.9	2.882E+02
30.0	59.9	3.2	2.839E+02
40.0	60.5	0.6	2.715E+02
50.0	56.7	2.6	2.298E+02
60.0	59.1	12.2	1.372E+02
70.0	59.8	30.5	5.000E+01
80.0	55.9	7.3	1.213E+01
90.0	33.2	17.7	6.417E+00
99.9	41.6	292.2	4.362E+00

Demagnetization

Step (mT)	Inc	Dec	J (mA/m)
in24b:illite/acicular magnetite/saline/75°			
0.0	68.2	359.5	3.191E+02
2.5	69.1	3.7	3.338E+02
5.0	70.4	1.3	3.128E+02
10.0	69.3	2.1	3.112E+02
20.0	69.0	3.2	3.091E+02
30.0	70.2	5.2	3.049E+02
40.0	68.3	359.4	2.861E+02
50.0	71.1	1.6	2.318E+02
60.0	75.1	25.8	1.430E+02
70.0	63.7	4.7	5.999E+01
80.0	73.2	6.2	1.471E+01
90.0	58.7	50.9	5.263E+00
99.9	66.7	84.3	5.521E+00

Demagnetization Step (mT)	Inc	Dec	J (mA/m)
kn25a:kaolinite/acicular magnetite/saline/75°			
0.0	70.1	359.9	4.443E+02
2.5	70.1	6.4	4.433E+02
5.0	69.5	359.1	4.431E+02
10.0	69.8	0.9	4.431E+02
20.0	70.1	4.8	4.405E+02
30.0	71.0	1.2	4.348E+02
40.0	70.0	0.2	4.125E+02
45.0	70.2	355.2	3.815E+02
50.0	73.1	345.6	3.107E+02
60.0	75.7	344.6	1.783E+02
70.0	75.9	338.1	5.960E+01
80.0	70.2	330.2	1.518E+01
90.0	64.0	324.3	5.981E+00
99.9	80.4	136.5	3.140E+00

Demagnetization Step (mT)	Inc	Dec	J (mA/m)
kn25b:kaolinite/acicular magnetite/saline/60°			
0.0	55.6	359.3	4.057E+02
2.5	54.4	355.1	4.060E+02
5.0	55.6	359.8	4.053E+02
10.0	54.1	353.2	4.096E+02
20.0	56.1	356.3	4.039E+02
30.0	56.0	359.7	3.556E+02
40.0	56.2	0.8	3.289E+02
50.0	55.6	3.9	2.525E+02
60.0	55.0	352.7	1.429E+02
70.0	48.6	0.5	5.569E+01
80.0	55.6	40.4	1.525E+01
90.0	17.7	359.4	5.800E+00
99.9	21.4	216.0	3.518E+00

Demagnetization Step (mT)	Inc	Dec	J (mA/m)
kn26:kaolinite/acicular magnetite/saline/45°			
0.0	33.9	348.6	5.521E+02
2.5	33.6	351.3	5.516E+02
5.0	33.9	350.3	5.539E+02
10.0	33.3	535.4	5.505E+02
20.0	33.8	349.1	5.485E+02
30.0	33.1	351.5	5.344E+02
40.0	33.9	351.4	5.064E+02
50.0	34.5	349.9	3.877E+02
60.0	33.0	359.9	2.619E+02
70.0	40.4	346.1	7.525E+01
80.0	32.3	1.7	2.220E+01
90.0	70.3	351.7	3.771E+00

Demagnetization

Step (mT)	Inc	Dec	J (mA/m)
kn30a:kaolinite/acicular magnetite/saline/30°			
0.0	21.3	347.8	7.166E+02
5.0	21.5	348.2	7.166E+02
10.0	21.6	348.2	7.163E+02
20.0	21.3	350.5	7.143E+02
30.0	21.5	347.2	7.026E+02
35.0	21.2	346.5	6.886E+02
40.0	21.7	348.6	6.533E+02
45.0	21.9	345.5	5.931E+02
50.0	23.1	346.5	4.990E+02
60.0	24.8	354.7	2.732E+02
70.0	17.5	340.5	1.144E+02
80.0	23.7	359.3	3.624E+01
90.0	46.0	35.5	6.084E+00
99.9	53.5	83.3	3.242E+00

Demagnetization

Step (mT)	Inc	Dec	J (mA/m)
cdla:chlorite/acicular magnetite/saline/45°			
0.0	62.8	23.8	2.801E+02
2.5	59.3	26.2	3.036E+02
5.0	57.3	17.2	2.459E+02
10.0	47.7	95.2	4.336E+01
15.0	72.5	68.1	1.051E+02
20.0	56.4	109.9	4.671E+01
25.0	70.4	73.7	5.616E+01
30.0	53.0	314.5	4.660E+01
40.0	66.2	21.7	6.427E+01
50.0	78.4	220.6	9.201E+01
60.0	80.6	124.8	1.041E+02

Demagnetization

Step (mT)	Inc	Dec	J (mA/m)
cdlb:chlorite/acicular magnetite/saline/75°			
0.0	67.3	19.1	2.611E+02
2.5	66.0	19.1	2.330E+02
5.0	71.1	21.9	6.530E+01
10.0	-0.8	10.5	1.382E+02
15.0	77.1	356.4	7.303E+01
20.0	79.5	10.5	3.546E+01
25.0	64.2	110.8	2.705E+01
30.0	34.8	151.0	1.897E+01
35.0	41.6	183.2	2.074E+01
40.0	51.5	199.1	1.986E+01

45.0	74.4	115.6	1.591E+01
50.0	65.9	248.7	1.943E+01
60.0	43.0	246.5	3.401E+01
70.0	68.1	3.8	5.533E+01
80.0	45.1	147.6	4.491E+01
90.0	53.3	28.4	5.237E+01
99.9	-21.1	159.0	1.390E+01

Demagnetization

md3a:montmorillonite/acicular magnetite/saline/75°

Step (mT)	Inc	Dec	J (mA/m)
0.0	68.0	356.3	2.199E+02
2.5	67.7	3.1	2.189E+02
5.0	67.9	4.9	2.186E+02
10.0	67.9	6.3	2.187E+02
20.0	67.5	5.6	2.184E+02
30.0	66.5	2.0	2.150E+02
40.0	66.9	1.0	2.030E+02
45.0	68.3	354.6	1.856E+02
50.0	67.5	353.3	1.641E+02
60.0	70.6	11.3	8.478E+02
70.0	71.6	12.4	3.190E+01
80.0	56.8	38.5	8.732E+00
90.0	70.6	182.8	2.531E+00
99.9	49.6	320.7	1.555E+00

Demagnetization

md3b:montmorillonite/acicular magnetite/saline/60°

Step (mT)	Inc	Dec	J (mA/m)
0.0	50.9	31.7	1.546E+02
5.0	51.3	30.5	1.538E+02
10.0	51.5	28.1	1.535E+02
20.0	51.1	29.9	1.535E+02
30.0	51.3	29.0	1.508E+02
40.0	51.4	32.9	1.431E+02
50.0	49.8	23.7	1.162E+02
60.0	49.0	22.2	6.007E+01
70.0	51.1	40.0	2.173E+01
80.0	53.6	5.9	5.840E+00
90.0	76.7	29.5	1.931E+00
99.9	68.8	336.4	1.235E+00

Demagnetization

md4a:montmorillonite/acicular magnetite/saline/45°

Step (mT)	Inc	Dec	J (mA/m)
0.0	31.2	3.5	2.612E+02
5.0	31.2	2.7	2.611E+02
10.0	31.6	0.7	2.613E+02
20.0	32.1	1.3	2.602E+02
30.0	30.9	1.4	2.566E+02

40.0	32.7	357.6	2.411E+02
50.0	34.0	357.2	1.872E+02
60.0	37.4	11.8	1.179E+02
70.0	27.5	10.0	5.167E+01
80.0	33.4	24.2	1.188E+01
90.0	21.8	351.7	2.903E+00
99.9	14.0	222.2	2.583E+00

Demagnetization

Step (mT)	Inc	Dec	J (mA/m)
md4b:montmorillonite/acicular magnetite/saline/30°			
0.0	21.5	4.9	4.348E+02
5.0	23.1	1.4	4.384E+02
10.0	22.8	4.8	4.397E+02
20.0	22.6	4.0	4.368E+02
30.0	22.9	359.5	4.300E+02
40.0	23.4	6.0	4.084E+02
50.0	22.6	4.2	3.182E+02
60.0	23.3	359.4	1.663E+02
70.0	15.4	354.6	7.926E+01
80.0	27.6	340.8	1.902E+01
90.0	44.3	1.9	2.468E+00
99.9	85.9	360.0	1.632E+00

Demagnetization

Step (mT)	Inc	Dec	J (mA/m)
mmd11:marine sediment/natural magnetite/30°			
0.0	25.1	359.7	1.399E+02
2.5	29.2	2.0	1.163E+02
5.0	28.7	359.8	1.185E+02
10.0	23.7	6.5	1.027E+02
15.0	27.5	359.2	9.100E+01
20.0	27.1	354.9	7.865E+01
30.0	27.0	353.6	4.770E+01
40.0	24.8	353.6	3.085E+01
45.0	26.0	357.8	2.553E+01
50.0	27.5	357.3	1.860E+01
60.0	28.5	4.3	1.328E+01
70.0	31.7	359.3	8.471E+00

Demagnetization

Step (mT)	Inc	Dec	J (mA/m)
mmd11b:marine sediment/natural magnetite/45°			
0.0	31.9	4.7	1.073E+02
2.5	34.4	5.4	9.966E+01
5.0	35.6	4.8	9.658E+01
10.0	35.6	8.2	8.299E+01
20.0	31.8	8.8	6.230E+01
30.0	33.9	8.4	3.998E+01
40.0	34.6	5.4	2.318E+01
50.0	35.4	8.7	1.455E+01
60.0	37.8	9.7	1.013E+01
70.0	37.8	5.7	7.698E+00
80.0	43.2	11.5	4.588E+00

Demagnetization

Step (mT)	Inc	Dec	J (mA/m)
mmd14:marine sediment/natural magnetite/60°			
0.0	46.6	357.2	1.063E+02
2.5	47.2	359.7	1.051E+02
5.0	48.5	352.7	9.240E+01
10.0	46.7	1.2	8.920E+01
20.0	47.8	359.1	6.180E+01
30.0	46.8	3.5	5.840E+01
40.0	49.9	359.2	2.340E+01
50.0	48.4	360.0	1.540E+01
60.0	53.9	359.4	9.680E+00
70.0	48.0	359.4	7.350E+00

Demagnetization

Step (mT)	Inc	Dec	J (mA/m)
mmd14b:marine sediment/natural magnetite/75°			
0.0	70.1	351.5	1.420E+02
22.5	69.1	351.9	6.840E+01
30.0	65.7	0.1	5.160E+01

35.0	70.4	0.2	4.030E+01
40.0	69.3	1.4	3.240E+01
45.0	72.0	344.7	2.400E+01
50.0	73.6	354.4	1.920E+01
60.0	68.8	354.0	1.350E+01
70.0	71.3	349.9	9.710E+00
80.0	69.9	0.3	6.630E+00

Demagnetization

Step (mT)	Inc	Dec	J (mA/m)
msd16:marine silty sediment/natural magnetite/75°			
0.0	71.2	7.6	7.062E+01
5.0	73.4	334.9	7.050E+01
10.0	72.4	358.0	6.250E+01
15.0	71.7	10.1	5.270E+01
20.0	71.6	7.2	4.360E+01
25.0	68.8	7.5	3.510E+01
30.0	73.0	4.3	2.800E+01
35.0	74.8	5.8	2.150E+01
40.0	75.0	7.7	1.660E+01
50.0	71.7	12.3	1.140E+01
60.0	79.4	329.0	8.440E+00
70.0	84.1	55.9	4.670E+00

Demagnetization

Step (mT)	Inc	Dec	J (mA/m)
msd17:marine silty sediment/natural magnetite/60°			
0.0	59.2	359.1	5.140E+01
2.5	58.2	358.9	5.100E+01
5.0	53.7	14.0	5.904E+01
10.0	58.4	357.9	4.440E+01
15.0	57.4	6.2	3.820E+01
20.0	57.9	359.8	3.090E+01
25.0	58.5	2.7	2.430E+01
30.0	57.2	7.8	2.000E+01
35.0	57.3	1.2	1.530E+01
40.0	55.2	359.1	1.310E+01
45.0	58.6	6.8	9.340E+00
50.0	60.9	10.7	8.090E+00
60.0	77.6	58.4	4.640E+00

Demagnetization

Step (mT)	Inc	Dec	J (mA/m)
msd17b:marine silty sediment/natural magnetite/45°			
0.0	39.1	356.2	5.630E+01
2.5	39.7	357.7	5.590E+01
5.0	31.5	2.5	5.870E+01
10.0	39.0	358.9	4.720E+01
15.0	42.4	352.4	3.940E+01
20.0	39.6	354.6	3.440E+01
30.0	44.6	358.3	2.230E+01

40.0	39.2	351.4	1.400E+01
50.0	49.0	347.2	8.560E+00
55.0	48.1	0.9	6.450E+00
60.0	43.8	5.5	6.400E+00
70.0	49.8	356.9	4.570E+00
80.0	48.4	2.3	3.660E+00

Demagnetization

Step (mT)	Inc	Dec	J (mA/m)
msd18:marine silty sediment/natural magnetite/30°			
0.0	26.6	350.3	7.830E+01
2.5	26.2	348.8	7.740E+01
5.0	21.0	0.3	7.540E+01
10.0	26.1	355.3	6.300E+01
15.0	25.9	331.2	4.230E+01
20.0	26.6	342.6	3.970E+01
30.0	17.3	350.1	2.800E+01
35.0	23.1	350.6	2.530E+01
40.0	28.5	349.7	1.770E+01
50.0	32.8	353.2	1.200E+01
60.0	38.0	354.6	6.180E+00
70.0	50.5	5.0	4.390E+00
80.0	36.0	357.1	4.490E+00

Demagnetization

Step (mT)	Inc	Dec	J (mA/m)
rej11:reconstructed sediment/natural magnetite/saline/45°			
0.0	47.6	5.4	1.520E+02
2.5	47.0	7.7	1.480E+02
5.0	47.1	7.9	1.400E+02
10.0	47.6	10.1	1.100E+02
20.0	46.9	359.9	7.090E+01
30.0	49.3	15.6	3.430E+01
40.0	55.4	13.3	1.870E+01
45.0	47.8	2.1	1.590E+01
50.0	58.2	357.3	1.050E+01
60.0	56.9	128.1	1.480E+01

Demagnetization

Step (mT)	Inc	Dec	J (mA/m)
rej11a:reconstructed sediment/natural magnetite/saline/60°			
0.0	61.7	347.6	1.230E+02
2.5	61.5	346.2	1.220E+02
5.0	61.3	344.4	1.160E+02
10.0	61.9	346.5	9.760E+01
20.0	63.3	351.2	5.900E+01
25.0	63.7	353.2	4.120E+01
30.0	62.3	1.7	3.180E+01
40.0	65.9	354.1	1.770E+01
50.0	66.4	0.9	9.800E+00
60.0	73.9	4.9	7.210E+00

70.0	62.3	350.8	5.470E+00
80.0	69.2	40.8	3.520E+00

Demagnetization Step (mT) Inc Dec J (mA/m)

rej12:reconstructed sediment/natural magnetite/saline/75°

0.0	70.7	3.4	1.680E+02
5.0	68.5	6.9	1.560E+02
10.0	71.0	7.9	1.300E+02
20.0	71.8	0.8	7.400E+01
30.0	76.8	350.1	4.230E+01
40.0	72.4	348.7	2.340E+01
50.0	74.3	357.6	1.360E+01
60.0	80.7	35.3	9.040E+00
70.0	72.9	62.6	5.380E+00

Demagnetization Step (mT) Inc Dec J (mA/m)

rej13:reconstructed sediment/natural magnetite/saline/30°

0.0	30.0	356.1	2.080E+02
2.5	33.7	354.0	2.000E+02
5.0	34.4	352.2	1.900E+02
10.0	30.6	359.0	1.650E+02
20.0	31.3	359.7	9.560E+01
25.0	31.6	0.4	7.730E+01
30.0	33.0	353.2	5.250E+01
35.0	33.7	352.8	4.080E+01
40.0	34.1	1.2	2.890E+01
50.0	36.8	1.9	1.740E+01
60.0	30.6	6.7	1.180E+01
70.0	50.9	4.3	6.290E+00
80.0	34.1	15.2	5.950E+00
90.0	71.2	24.4	4.070E+00

Demagnetization Step (mT)	Inc	Dec	J (mA/m)
id22:illite/equi-magnetite/saline/50°			
0.0	49.2	354.6	9.350E+01
2.5	49.9	349.6	9.770E+01
5.0	50.0	352.1	9.590E+01
10.0	50.0	351.7	9.330E+01
20.0	49.1	349.1	8.720E+01
30.0	49.2	352.7	7.630E+01
40.0	50.2	345.9	6.150E+01
45.0	50.2	349.9	5.000E+01
50.0	50.2	352.0	4.190E+01
60.0	50.8	355.0	2.790E+01
70.0	48.2	359.9	1.640E+01
80.0	54.9	1.6	7.540E+00
90.0	68.2	337.5	4.500E+00

Demagnetization Step (mT)	Inc	Dec	J (mA/m)
kd22:kaolinite/equi-magnetite/saline/50°			
2.5	32.5	330.6	1.530E+02
5.0	32.6	330.5	1.520E+02
10.0	33.2	327.7	1.430E+02
20.0	34.3	330.9	1.160E+02
30.0	42.2	330.1	7.700E+01
35.0	42.5	335.1	6.430E+01
40.0	41.8	335.6	5.430E+01
45.0	43.1	335.0	4.230E+01
50.0	43.0	339.3	3.390E+01
60.0	38.4	333.1	2.200E+01
70.0	36.6	336.5	1.330E+01
80.0	32.7	334.6	9.160E+00
90.0	30.3	327.9	5.040E+00

Demagnetization Step (mT)	Inc	Dec	J (mA/m)
md23:montmorillonite/equi-magnetite/saline/50°			
0.0	44.4	5.4	7.090E+01
2.5	43.3	7.4	7.170E+01
10.0	44.0	2.7	7.020E+01
20.0	42.9	4.5	6.700E+01
30.0	43.2	1.6	5.770E+01
40.0	42.7	5.0	4.680E+01
45.0	43.0	1.1	3.910E+01
50.0	44.4	357.3	3.030E+01
55.0	45.3	0.5	2.310E+01
60.0	44.1	1.1	1.820E+01
70.0	45.2	353.4	1.040E+01
80.0	45.8	347.1	5.650E+00

Demagnetization

Step (mT)	Inc	Dec	J (mA/m)
id28:illite/equi-magnetite/saline/50°			
0.0	45.6	346.5	5.730E+01
5.0	46.1	336.8	5.830E+01
10.0	46.1	341.9	5.740E+01
20.0	46.4	345.5	5.310E+01
30.0	47.6	340.8	4.570E+01
35.0	47.8	342.3	4.120E+01
40.0	47.7	346.1	3.590E+01
45.0	47.5	342.4	3.170E+01
50.0	46.5	337.6	2.470E+01
60.0	51.2	341.5	1.520E+01
70.0	46.6	335.4	9.610E+00
80.0	52.4	347.9	4.210E+00

Demagnetization

Step (mT)	Inc	Dec	J (mA/m)
md30:montmorillonite/equi-magnetite/saline/50°			
0.0	44.7	1.6	9.870E+01
2.5	44.4	355.1	9.880E+01
5.0	45.2	357.2	9.830E+01
10.0	45.0	359.0	9.780E+01
20.0	44.8	357.0	9.410E+01
30.0	44.7	358.4	8.390E+01
40.0	44.2	357.6	7.170E+01
50.0	46.2	358.5	4.990E+01
60.0	48.1	355.5	2.720E+01
70.0	45.2	355.0	1.680E+01
80.0	49.1	354.4	7.980E+00
90.0	55.5	355.9	4.120E+00

Demagnetization

Step (mT)	Inc	Dec	J (mA/m)
kj15:kaolinite/natural+equi-magnetite/water/60°			
0.0	61.9	343.8	1.760E+02
2.5	61.9	339.3	1.590E+02
5.0	64.9	339.3	1.330E+02
10.0	63.3	350.0	1.040E+02
15.0	62.5	353.4	7.700E+01
20.0	58.1	355.1	5.630E+01
25.0	63.2	358.0	4.100E+01
30.0	62.8	353.1	3.080E+01
35.0	63.2	350.8	2.420E+01
40.0	58.2	343.1	1.770E+01

45.0	58.1	341.9	1.300E+01
50.0	60.9	348.6	9.340E+00
60.0	67.1	340.2	5.790E+00
70.0	62.4	323.5	3.800E+00
80.0	63.5	310.9	2.980E+00
90.0	72.2	269.8	2.020E+00

Demagnetization

Step (mT)	Inc	Dec	J (mA/m)
kj15a:kaolinite/natural+equi-magnetite/water+NaOH/60°			
0.0	62.7	1.2	1.510E+02
2.5	62.2	0.0	1.460E+02
5.0	61.6	359.6	1.390E+02
10.0	58.9	10.6	1.250E+02
15.0	59.6	2.5	1.210E+02
20.0	59.1	356.7	1.060E+02
25.0	58.8	358.2	1.040E+02
30.0	57.4	356.1	9.730E+01
35.0	58.1	354.8	8.590E+01
40.0	57.8	359.0	7.530E+01
45.0	57.3	3.9	6.440E+01
50.0	57.8	359.8	4.850E+01
60.0	57.1	6.3	3.350E+01
70.0	56.0	5.0	1.920E+01
80.0	60.1	359.3	9.200E+00
90.0	61.4	354.9	5.200E+00
99.9	64.6	10.9	2.710E+00

Demagnetization

Step (mT)	Inc	Dec	J (mA/m)
mf2:montmorillonite/natural+equi-magnetite/water/60°			
0.0	53.5	22.0	2.039E+02
2.5	53.1	23.5	1.901E+02
5.0	52.0	25.0	1.760E+02
10.0	51.3	28.5	1.550E+02
15.0	51.3	27.9	1.380E+02
20.0	51.0	24.4	1.260E+02
25.0	50.0	23.1	1.160E+02
30.0	50.7	22.6	1.010E+02
40.0	49.3	30.5	8.340E+01
45.0	50.9	24.2	6.610E+01
50.0	51.4	24.2	5.210E+01
60.0	51.5	29.7	3.520E+01
70.0	51.5	27.3	2.070E+01
80.0	55.8	21.6	9.230E+00

Demagnetization

Step (mT)	Inc	Dec	J (mA/m)
if2:illite/natural+equi-magnetite/water/60°			
0.0	50.7	350.0	1.890E+02
2.5	52.2	347.6	1.770E+02
5.0	54.9	349.4	1.520E+02
10.0	55.0	352.9	1.190E+02
15.0	53.1	355.9	9.180E+01
20.0	52.2	356.3	7.130E+01
25.0	54.6	353.2	5.070E+01
30.0	55.8	353.6	4.060E+01
35.0	54.0	354.8	2.940E+01
40.0	53.0	354.9	2.220E+01
45.0	53.9	354.2	1.810E+01
50.0	57.9	3.0	1.200E+01
60.0	56.7	1.9	8.790E+00
70.0	60.7	347.5	4.870E+00

Vita

Gay A. Howell Deamer graduated from Penn State University in 1976 with a B.S. degree in geology. She received a master's degree in metallurgical engineering at Lehigh University in 1980, and worked in industry for six years before returning to Lehigh for a master's degree in geology.

Compaction-Induced Inclination Shallowing in Synthetic and Natural Sediments

by Gay Deamer

ABSTRACT

A model proposing a mechanism for inclination shallowing of compacting sediments (Anson and Kodama, 1987) in which magnetite particles are electrostatically attracted to negatively charged clay particles was tested. Equidimensional and acicular magnetite (0.5 microns in size) were mixed with kaolinite, chlorite, montmorillonite or illite in either saline or distilled water to produce clay slurries which were given PDRM's by stirring them in fields with inclinations of 30°, 45°, 60°, and 75° and compacted to maximum pressures ranging from 0.14 to 0.19 MPa. Although no evidence for electrostatic attraction between magnetite and clay particles was found, there is evidence that clay and magnetite somehow interact.

The shallowing rate for most samples is rapid at low pressures, and decreases abruptly at higher pressures. This change in shallowing rate occurs at the same pressure as an abrupt change in compaction rate with pressure. This behavior closely resembles the behavior of compacted slurries studied by McConnachie (1974). He found that the orientation of clay particles during compaction was initially rapid, but then the clays stopped orienting at the same pressure at which he observed a change in the compaction rate. It is inferred that since clay orientation and inclination shallowing exhibit very similar behavior with increasing pressure, the magnetite particles are attached to clay platelets.

The change in intensity of magnetization according to field inclination angle during compaction suggests that magnetite particles are not perfectly aligned before compaction, but are dispersed about the mean direction. Compaction causes a decrease in magnetic intensity accompanying shallowing, suggesting that compaction increases the dispersion, similar to the effect found by Cogne (1987) in strained synthetic materials.